Russian Original Vol. 38, No. 6, June, 1975

December, 1975

SATEAZ 38(6) 469-570 (1975)

SOVIET ATOMIC ENERGY

АТОМНАЯ ЭНЕРГИЯ
(ATOMNAYA ÉNERGIYA)

TRANSLATED FROM RUSSIAN

c/b CONSULTANTS BUREAU, NEW YORK

SOVIET ATOMIC ENERGY

Soviet Atomic Energy is a cover-to-cover translation of *Atomnaya Énergiya*, a publication of the Academy of Sciences of the USSR.

An agreement with the Copyright Agency of the USSR (VAAP) makes available both advance copies of the Russian journal and original glossy photographs and artwork. This serves to decrease the necessary time lag between publication of the original and publication of the translation and helps to improve the quality of the latter. The translation began with the first issue of the Russian journal.

Consultants Bureau journals appear about six months after the publication of the original Russian issue. For bibliographic accuracy, the English issue published by Consultants Bureau carries the same number and date as the original Russian from which it was translated. For example, a Russian issue published in December will appear in a Consultants Bureau English translation about the following June, but the translation issue will carry the December date. When ordering any volume or particular issue of a Consultants Bureau journal, please specify the date and, where applicable, the volume and issue numbers of the original Russian. The material you will receive will be a translation of that Russian volume or issue.

Subscription
$87.50 per volume (6 Issues)

Single Issue: $50
Single Article: $15

Prices somewhat higher outside the United States.

CONSULTANTS BUREAU, NEW YORK AND LONDON

227 West 17th Street
New York, New York 10011

4a Lower John Street
London W1R 3PD
England

Published monthly. Second-class postage paid at Jamaica, New York 11431.

Soviet Atomic Energy is abstracted or indexed in *Applied Mechanics Reviews, Chemical Abstracts, Engineering Index, INSPEC—Physics Abstracts and Electrical and Electronics Abstracts, Current Contents,* and *Nuclear Science Abstracts.*

SOVIET ATOMIC ENERGY

A translation of *Atomnaya Énergiya*

December, 1975

Volume 38, Number 6 June, 1975

CONTENTS

CONTENTS

(continued)

The Russian press date (podpisano k pechati) of this issue was 5/28/1975. Publication therefore did not occur prior to this date, but must be assumed to have taken place reasonably soon thereafter.

ARTICLES

OPTIMIZATION OF THE OPERATING CONDITIONS OF MASS-DIFFUSION CASCADE INSTALLATIONS

V. A. Chuzhinov, N. I. Laguntsov,
B. I. Nikolaev, and G. A. Sulaberidze

UDC 621.039.31

In the design and execution of practical cascade installations a calculation of the optimum operating conditions of the separating devices is extremely vital. A correct choice of conditions enables the number of such devices in the cascade and the energy capacity of production to be reduced for special external working conditions.

When solving problems of the type encountered in separation practice, it is desirable in a number of cases to use the method of mass diffusion; this has the advantages of servicing simplicity, fairly short times of installation, compactness of apparatus, universality, and speed of operation, i.e., it enables isotopes of a variety of elements to be produced in the same apparatus in a very short time [1, 2]. However, the absence of published data as to methods of optimizing mass-diffusion apparatus, as distinct from such classical methods of separation as thermal diffusion and distillation [3-8], makes it difficult to create effective mass-diffusion separators.

This paper is devoted to questions of optimizing mass-diffusion units (columns or pumps) in cascades. Since the creation and operation of practical separating installations involve the expenditure of considerable material resources and electrical power, optimization of the cascade is best carried out by reference to a criterion as fully as possible reflecting the economy of the method and the separating process.

One such criterion is the net cost of the resultant product. An analytical expression for estimating the net cost of an isotope mixture enriched with the valuable component may be obtained if we take account of the main expenses incurred in the production of an isotope in the cascade (for example, one consisting of mass-diffusion columns).

For simplicity, let us assume that all the columns in the cascade work in the same mode. The form efficiency of the cascade η, defined as the ratio of the separating power ΔU_{id} of an ideal cascade having specified values of individual flows and concentrations [F and c_F in the feed, P and c_P in the outgoing materials (product), and W and c_W in the spent materials (waste)], to the separating power ΔU of a real cascade with the same flows and concentrations at the input and outputs, may be expressed in the following form [4]:

$$\eta = \frac{\Delta U_{id}}{\Delta U} = \frac{1}{(H^2/4K)\, l_\Sigma} [P\Phi(c_P) + W\Phi(c_W) - F\Phi(c_F)], \quad (1)$$

where $H^2/4K = \delta U$ is the specific separating power of the column, H and K are the coefficients of the transfer equation for the column, l_Σ is the total length of all the columns in the cascade, $\Phi(c) = (2c-1) \ln [c/(1-c)]$ is the separating potential.

From Eq. (1) we obtain an expression for the total length of the columns in a real cascade:

$$l_\Sigma = \frac{1}{(H^2/4K)\, \eta} [P\Phi(c_P) + W\Phi(c_W) - F\Phi(c_F)]. \quad (2)$$

Since mass diffusion relates to irreversible methods of separation, we may consider that the energy required by the cascade and the amount of cooling liquid employed are proportional to the length of the

Translated from Atomnaya Énergiya, Vol. 38, No. 6, pp. 363-366, June, 1975. Original article submitted July 1, 1974.

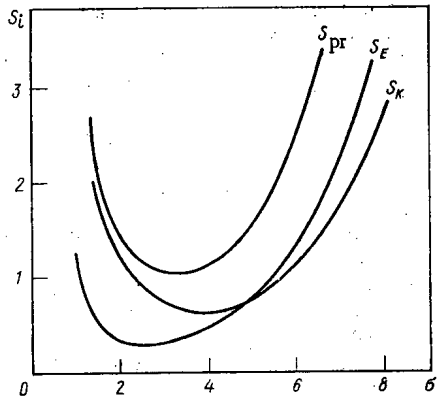

Fig. 1. Net cost and cost components as functions of the vapor flow.

cascade. Using a_K to denote the cost of unit length of the column, we may write the capital expenditure y_K required for creating the cascade in the form

$$y_K = a_K l_\Sigma. \tag{3}$$

If T_0 is the period of service of the cascade, determined in accordance with established norms, while t is the time of operation required to obtain a specified amount of product, the part of the cost of the cascade which is transferable to the cost of the isotope (amortization deductions) will be

$$y_a = a_K l_\Sigma t/T_0. \tag{4}$$

Since the power consumed by the cascade installation is proportional to the total flow of vapor, its magnitude may be defined as

$$Q = bql_\Sigma, \tag{5}$$

where q is the flow of vapor associated with unit length of the cascade, b is the energy consumed in creating unit vapor flow.

The specific flow of the vapor q may be expressed in terms of the working parameters of the column:

$$q = 2\pi r_2 u = 2\pi n D_{10}\sigma. \tag{6}$$

Here r_2 is the radius of the inner condenser of the column, u is the density of the vapor flow at the condensing surface, n is the molar density, D_{10} is the diffusion coefficient of the separated gas in the vapor of the working liquid, $\sigma = ur_2/nD_{10}$ is a dimensionless parameter of the column, an analog of the Peclet diffusion number.

Hence the energy needed in order to obtain a specified quantity of the isotope is

$$E = 2\pi bnD_{10}\sigma t l_\Sigma, \tag{7}$$

and its cost may be written in the following form

$$y_E = 2\pi a_E D_{10}\sigma t l_\Sigma, \tag{8}$$

where $a_E = b a_{0E}$ (a_{0E} is the distribution cost of the unit of energy).

In an analogous manner, for estimating the expenditure on cooling liquid we obtain the expression

$$y_b = 2\pi a_b n D_{10}\sigma t l_\Sigma, \tag{9}$$

where a_b is a coefficient allowing for the coolant expenses associated with unit flow of the vapor q.

Apart from these components, the net cost of the isotope must include the expenditure on the raw material required to produce the specified amount of isotope $y_F = a_F Ft$, the expenditure of the wages of the servicing personnel $y_{wg} = a_{wg}t$, and also the expenditure on repairing the cascade installation. The coefficients a_F and a_{wg} represent the distribution cost of one unit of raw material and the wages per unit time respectively. The cost of the capital and preventive repairs of the separating apparatus we define as a part of the capital outlay; we allow for these in the expression for the net cost of the product by means of a coefficient k_1. The value of k_1 depends on the complexity and specific characteristics of the apparatus employed and is chosen on the basis of experience in the use of analogous installations.

Thus the expression for estimating the total cost of the product being manufactured (the isotope) assumes the form

$$Y = \frac{t1}{(H^2/4K)\eta}\left[P\Phi(c_P) + W\Phi(c_W) - F\Phi(c_F)\right]\left[\frac{a_K(1+k_1)}{T_0} + 2\pi nD_{10}\sigma(a_E + a_b)\right] a_F Ft + a_{wg}t. \tag{10}$$

Let us consider various possible cases of the use of this function.

If in a natural isotope mixture only one isotope is valuable, then, allowing for the balance equation relating to the whole cascade

$$P+W=F;$$
$$Pc_P+Wc_W=Fc_F,$$

we obtain the following expression for the net cost of the isotope from Eq. (10):

$$S_{pr}=\frac{Y}{Pt}=\frac{1}{(H^2/4K)\eta}\left[\Phi(c_P)+\frac{c_P-c_F}{c_F-c_W}\Phi(c_W)-\frac{c_P-c_W}{c_F-c_W}\Phi(c_F)\right]\left[\frac{a_K(1+k_1)}{T_0}+2\pi nD_{10}\sigma(a_E+a_b)\right]$$
$$+a_F\frac{c_P-c_W}{c_F-c_W}+\frac{a_{wg}}{P}. \quad (11)$$

For a specified geometry of the column the specific separating capacity $\delta U = H^2/4K$ is determined by the dimensionless flow of vapor σ and by the circulation, the maximum value of which is in turn proportional to σ. Since the separating capacity (for a fixed flow of vapor) increases monotonically with increasing circulation, tending toward a limiting value δU_{lim}, it is desirable to establish the value of the circulation for which δU is close to δU_{lim}. Then the choice of operating conditions for the columns in the cascade will be determined simply by the vapor flow.

Since the capital outlay is proportional to $1/\delta U$ and the power required to the quantity $\sigma/\delta U$, it follows from Eq. (11) that the energy and apparatus optima for a cascade of mass-diffusion columns do not coincide. Hence the operating conditions of the columns in the cascade have to be chosen in such a way that the net cost of the resultant produce may be a minimum.

It is also useful to use the net-cost function (11) in order to optimize the cascade with respect to the dimensions of the stripping section. For this purpose it is sufficient to find the minimum of S_{pr} with respect to the value of c_W. In the particular case in which the net cost of the raw material is small, or when the product obtained in the spent materials may be realized at the original (supply) price, there is no need to consider the spent-materials section, and the expression for the net cost may be written in the form:

$$S_{pr}=\frac{\Phi(c_P, c_F)}{(H^2/4K)\eta}\left[\frac{a_K(1+k_1)}{T_0}+2\pi nD_{10}\sigma(a_E+a_b)\right]+\frac{a_{wg}}{P}, \quad (12)$$

where

$$\Phi(c, c_F)=(2c-1)\ln\frac{c(1-c_F)}{c_F(1-c)}+\frac{(c-c_F)(1-2c_F)}{c_F(1-c_F)}. \quad (13)$$

Also of interest is the case in which both isotopes of the separated mixtures are valuable. Then in addition to the value of C_P we must specify the required concentration of the second isotope $1-c_W$, which is enriched at the other end of the cascade. We may consider that the expenses incurred in producing each isotope are proportional to the total length of the columns of the particular section in which the isotope under consideration is enriched:

$$Y=Y_P+Y_W; \quad (14)$$
$$\frac{Y_P}{Y_W}=\frac{P\Phi(c_P, c_F)}{W\Phi(c_W, c_F)}, \quad (15)$$

where Y_P and Y_W are the expenses associated with the creation and exploitation of the enriched and spent (waste) sections of the cascade respectively. The net cost of each isotope will in this case be determined by an expression analogous to Eq. (12):

$$S_{pr}^P=\frac{Y_P}{Pt}=\frac{1}{(H^2/4K)\eta}\frac{P\Phi(c_P, c_F)}{P\Phi(c_P, c_F)+W\Phi(c_W, c_F)}\left\{\left[\Phi(c_P)+\frac{c_P-c_F}{c_F-c_W}\Phi(c_W)-\frac{c_P-c_W}{c_F-c_W}\Phi(c_F)\right]\right.$$
$$\left.\times\left[\frac{a_K(1+k_1)}{T_0}+2\pi nD_{10}\sigma(a_E+a_b)\right]+a_F\frac{c_P-c_W}{c_F-c_W}+\frac{a_{wg}}{P}\right\}; \quad (16)$$

$$S_{pr}^W=\frac{Y_W}{Wt}=\frac{1}{(H^2/4K)\eta}\frac{W\Phi(c_W, c_F)}{P\Phi(c_P, c_F)+W\Phi(c_W, c_F)}\left\{\left[\frac{c_F-c_W}{c_P-c_F}\Phi(c_P)+\Phi(c_W)-\frac{c_P-c_W}{c_P-c_F}\Phi(c_F)\right]\right.$$
$$\left.\times\left[\frac{a_1(1+k_1)}{T_0}+2\pi nD_{10}\sigma(a_E+a_b)\right]+a_F\frac{c_P-c_W}{c_P-c_F}+\frac{a_{wg}}{W}\right\}. \quad (17)$$

By repeating the discussions outlined above we may obtain a function for the net cost of the isotopes concentrated in a cascade of mass-diffusion (Hertz) pumps. In this case, in order to estimate the total net cost of the product, we must replace the separating power $H^2/4K$ in Eq. (10) by the separating power of the pump δU_H expressed in terms of its working and geometrical parameters [9, 10]. The term allowing for the energy expenses also changes slightly. For a cascade of mass-diffusion pumps with specified geometry and working conditions Eq. (10) takes the form

$$Y_{\text{н}} = \frac{t}{\delta U_{\text{н}} \eta} [P\Phi(c_P) + W\Phi(c_W) - F\Phi(c_F)] \left[\frac{a'_{\text{к}}(1+k'_1)}{T_0} + \frac{Z}{l_{\text{e}}} nD_{10} \frac{1}{1-\theta_n} \ln q (a'_{\text{E}} + a'_b) \right] + a_F Ft + a_{\text{wg}} t. \quad (18)$$

Here Z is the area of the porous diaphragm, l_{e} is the effective diffusion length [10], $\ln q = ul_{\text{e}}/nD_{10}$ is the Peclet diffusion number, θ_{n} is the partition coefficient of the vapor flow, a'_{K} k'_1 a'_{E}, a'_{b} are coefficients allowing for the corresponding expenses. From Eq. (18) we may easily obtain the net-cost function for various cases of transferring the total expenses to the isotopes produced.

Figure 1 shows the net cost of 99% $^{13}CH_4$ calculated from Eq. (12) and also the components allowing for the capital (S_{K}) and energy (S_{E}) expenditure on the creation and exploitation of the installation as functions of the quantity σ. The data required for the calculation were obtained during laboratory research into mass-diffusion columns carried out earlier [1]. The values of S_{K}, S_{E}, and S_{pr} are given in relative units. The terms of Eq. (12) allowing for the wages of the servicing personnel and the cost of the original materials are omitted, since these have no effect on the appearance of the curves. We see from Fig. 1 that, as a result of the noncoincidence of the optimal energy and capital outlays, the value of σ corresponding to the minimum net cost is smaller than the value of σ corresponding to the maximum separating power of the column.

By using the method proposed we may generalize the resultant net-cost function to other methods of separation (thermal diffusion, gas diffusion, and so on). It is clear that in every specific case the optimization parameters are to be chosen with due regard for the special features of the separating method and the separating devices. The results may be used in designing mass-diffusion separating installations and also when comparing the efficiency of methods used for separating various isotopes.

The authors wish to thank G. A. Tevzadze for discussing the work and also for valuable comments.

LITERATURE CITED

1. B. I. Nikolaev et al., At. Énerg., 23, No. 1, 62 (1967).
2. B. I. Nikolaev et al., Isotopenpraxis, 6, No. 11, 417 (1970).
3. K. Jones and W. Ferry, Separation of Isotopes by Thermal Diffusion [Russian translation], IL, Moscow (1947).
4. A. M. Rozen, Theory of Isotope Separation in Columns [in Russian], Atomizdat, Moscow (1960).
5. G. D. Rabinovich, R. Ya. Gurevich, and G. I. Bobrova, Thermal Diffusion Separation of Liquid Mixtures [in Russian], Nauka i Tekhnika, Minsk (1971).
6. W. Rutherford et al., Rev. Sci. Instrum., 39, No. 1, 94 (1968).
7. M. P. Malkov et al., in: Transactions of the Second Geneva Conference, Vol. 10 [in Russian], Atomizdat Moscow (1969), p. 54.
8. Ya. D. Zel'venskii, A. A. Raitman, and A. P. Timashev, Khim. Prom., No. 7, 538 (1973).
9. G. F. Barvikh and R. Ya. Kucherov, in: Transactions of the All-Union Scientific-Technical Conference on the Use of Radioactive and Stable Isotopes in the National Economy [in Russian], Izd. AN SSSR, Moscow (1958), p. 120.
10. I. G. Gverdtsiteli, R. Ya. Kucherov, and V. K. Tskhakaya, in: Transactions of the Second Geneva Conference, Vol. 10 [in Russian], Atomizdat, Moscow (1969), p. 69.

MATHEMATICAL SIMULATION OF THE EXTRACTIVE REPROCESSING OF NUCLEAR FUEL

3. REDOX REEXTRACTION USING IRON SALTS*

A. M. Rozen, M. Ya. Zel'venskii, and I. V. Shilin

UDC 621.039.59.001.57

Processes of separative reextraction play an important part in radiochemical technology; they are used to separate plutonium and neptunium from each other and from uranium. However, the mathematical extraction model developed in earlier treatments [1-4] is insufficient for describing these processes, since it takes no account of the kinetics of redox reactions.

The aim of the present investigation was to develop a mathematical model and a computing algorithm for the redox reextraction of neptunium and plutonium with due allowance for the kinetics of the chemical reactions in the aqueous phase, and also to analyze the influence of the basic parameters of the process on its efficiency, leading to a rational choice of the optimum conditions of operation. As redox reagent we took the Fe^{2+}—Fe^{3+} system, for which a relatively large number of kinetic data have been published; however, the algorithm developed in this connection is of a general character, and may be used for processes involving other nonextracted redox reagents.

Kinetics of the Reduction of Plutonium and Oxidation of Neptunium by Iron Salts

The reduction of plutonium (IV) by iron (II) proceeds in accordance with the reaction $Pu^{4+} + Fe^{2+} \rightleftharpoons Pu^{3+} + Fe^{3+}$, while the oxidation of neptunium (IV) by iron (III) obeys $Np^{4+} + Fe^{3+} + 2H_2O \rightleftharpoons NpO_2^+ + Fe^{2+} + 4H^+$.

The kinetic equations of these reactions are

*Parts 1 and 2, see At. Énerg., 37, No. 3 (1974).

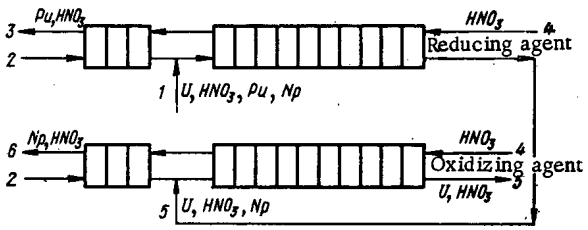

Fig. 1. Arrangement of reextraction unit: 1) Flow of original organic solution; 2) flow of extraction agent; 3) aqueous flow from the first extractor; 4) flow of reextraction agent in the first and second extractors; 5) extract from the first extractor (also forming the original solution for the second) and from the second extractor; 6) reextract from the second extractor.

Translated from Atomnaya Énergiya, Vol. 38, No. 6, pp. 367-371, June, 1975. Original article submitted July 18, 1974; revision submitted January 3, 1975.

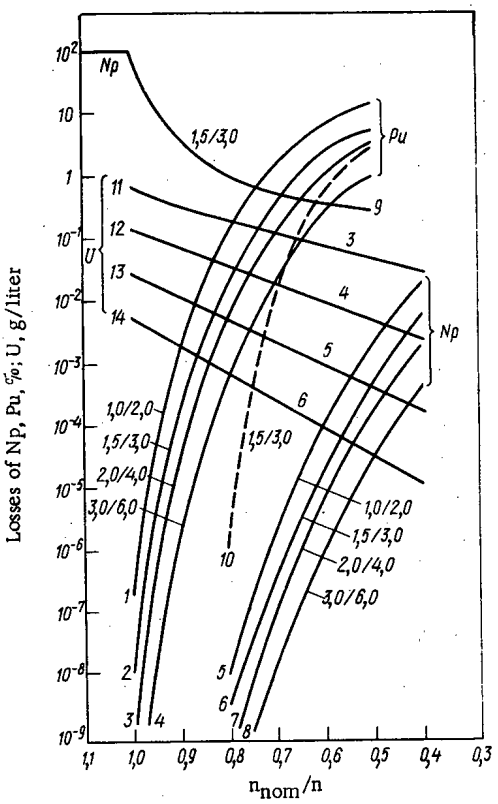

Fig. 2

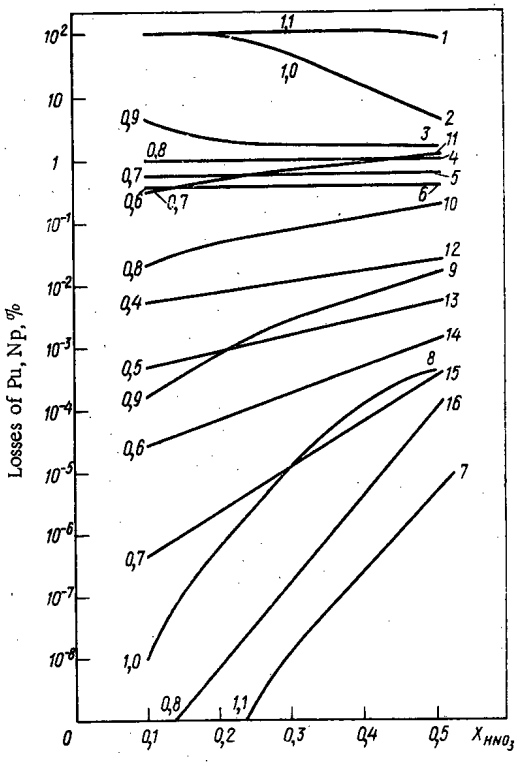

Fig. 3

Fig. 2. Loss of valuable components (Pu and Np, % of the original content) as a function of the ratio of the flows $n_{nom}/n = L/L_{nom}$ for X_{HNO_3} = 0.1 M: 1)-4) losses of plutonium from the organic phase of the first reextractor; 5)-8) losses of neptunium from the organic phases of the second reextractor; 9) losses of neptunium from the aqueous phase of the first reextractor; 10) losses of plutonium from the organic phase of the first reextractor for the ideal-displacement situation; 11)-14) losses of uranium from the aqueous phase of the second reextractor. (The figures on curves 1-10 give the contact time in the mixing and settling chambers of the stage in min; those of 11-14 give the number of stages in the uranium preextraction section.)

Fig. 3. Dependence of the neptunium and plutonium losses on the acidity of the reextraction agent: 1)-6) losses of neptunium from the aqueous phase of the first reextractor; 7)-11) losses of plutonium from the organic phase of the first reextractor; 12-16) losses of neptunium from the organic phase of the second reextractor. (Numbers on the curves indicate the values of $L/L_{nom} = n_{nom}/n$.)

$$\frac{d[\mathrm{Pu(III)}]}{dt} = k_1^{\mathrm{Pu}}[\mathrm{Pu(IV)}] - k_2^{\mathrm{Pu}}[\mathrm{Pu(III)}]; \quad (1)$$

$$\frac{d[\mathrm{Np(V)}]}{dt} = k_1^{\mathrm{Np}}[\mathrm{Np(IV)}] - k_2^{\mathrm{Np}}[\mathrm{Np(V)}]. \quad (2)$$

By approximating the experimental data of [5-9] we obtain equations for the constants

$$k_1^{\mathrm{Pu}} = \frac{1620[\mathrm{Fe(II)}]}{(1+2.9[\mathrm{NO_3^-}])[\mathrm{H^+}]}; \quad k_2^{\mathrm{Pu}} = \frac{k_1^{\mathrm{Pu}}[\mathrm{Fe(III)}]}{600[\mathrm{H^+}]};$$

$$k_1^{\mathrm{Np}} = \exp(-0.368\mu + 0.345)[\mathrm{Fe(III)}]/[\mathrm{H^+}]^3; \quad (3)$$

$$k_2^{\mathrm{Np}} = \exp(0.506\mu + 3.1)[\mathrm{Fe(II)}][\mathrm{H^+}],$$

where $\mu = 3[UO_2(NO_3)_2] + [HNO_3]$ is the ionic strength; $[NO_3^-] = 2[UO_2(NO_3)_2] + [HNO_3]$ is the concentration of nitrate ions.

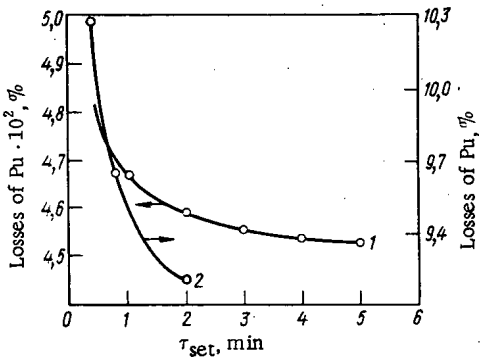

Fig. 4

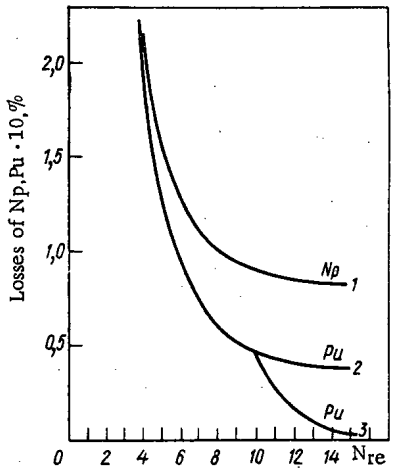

Fig. 5

Fig. 4. Influence of the time of contact in the settling chamber on the losses of plutonium from the organic phase of the first reextractor (L/L_{nom} = 0.8; X_{HNO_3} = 0.2 M): 1) for ordinary mixer—settlers, τ_{mix} = 1.5 min; 2) for centrifugal extractors τ_{mix} = 0.2 min.

Fig. 5. Dependence of the plutonium and neptunium losses on the number of stages in the reextraction section of the first extractor (L/L_{nom} = 0.8; X_{HNO_3} = 0.2 M): 1), 2) neptunium and plutonium losses for a constant total time of contact in the extractor $N_{re}\,\tau_{mix}$ = 15 min and τ_{mix}: τ_{set} = 1:2; 3) plutonium losses on adding stages with a standard contact time (τ_{mix} = 1.5 min, τ_{set} = 3.0 min).

Mathematical Description of the Process in Each Stage, and Algorithm for Calculating the Distribution of the Microcomponents with respect to the Various Stages of the Extraction Apparatus under Steady-State Conditions

We shall assume that the reextraction process does not amount to a slow chemical reaction, and that its velocity, determined by mass-transfer processes, is fairly high; owing to the smallness of their distribution coefficients, the extractability of Pu(III) and Np(V) may be neglected. We shall consider that the distribution coefficients of Pu(IV) and Np(IV) as microcomponents do not depend on their own concentration but are determined by the concentration of uranium and nitric acid in the aqueous phase.

The mathematical description of the process at the i-th stage comprises the equations of material balance (allowing for the structure of the flows) (a), the equations of extractive equilibrium (b), and the kinetic equations of the redox reactions in the aqueous phase (c). The equations describing the process are exactly the same for both plutonium and neptunium (the only difference lies in the numerical values of the kinetic constants and the distribution coefficients) and take the following form:

for the mixing chamber of the stage

$$\left.\begin{aligned} &\text{a)}\ x_{5,\,i-1} + x_{4,\,i-1} + ny_{i+1} \\ &\quad - \bar{x}_{5,\,i} - \bar{x}_{4,\,i} - n\bar{y}_{4,\,i} = 0; \\ &\text{b)}\ \bar{y}_{4,\,i} = \alpha_i \bar{x}_{4,\,i}; \\ &\text{c)}\ \frac{d\bar{x}_{5,\,i}}{dt} = k_{1,\,i}\bar{x}_{4,\,i} - k_{2,\,i}\bar{x}_{5,\,i}; \end{aligned}\right\} \quad (4)$$

for the settling chamber of the stage

$$\left.\begin{aligned} &\text{a)}\ \bar{x}_{4,\,i} + \bar{x}_{5,\,i} - x_{4,\,i} - x_{5,\,i} = 0; \\ &\text{b)}\ \bar{y}_{4,\,i} = y_{4,i}; \\ &\text{c)}\ \frac{dx_{5,\,i}}{dt} = k_{1,\,i}x_{4,\,i} - k_{2,\,i}x_{5,\,i}, \end{aligned}\right\} \quad (5)$$

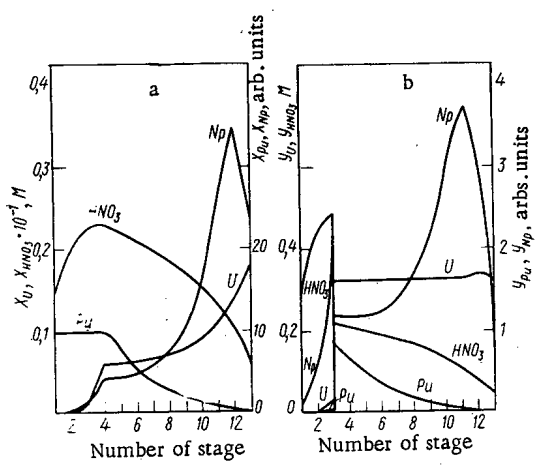

Fig. 6

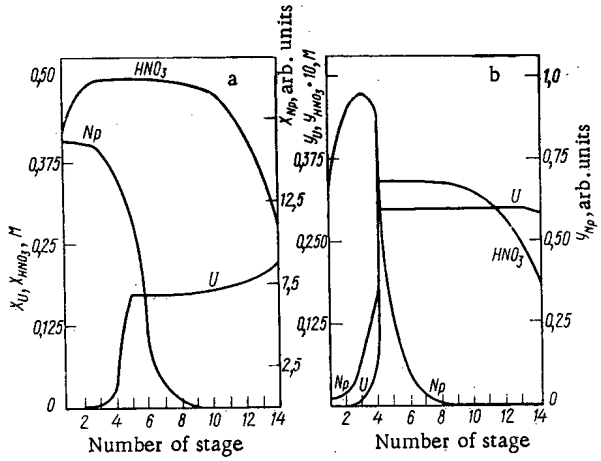

Fig. 7

Fig. 6. Distribution of the components with respect to the stages of the first extractor in the aqueous and organic phases (a and b respectively).

Fig. 7. Distribution of the components with respect to the stages of the second extractor in the aqueous and organic phases (a and b respectively).

where n is the ratio of the flows of the organic and aqueous phases, α is the distribution coefficient of Pu(IV) or Np(IV), x_4 is the concentration of Pu(IV) or Np(IV), x_5 is that of Pu(III) or Np(V) in the aqueous phase, y_4 is the concentration of Pu(IV) or Np(IV) in the organic phase. The index i means that the quantity relates to the yield in the i-th stage; intermediate values (at the outlet of the mixing chamber) are denoted by a stroke over the symbol.

The system (4), (5) reduces to a matrix equation describing the step as a whole:

$$\begin{vmatrix} y_{4,\ i+1} \\ x_{4,\ i} \\ x_{5,\ i} \end{vmatrix} = \begin{vmatrix} A_2/n\alpha_i A_9 & -\frac{1}{n} & (A_6-A_4-1)/nA_9 \\ (A_{10}+(1-A_8)A_6A_2/A_9)/\alpha_i & 0 & A_4(A_8-1)/(A_6-1) \\ (A_7+A_8A_6A_2/A_9)/\alpha_i & 0 & A_8A_4/A_9 \end{vmatrix} \times \begin{vmatrix} y_{4,\ i} \\ x_{4,\ i-1} \\ x_{5,\ i-1} \end{vmatrix} = S_i \begin{vmatrix} y_{4,\ i} \\ x_{4,\ i-1} \\ x_{5,\ i-1} \end{vmatrix}. \tag{6}$$

Here $A_1 = k_{1,i} + k_{2,i}$; $A_2 = 1 + \alpha_i n$; $A_3 = k_{1,i}/A_2 + k_{2,i}$; $A_4 = e^{-A_3\tau_{mix}}$ and $A_5 = e^{-A_1\tau_{set}}$ for the ideal displacement situation; $A_4 = (1 + A_3\tau_{mix})^{-1}$ and $A_5 = (1 + A_1\tau_{set})^{-1}$ for the ideal mixing situation; $A_6 = k_{1,i}(1-A_4)/(k_{1,i} + k_{2,i}A_2)$; $A_7 = k_{1,i}(1-A_5)/A_1$; $A_8 = (k_{2,i}A_5 + k_{1,i})/A_1$; $A_9 = 1-A_6$; $A_{10} = 1-A_7$, where τ_{mix} and τ_{set} are the times spent by the aqueous phase in the mixing and settling chambers of the stage.

For the whole extractor the expression analogous to (6) is

$$\begin{vmatrix} 0 \\ x_{4,\ out} \\ x_{5,\ out} \end{vmatrix} = S_N S_{N-1} \ldots S_{N'+2} \begin{vmatrix} \frac{y_{in} n_0}{n_e} \\ 0 \\ 0 \end{vmatrix} + S_N \ldots S_{N'+2} \begin{vmatrix} \frac{n_{re}}{n_e} & 0 & 0 \\ 0 & 1 & 0 \\ 0 & 0 & 1 \end{vmatrix} S_{N'} \ldots S_1 \begin{vmatrix} y_{4,\ out} \\ 0 \\ 0 \end{vmatrix}, \tag{7}$$

where n_e and n_{re} are the ratios of the flows in the extraction and reextraction sections of the apparatus, n_0 is the ratio of the flow of the reprocessed organic solution to the flow of the aqueous phase, N' is the number of stages in the whole extractor, with due allowance for the fictitious stage of feeding in the solution to be reprocessed, which has the number N' + 1.

In shortened form Eq. (7) appears thus:

$$\begin{vmatrix} 0 \\ x_{4,\ out} \\ x_{5,\ out} \end{vmatrix} = Q + R \begin{vmatrix} y_{out} \\ 0 \\ 0 \end{vmatrix} = \begin{vmatrix} q_1 \\ q_2 \\ q_3 \end{vmatrix} + \begin{vmatrix} r_{11} \\ r_{21} \\ r_{23} \end{vmatrix} y_{out}, \tag{8}$$

whence

$$y_{out} = \frac{-q_1}{r_{11}};\ x_{4,\ out} = q_2 - q_1\frac{r_{21}}{r_{11}};\ x_{5,\ out} = q_3 - q_1\frac{r_{31}}{r_{11}}. \tag{9}$$

Thus the algorithm for calculating the distribution of neptunium and plutonium over the various stages of the apparatus consists of the following: 1) calculation of the distribution of the macrocomponents, namely, uranium and nitric acid (for the methods of calculation see [4], which also gives the equilibrium equations); 2) calculation of the kinetic constants of the reactions by means of Eq. (5) and of the distribution coefficients (see [4]) at each stage; 3) construction of the matrices S_i in accordance with Eq. (6); 4) determination of the matrix R and the column Q in accordance with Eqs. (7) and (8); 5) calculation of the neptunium and plutonium concentrations in the flows of the aqueous and organic phases emerging from the extractor by means of Eq. (9); 6) successive calculation of the neptunium and plutonium concentrations in the two phases at each stage by means of Eq. (6), using the already prepared matrices S_i.

Calculations of the Redox Reextraction Process

Using the Minsk-32 computer we calculated a reextraction system consisting of two extractors (Fig. 1); the reduction and reextraction of plutonium took place in the first extractor, and the oxidation and reextraction of neptunium in the second. The aim of the calculations was to study the influence of the ratio of the flows, the acidity of the aqueous phase, the number of stages, and the time spent in the mixing and settling chambers on the extraction of the valuable components. We also determined the range of conditions for both extractors in which the losses of uranium, plutonium, and neptunium were lowest.

For the first extractor we took $n_0 = 8.0$; $n_e = 1.5$; $n_{re} = n_0 + n_e = 9.5$ as nominal conditions. The original organic solution contained 0.38 M uranium and 0.17 M HNO_3. The concentration of plutonium and neptunium in this solution was taken as unity. Into the preextraction section we fed a 30% solution of tributylphosphate (TBP) in synthine; reextraction was effected with 0.1 M HNO_3 containing 0.04 g-ion/liter Fe(II) with an admixture of 10% Fe(III) (produced by self-oxidation). Into the second reextractor we fed the organic flow from the first reextractor (at 80% of the nominal rating in the latter according to the ratio of the flows), containing 0.32 M uranium, 0.0333 M HNO_3, 0.83444 arbitrary units of Np, and $1.7 \cdot 10^{-4}$ arbitrary units of Pu. The nominal ratios of the flows were $n_0 = 11.875$; $n_e = 1.125$; $n_{re} = 13.0$ The reextracting 0.1 M HNO_3 contained 0.04 g-ion/liter Fe(III).

The ratio of the flows in the two reextractors was varied by varying the flow of the aqueous phase $L[n = n_{nom}/(L/L_{nom})]$.

We see from Fig. 2 that an increase in the ratio of the flow increases the losses of the components from the organic phase (plutonium in the first extractor, neptunium in the second), but reduces the losses from the aqueous phase (neptunium in the first and uranium in the second). Whereas in the first reextractor the uranium concentration in the reextract is no greater than 1.5 mg/liter for any of the operating conditions calculated, in the second reextractor a three-stage preextraction section fails to provide an acceptable (10 mg/liter) degree of purity of the reextract with respect to uranium (Fig. 2, curve 11), and the number of stages must be increased from four to six (Fig. 2, curves 12-14).

Increasing the acidity of the reextraction agent increases the losses of the components from the aqueous phase (Fig. 3); hence it is desirable to conduct the whole process at a low acidity.

The time spent in the stage has a substantial influence on the losses of neptunium and plutonium (Fig. 2), and due allowance for the kinetics of the redox reactions must therefore never be neglected. This may at first glance appear paradoxical, since the velocity constants are high and the relaxation time of the process ($t_0 = 1/k$) should be short (for example, in the case of $X_{HNO_3} = 1$ M and [Fe(II)] = 0.04 g-ion/liter; $k_1^{Pu} = 16.2$ min^{-1} and $t_0 = 1/k_1^{Pu} = 0.06$ min, while $\tau_{mix} = 1.5$ min, i.e., 25 times greater than t_0). However, one characteristic of the process in the two-phase system is a transition of the plutonium (neptunium) to a state of reduction (oxidation) on passing into the aqueous phase from the organic phase, in accordance with its distribution coefficient; the velocity constant then falls by a factor of $(1 + \alpha n)$, while the relaxation time correspondingly increases. This leads to a considerable retardation of the redox processes in the extractive stage by comparison with the same process in the aqueous phase.

The calculations also showed that, despite the occurrence of redox reactions in the mixing and settling chambers, the role of the latter was insignificant owing to the absence of mass transfer in these chambers even for small values of τ_{mix} (Fig. 4).

Influence of the Number of Stages. We found (Fig. 5, curves 1 and 2) that for a constant total time of contact in the apparatus ($N_{re}\tau_{mix} = \text{const}$) it was advantageous to have more stages with a shorter contact time in each. Increasing the number of reextraction stages while preserving their standard dimensions naturally reduces the losses of the components (curve 3).

Structure of the Flows. A comparison between the results of calculations relating to the operating conditions of the process for the case of ideal displacement and ideal mixing (Fig. 2, curves 2 and 10) once again [2] indicates the considerable advantage of using piston-type flow rather than ideal mixing.

The range of acceptable operating conditions is determined by the completeness of the plutonium, neptunium, and uranium separation required. Since many parameters of the process act in contradictory ways on the losses of these components, this range is comparatively narrow. For the first reextractor the best arrangement is that corresponding to 80% nominal (flow ratios $n_0 = 10.0$; $n_e = 1.875$; $n_{re} = 11.875$) with a reextraction-agent acidity of no greater than 0.2 M. Under these conditions the plutonium losses are no greater than 0.05%, and the neptunium losses no greater than 1%. A shift in the direction of lower values of n leads to an increase in the losses of neptunium with the aqueous phase, while higher values of n lead to an increase in the losses of plutonium with the organic flow passing into the second reextractor. (The distribution of the components with respect to the stages in this condition is indicated in Fig. 6.) In order to widen the range of acceptable conditions it is essential to enlarge the reextraction section of the apparatus.

The second reextractor should have at least four stages in the uranium preextraction section, the best working condition being that corresponding to 60% nominal (ratios of the flows $n_0 = 19.8$; $n_e = 1.87$; $n_{re} = 21.7$). For an X_{HNO_3} no greater than 0.5 M the neptunium losses then fall below $1 \cdot 10^{-3}$% and the amount of uranium in the reextract is no greater than 10 mg/liter. (The distribution of the components with respect to the stages in this situation is indicated in Fig. 7.) Increasing the preextraction section to six stages leads to a considerable expansion of the range of acceptable conditions, which is then only restricted by upper limits of $n_0 = 30.0$ and $n_e = 2.8$; the losses of neptunium are no greater than $5 \cdot 10^{-3}$%.

We note that the ratios of the flows corresponding to the nominal operating mode of the first reextractor (as well as values lower than these), together with a reextraction-agent acidity of no greater than 0.2 M, ensure an almost complete transition of the neptunium and plutonium into the aqueous phase in one extractor (the amount of uranium in this section will then lie below ~1 mg/liter). Thus depending on the technological requirements either individual or combined separation of Pu and Np from U may be achieved.

Influence of Temperature. Since the activation energies for the reduction of plutonium and oxidation of neptunium (19.7 and 35.2 kcal/mole respectively [7]) are comparatively high, the velocity constants increase sharply with temperature, i.e., increasing the temperature reduces the losses of plutonium and neptunium, or alternatively reduces the contact time (calculation shows, for example, that on conducting the process in centrifugal extractors, in which τ_{mix} = 5-10 sec, t^0 should be raised to ~ 40°C).

LITERATURE CITED

1. A. M. Rozen et al., Third Geneva Conference, Paper No. 346 (1964).
2. A. M. Rozen et al., in: Liquid Extraction [in Russian], Khimiya, Leningrad (1969), p. 5.
3. A. M. Rozen, Yu. V. Reshet'ko, and M. Ya. Zel'venskii, in: Transactions of the Comecon Symposium on Research in the Reprocessing of Irradiated Fuel, Vol. 1 [in Russian], Czechoslovakian Atomic Energy Commission, Prague (1972), p. 118.
4. A. M. Rozen, Yu. V. Reshet'ko, and M. Ya. Zel'venskii, At. Énerg., 37, No. 3, 187 (1974).
5. T. Newton et al., J. Phys. Chem., 64, 244 (1960).
6. J. Huizenga and L. Magnusson, J. Amer. Chem. Soc., 73, 3902 (1951).
7. V. S. Koltunov, Kinetics of Redox Reactions of Uranium, Neptunium, and Plutonium in Aqueous Solution [in Russian], Atomizdat, Moscow (1965).
8. G. Best, J. Inorg. and Nucl. Chem., 12, 136 (1959).
9. M. Germain, ibid., 32, 245 (1970).

TWO-DIMENSIONAL DIFFUSION PROGRAM HEXAGA II FOR MANY-GROUP CALCULATIONS OF HEXAGONAL LATTICES

T. Apostolov and Z. Woznicki

UDC 621.039.51

The HEXAGA II program uses a uniform triangular difference mesh employed for the calculations for various reactors of basically the water-moderated water-cooled type. The program is written in FORTRAN IV for the systems SYBER-70 and EC-1040. HEXAGA II enables one to solve diffusion equations in the approximation from two to ten groups with allowance for diffusion of neutrons from high to low energy groups. Neutron scattering accompanied by an increase of energy is taken into account when the model is used with two or more thermal groups. The first variant of the program calculated the neutron fluxes at 5000 points of the reactor lattice, and for the subsequent variants this number increases to 10,000 and more.

The many-grouped model of neutron diffusion is a search for a solution of the system of adjoint elliptic second-order partial differential equations

$$-\operatorname{div}\left[D^g \operatorname{grad} \Phi^g\right] + \Sigma^g \Phi^g - \sum_{\substack{g'=1 \\ g' \neq g}}^{G} \Sigma^{g' \to g} \Phi^{g'} = \frac{1}{K} \sum_{g'=1}^{G} F^{g' \to g} \Phi^{g'}, \quad g = 1, 2, \ldots, G \tag{1}$$

(all the notation in (1) is standard and given in [1]).

The extraction cross section for the given group, Σ^g, is represented by the equation

$$\Sigma^g = \Sigma_a^g + \sum_{\substack{g'=1 \\ g' \neq g}}^{G} \Sigma^{g \to g'}.$$

Equation (1) is augmented by the boundary conditions on the surface of the reactor:

$$D^g \frac{\partial \Phi^g}{\partial n} + \alpha^g \Phi^g = 0 \tag{2}$$

(the derivative is along the outer normal to the boundary of the region).

Equations (1) and (2) are solved by the source-iteration method. For the numerical solution of the problem in the group, one uses a finite-difference approximation in the triangular lattice. Thus, finite-difference equations are obtained and these can be represented for each group by a system of linear equations:

$$A\Phi = c, \tag{3}$$

where A is a nondegenerate matrix of coefficients; Φ is the required vector of the solution for the given group; c is the known source vector, whose components take into account the processes of fission and scattering for the given group. For the solution of such linear systems, factorization iterative methods have been developed, for example, the method of Buleev [2], OLIPHANT [3, 4], STONE [5, 6], DUPONT [7], and others. In [8], factorization iterative methods called two-pass iteration methods were developed.

The essence of such a method, used in the HEXAGA II program to solve a system of linear equations [2], is as follows.

Institute of Nuclear Research and Nuclear Energy, Sofia, Bulgaria. Institute of Nuclear Research, Swierk, Poland. Translated from Atomnaya Énergiya, Vol. 38, No. 6, pp. 372-374, June, 1975. Original article submitted February 28, 1974; revision submitted November 12, 1974.

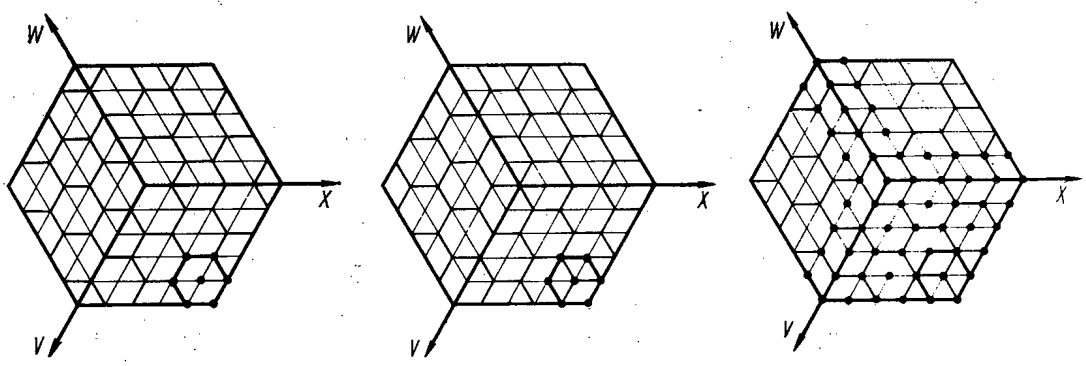

Fig. 1. Different arrangements of the hexagonal lattice relative to the central axis of the reactor.

We represent the matrix A in the form

$$A=K-L-U, \tag{4}$$

where $K = \mathrm{diag}(k_{ii}) \geq 0$ is a diagonal matrix in which $k_{ii} > 0$ for all $1 \leq i \leq n$; $L = (l_{ij}) \geq 0$ is the lower triangular matrix in which $l_{ij} = 0$ for all $i \leq j$; $U = (u_{ij}) \geq 0$ is the upper triangular matrix in which $u_{ij} = 0$ for all $i \geq j$ and

$$k_{ii} \geqslant \sum_{j=1}^{n} (|l_{ij}|+|u_{ij}|)$$

for all $1 \leq i \leq n$, and for at least one i there is a rigorous equation which guarantees nonnegativity of the matrix A and the existence of $A^{-1} \geq 0$.

The matrix A can be represented as

$$A=K-P_A-(L+H)-(U+Q)+P_A+H+Q, \tag{5}$$

where $P_A = \mathrm{diag}(p_{ii}) \geq 0$, in which $p_{ii} \geq 0$ for all $1 \leq i \leq n$; $H = (h_{ij}) \geq 0$ is the lower triangular matrix in which $h_{ij} = 0$ for all $i \leq j$; $Q = (q_{ij}) \geq 0$ is the upper triangular matrix in which $q_{ij} = 0$ for all $i \geq j$.

Further, one assumes

$$K \geqslant P_A \geqslant 0, \tag{6}$$

where $k_{ii} > p_{ii} > 0$ for all $1 \leq i \leq n$. Then

$$D_A=K-P_A \geqslant 0 \tag{7}$$

is a nonnegative diagonal matrix in which $D_A^{-1} \geq 0$ for all $1 \leq i \leq n$.

After transformations, we obtain

$$A=D_A-(L+H)-(U+Q)+P_A+H+Q. \tag{8}$$

In what follows, we use the equation

$$\begin{aligned} &D_A-(L+H)-(U+Q) \\ &=[I-(L+H)D_A^{-1}]D_A[I-D_A^{-1}(U+Q)] \\ &\quad -(L+H)D_A^{-1}(U+Q). \end{aligned} \tag{9}$$

The nonnegative matrix $(L + H) D_A^{-1} (U + Q)$ can be expressed by the sum

$$(L+H)D_A^{-1}(U+Q)=R_1+T_A+H_1+Q_1,$$

where $R_1 = \mathrm{diag}[(L + H) D_A^{-1} (U + Q)]$.

If we choose matrices P_A, H, and Q such that $P_A = R_1$, $H = H_1$, and $Q = Q_1$, then

$$A=M_A-N_A, \tag{10}$$

where $M_A = [I-(L + H) D_A^{-1}] D_A[I-D_A^{-1}(U + Q)]$ and $N_A = T_A$, and

$$M_A^{-1} \geqslant 0 \text{ and } N_A \geqslant 0.$$

It is known from Varga's theorem [9] that the iteration matrix

$$\mathcal{A}_1 = M_A^{-1} N_A$$

has spectral radius $\rho(M_A^{-1}N_A) < 1$ and the iterative method

$$\Phi^{j+1} = M_A^{-1} N_A \Phi^j + M_A^{-1} c, \quad j \geqslant 0 \tag{11}$$

(where j is the number of the iteration) converges for the solution of a system of linear equations for all vectors $\Phi^{(0)}$.

In the practical use of the two-pass iteration methods one uses recursive formulas for some auxiliary vector β, after whose calculation the vector $\Phi^{(j+1)}$ is determined.

In our case the vector $\Phi^{(j+1)}$ is expressed in the form

$$\begin{aligned} \Phi^{(j+1)} = {} & [I - D_A^{-1}(U + Q)]^{-1} D_A^{-1} \\ & \times [I - (L + H) D_A^{-1}]^{-1} T_A \Phi^{(j)} \\ & + [I - D_A^{-1}(U + Q)]^{-1} D_A^{-1} [I - (L + H) D_A^{-1}]^{-1} c, \end{aligned} \tag{12}$$

where $j \geq 0$.

After multiplication of (12) by the matrix $[I - D_A^{-1}(U + Q)]$, we obtain

$$\Phi^{(j+1)} = D_A^{-1} \{(U + Q) \Phi^{j+1} + [I - (L + H) D_A^{-1}]^{-1} (T_A \Phi^{(j)} + c)\}. \tag{13}$$

We introduce the vector $\beta^{(j+1)}$:

$$\beta^{(j+1)} = [I - (L + H) D_A^{-1}]^{-1} (T_A \Phi^{(j)} + c). \tag{14}$$

After multiplication of (14) by the matrix $[I - (L + H) D_A^{-1}]$, we obtain

$$\begin{aligned} \beta^{(j+1)} &= (L + H) D_A^{-1} \beta^{(j+1)} + T_A \Phi^{(j)} + c; \\ \Phi^{(j+1)} &= D_A^{-1} [(U + Q) \Phi^{(j+1)} + \beta^{(j+1)}]. \end{aligned} \tag{15}$$

This approach is none other than the elimination method of Gauss and is equivalent in this case to the sweep method for three-diagonal matrices. To accelerate the convergence, the method of upper relaxation can be used.

In [8] this method is compared with the Gauss—Seidel method and it is shown that

$$0 < \rho(\mathcal{A}_1) < \rho(L_1) < 1, \tag{16}$$

where L_1 is the iteration matrix in the Gauss—Seidel method:

$$L_1 = (I - K^{-1})^{-1} K^{-1} U. \tag{17}$$

In the determination of the region of the solution in the program it is borne in mind that the majority of reactors with hexagonal lattice of the core have angular symmetry (every 120°). Such an approach is used in reactors of the water-moderated water-cooled type. Figure 1 shows three arrangements of the hexagonal lattice relative to the central axis of the reactor. The neutron fluxes at arbitrary but symmetric points in the regions I, II, and III also have the same values. Thus, to describe the lattice one need consider only one of the regions and it is not necessary to determine the logarithmic boundary conditions on the axes X and V, whose values are obtained from the symmetry condition. It is only necessary to determine the logarithmic conditions on the boundaries parallel to the X and V axes lying within the core, on its boundary or outside it. One also considers a variant using logarithmic conditions on four boundaries of the region (Figs. 2 and 3).

In one of the program variants, the regions may have the form of a parallelogram (see Fig. 2; such a form of the region is used in the program PDQ-7); in others, they can have the form of a hexagon (see Fig. 3), which simplifies the problem and makes the use of programs convenient.

Besides the described lattice form, one also considers a combined configuration of hexagonal and oblique-angled polygons, and also a combined configuration of hexagonal lattices and lattices with (r, θ) geometry. The combination of such lattices enables one to represent more accurately the actual geometry and the material properties of the reactor lattice. However, the programming of the problem is then much more complicated.

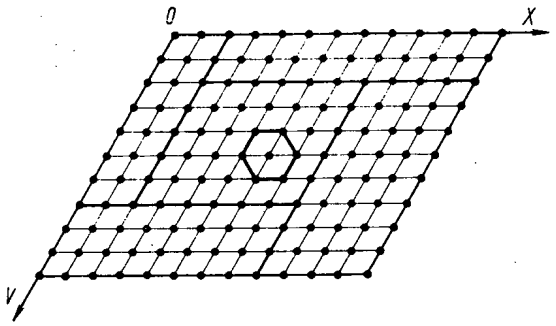

Fig. 2. Regions of the reactor having the the form of a parallelogram.

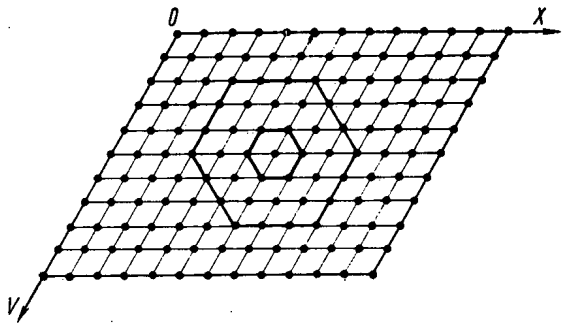

Fig. 3. Hexagonal form of reactor regions.

Two-pass iterative methods were used in the two-dimensional programs EWA II [4, 6] and AGA II to make a calculation for reactors with rectangular lattice on the GIER computer. The results show that the rate of convergence of these methods is 5-10 times faster than methods based on the Gauss–Seidel computational model.

It is to be expected that the use of two-pass iteration methods of solution of the diffusion equations for a hexagonal lattice will increase the rate of convergence compared with the case of a rectangular lattice. However, to confirm this conjecture concrete results are necessary; these are expected very shortly.

It should be pointed out that the number of arithmetic operations for one point in one group and one iteration when one uses the two-pass method and the method of upper relaxation (of the HEXAGA II program) exceeds ten operations of multiplication and ten operations of addition. When the Gauss–Seidel method is used, there are eight operations of multiplication and eight of addition.

It is assumed that if a two-dimensional program is used for cylindrical and flat (y, z) geometry (30 groups and 4000 points), it will be possible to calculate the group geometric parameters B_Z^2 needed for HEXAGA II. The algorithm EWA II is based on the modified two-pass iteration method. The program is written in FORTRAN IV for the IBM-360/40 computer.

LITERATURE CITED

1. G. Habettler and M. Martino, in: Proc. Symp. on Appl. Math., Amer. Math. Soc., Providence, Rhode Island, 11, 127 (1961).
2. N. Buleev, Matem. Sb., 51, 227 (1960).
3. T. Oliphant, Quart. Appl. Math., 20, 257 (1962).
4. T. Oliphant, ibid., 19, 221 (1961).
5. H. Stone, Trans. Amer. Nucl. Soc., 13, 180 (1970).
6. H. Stone, SIAM J. Number. Anal., 5, 530 (1968).
7. T. Dupont, ibid., 753.
8. Z. Woznicki, Doctoral Dissertation, Computing Center CYFRONET, Institute of Nuclear Research, Swierk (1973).
9. R. Varga, Matrix Iterative Analysis, Prentice Hall (1962).

INVESTIGATION OF THE ADIABATIC OUTFLOW OF WATER THROUGH CYLINDRICAL CHANNELS

V. S. Aleshin, Yu. A. Kalaida, and V. V. Fisenko

UDC 621.039.001.5

Partial evaporation of the fluid along the channel length occurs during the outflow of saturated and underheated water with high initial parameters through a cylindrical channel with pointed entrance edges, and the stream is two-phasal at the exit from the channel. A large number of papers, including the surveys [1, 2], is devoted to the investigation of the adiabatic flow of saturated water. However, up to now there have been no reliable methods of estimating the weight discharge for a broad range of initial parameters and the total picture of the flow of evaporating water in cylindrical channels has been studied inadequately. This is explained by the complexity of the heat and mass exchange processes between the liquid and vapor phases flowing in the channel and by the influence of various factors (the initial parameters, the l/d ratio, where l is the channel length and d is its diameter, the counter-pressure at the exit, etc.) on the outflow processes.

The results of investigating the outflow of hot water through cylindrical channels of 5 and 9.53 mm diameter with pointed entrance edges and an l/d ratio between 0.5 and 18 are examined in this paper as the pressure p_1 changes ahead of the outflow channel between 25 and 150 kg/cm^2 and the water underheating Δt_s is 0-100°C up to saturation.

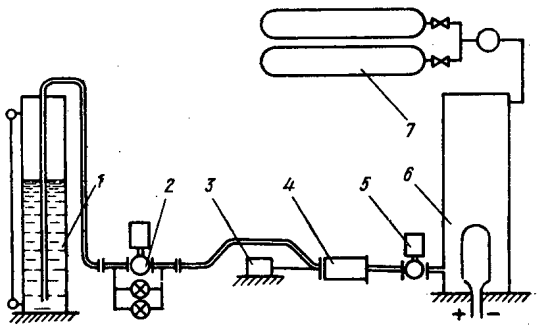

Fig. 1

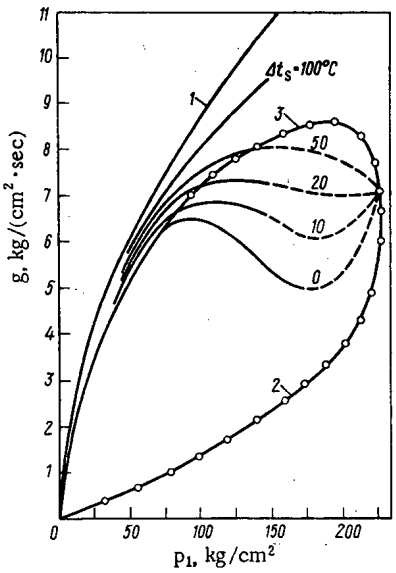

Fig. 2

Fig. 1. Schematic diagram of the apparatus: 1) disposal section; 2) valves to produce counterpressure; 3) probe; 4) outflow valve; 5) quick-shutoff valve; 6) hot-water chamber; 7) high-pressure air system.

Fig. 2. Dependence of the stream discharge on the initial pressure for different Δt_s (d = 5 mm, l/d = 0.5): 1) discharge of cold water at t = 18°C; 2) rated discharge of dry saturated vapor; 3) rated discharge of saturated water (x = 0).

Atomnaya Énergiya, Vol. 38, No. 6, pp. 375-378, June, 1975. Original article submitted April 30, 1974.

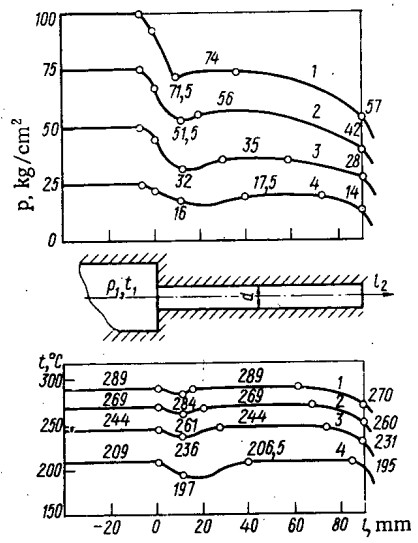

Fig. 3

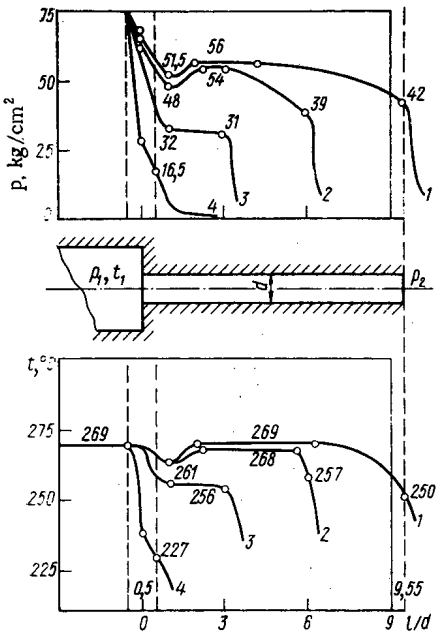

Fig. 4

Fig. 3. Change in medium parameters (p and t) along the channel length for d = 9.53 mm, l/d = 9.55, Δt_s = 20°C for different initial pressures p_1, kg/cm²: 1) 100; 2) 75; 3) 50; 4) 25.

Fig. 4. Change in parameters of the medium (p and t) along the channel length for p_1 = 75 kg/cm², Δt_s = 20°C, d = 9.53 mm for different l/d: 1) l/d = 9.55; 2) l/d = 6; 3) l/d = 3; 4) l/d = 0.5.

The experimental apparatus (Fig. 1) consists of a 350 liter (hot water) chamber to obtain hot water at pressures to 150 kg/cm² and a temperature to 350°C; an outflow section of telescope type, which permits altering the working channel without disassembly of the apparatus; a tank for disposal of the outflowing medium through a throttling unit under a layer of water; a high-pressure air system to maintain a given pressure ahead of the outflow section and to assure its constancy during the outflow process.

The hot water chamber was filled with water purified in special filters, and the water was deaerated before each test. The cold water hydraulic characteristics were recorded for each of the channels before the tests.

The error in measuring the temperature and pressure in the hot water chamber, at the entrance to the outflow channel, and at its exit was no higher than ±5%.

The stream static pressure and temperature along the outflow channel length were measured by using a probe. The impulse hole to determine the pressure and the microthermocouple imbedded in the probe permitted a record of both the continuous diagram along the channel length, and the parameters at fixed points.

The discharge of the outflowing medium was measured with a flowmeter with a continuous recorder tape, which is important in investigations of the critical flow modes.

Weight Discharge of Water. To determine the influence of the initial pressure p_1, the degree of underheating of the water below boiling Δt_s, and the l/d ratio on the weight discharge characteristics, a series of tests was conducted in which only one of the factors listed above was altered while the other conditions remained equal. Presented in Fig. 2 is a graph of the dependence of the ratio between the weight discharge and the channel cross-sectional area on the pressure ahead of the entrance to the outflow section for a channel with l/d = 0.5 (the dashes show the assumed weight discharge at an initial pressure above 150 kg/cm²). It follows from Fig. 2 that the experimental discharge characteristics almost agree with the hydraulic characteristics up to a 70-75 kg/cm² pressure for any degree of underheating. The vapor formation in the stream becomes so intense at pressures above 75 kg/cm² and a 0-50°C degree of underheating that the presence of the vapor phase noticeably diminishes the stream density and reduces the weight discharge.

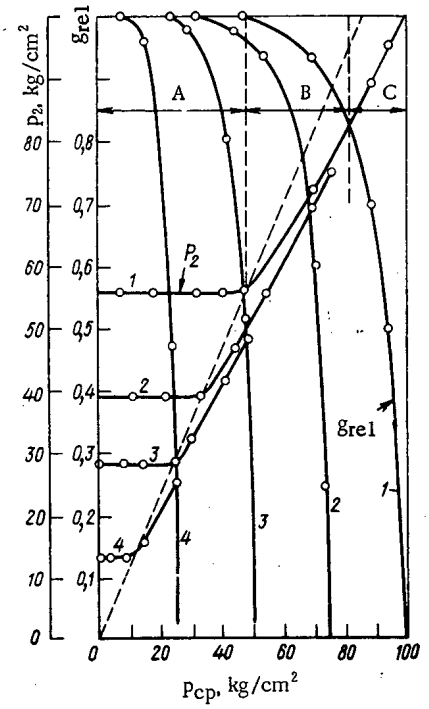

Fig. 5

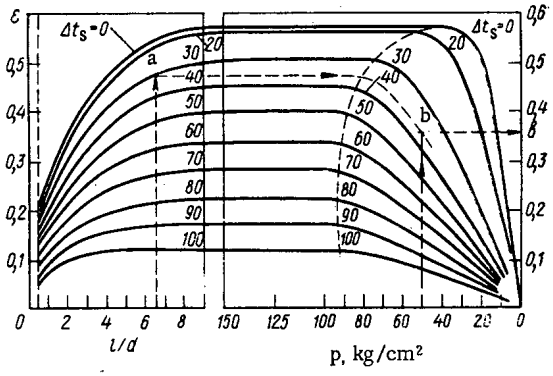

Fig. 6

Fig. 5. Dependence of g_{rel} and p_2 on the counterpressure p_{cp} for d = 6.4 mm, l/d = 7.26, Δt_s = 20°C and different p_1, kg/cm²: 1) 100; 2) 75; 3) 50; 4) 25.

Fig. 6. Dependence of $\varepsilon = p_2/p_1$ on l/d, Δt_s, and p_1.

Analogous graphs have been obtained for weight discharges for other l/d ratios(0.5; 2.0; 3.0; 4.0; 5.0; 6.0; 9.0; 18.0). It follows from the graphs that a deviation of the experimental from the hydraulic curves sets in at a lower pressure as l/d increases. Thus, for $l/d > 6$-8 the diminution in discharge starts at $p \approx 25$ kg/cm² as compared with the hydraulic value.

Pressure and Temperature Distribution. The temperature and pressure along the channel axis were measured by displacement of a probe. The investigations were carried out in 9.53 mm channels for an l/d between 0.5 and 9.55. More than 100 combined diagrams were obtained. Some are presented in Figs. 3 and 4. Analysis of the test curves shows that three characteristic sections are formed along the channel length in channels with $l/d > 6$-8. An abrupt pressure drop below the saturation pressure corresponding to the initial temperature is observed in the first section in the area of the entrance edge, and intensive vapor formation occurs, whereupon the temperature of the medium drops. A certain lag in the temperature drop as compared with the pressure reduction as the water moves (particularly for saturated water) indicates its possible overheating and a metastability of the process in progress. Then the velocity of the stream motion diminishes as the stream broadens beyong the leading edge, the pressure rises and the process of vapor condensation is observed, as the rise in stream temperature indicates.

The nature of the pressure drop depends on the initial temperature. The higher the stream temperature, the smaller the fraction of the pressure drop at the entrance section and the greater the fraction at the exit of the channel.

Let us note that the phenomenon of a sharp pressure drop and its subsequent rise at the leading edge has not been observed in researches performed earlier either because of the low initial parameters (a pressure less than 25 kg/cm²) or of the absence of a continuous record of the pressure and temperature along the channel length.

Depending on the initial values of p_1 and t_1, either a recovered hydraulic stream of saturated water at a temperature corresponding to the initial temperature (for $\Delta t_s > 20$°C) or a two-phase stabilized stream with a temperature somewhat lower than the initial value (for $\Delta t_s < 20$°C) flows in the second section, the section of stabilized parameters. As the underheating is reduced, the vapor content increases in the stream and reaches a maximum at the outflow of the saturated water. The lower the initial water temperature, the closer will the stabilized parameters section be to the exit section. The vapor formation

process starts again in the third section of the channel as the stream approaches the exit edge; the stream temperature also drops as the pressure drops. The pressure drops to p_2 in the exit section, a value greater than atmospheric and dependent on the initial parameters. Thus, for example, as p_1 rises from 25 to 100 kg/cm^2 at Δt_s = 20°C the pressure p_2 grows from 14 to 57 kg/cm^2, and the pressure ratio $\varepsilon = p_2/p_1$ remains practically constant. A steady, equilibrium two-phase stream for which $\varepsilon \approx 0.55$ flows out of the channel. As the underheating increases because of the diminution in the vapor phase content in the stream, the quantity ε drops. Thus, for Δt_s = 59°C, ε is reduced to 0.334.

Shown in Fig. 4 is the nature of the change in the stream p and t along the channel length as a function of l/d for saturated water flowing out at an initial pressure of 75 kg/cm^2. The nature of the process in long channels with $l/d > 6$-8 is described above. Diminution in the channel length is accompanied by the growth in metastability of the stream, by a rise in its density, and by an increase in the weight discharge. Thus, for l/d = 0.5 the stream turns out to be overheated 45°C in the exit section. The pressure at the exit from the channel drops more sharply in short channels. It is characteristic that there may be a section with stabilized parameters even in short channels with l/d = 3.0.

It also follows from Fig. 4 that the pressure drop along the channel length is accompanied by an abrupt reduction in temperature, and therefore, by a continuous vapor formation process.

Investigation of the Critical Modes. A series of tests was conducted in channels of 6.4 mm diameter with l/d = 0.5-7.26 and Δt_s = 0-100°C to investigate the critical flow modes of boiling water. The initial pressure varied between 25 and 150 kg/cm^2. Processing the test results permitted construction of dependences of the relative discharge $g_{rel} = g_{cp}/g_0$ (g_0 is the discharge for a stream outflow into the atmosphere, and g_{cp} is the discharge at a variable counterpressure p_{cp}) and of the pressure p_2 at the exit section on the counterpressure. One of the graphs is presented in Fig. 5. It follows therefrom that the passage over to the critical mode occurs more smoothly as boiling water flows out, the pressure at the exit edge p_2 tends to some constant value for a continuously diminishing counterpressure p_{cp}. The time of the onset of the flow crisis agrees with the time of build-up of a constant pressure in the exit section of the channel (the beginning of the critical flow mode is shown by dashes). This indicates that the critical channel section coincides with the exit, and the steady pressure ratio p_2/p_1 is critical.

The dependences $p_2 = f(p_{cp})$ and $g_{rel} = f(p_{cp})$ obtained permit establishment of three characteristic boiling water flow domains in the channel (the domain boundaries are shown for an initial pressure of p_1 = 100 kg/cm^2).

1. The critical mode domain (A). The weight discharge is a maximum in this domain and is independent of the counterpressure.
2. The near-critical domain (B). As the counterpressure increases in this domain the pressure in the exit section rises monotonely, remaining greater than p_{cp}. The discharge decreases insignificantly.
3. The third domain (C) is provisionally called the domain of the pseudohydraulic flow mode. It sets in at the time the pressure in the exit section equals the counterpressure and is retained down to total equalization of the pressure ($p_{cp} = p_1$). The discharge decreases sharply in this domain and is zero for $p_{cp} = p_1$.

Tests conducted with unchanged p_1 = 75 kg/cm^2 and Δt_s = 0-100°C showed that the crisis in the discharge sets in at lower counterpressures as Δt_s increases, i.e., $\varepsilon = p_2/p_1$ diminishes.

Processing the numerous experimental results permits construction of a nomogram (Fig. 6) of the dependence of ε on the initial pressure, the degree of underheating of the water to the saturation state, and the relative channel length. The dashes show the sequence in determining ε for a given l/d ratio and initial Δt_s and p_1.

The following dependences can be recommended to determine the specific weight discharges by generalizing the test results.

1) For $l/d > 0$, $\Delta t_s < 20$°C in the exit section, a critical pressure ratio is established as for dry saturated vapor ($\varepsilon_{cr} \approx 0.55$). In this case

$$g = 4.43 \cdot 10^{-2} \sqrt{\frac{p_1 (1 - \varepsilon_{cr})}{v_{mix}}} \text{ kg/cm}^2 \cdot \text{sec}.$$

Here $v_{mix} = xv_2'' + (1-x)v_2'$, where v_{mix} is the specific mixture volume, v_2'', v_2' are the specific volumes of the vapor and water in the exit section, taken for p_2 on the saturation line, and x is the vapor content in the exit section. The value of x is determined by the expression $x = s_1' - s_2'/s_2'' - s_2'$, where s_1', s_2' are the water entropy at the entrance to and exit from the channel, respectively, and s_2'' is the vapor entropy at the exit from the channel.

2) In all the remaining cases when $\varepsilon = p_2/p_1$ and does not reach the ratio ε_{cr} for dry saturated vapor in the channel exit section, it is possible to start from the assumption that a metastable stream of overheated fluid with a vapor formation process is incomplete in the channel. The design formula is

$$g = 4.43 \cdot 10^{-2} \mu_h \sqrt{\frac{p_1 (1-\varepsilon)}{v_1'}},$$

where μ_h is the hydraulic discharge coefficient, v_1' is the specific volume of saturated water taken at the initial temperature t_1. When using the dependence proposed, the value of ε should be determined from the nomogram in Fig. 6 for the initial parameters (l/d, Δt_s, p_1).

Comparison between the magnitudes of the discharges computed by the dependences proposed and the test results shows satisfactory agreement. The error does not exceed 10% in the domain of the parameters investigated.

LITERATURE CITED

1. G. B. Wallace, Simultaneous Two-Phase Flows [Russian translation], Mir, Moscow (1972).
2. H. Fauske, ANP-6633 (1962).

OXIDATION OF TRITIUM IN AIR UNDER THE ACTION OF INTRINSIC RADIATION

L. F. Belovodskii, V. K. Gaevoi,
V. I. Grishmanovskii, and N. V. Nefedov

UDC 546.11.02.3

To solve certain technological problems and predict the radiation surroundings when tritium is used, it is necessary to estimate the possibility of its oxidation in a definite time interval. This is due to the fact that the biological toxicity, the diffusion, sorption, and elution constants, and other principles of the behavior of free tritium and its oxide (HTO, T_2O) in the gas phase are different [1-3].

Under normal conditions in the presence of oxygen and moisture, the conversion of tritium to the oxide is due to reactions of radiation oxidation

$$T_2 + O_2 \rightarrow T_2O \quad (1)$$

and isotopic exchange

$$T_2 + H_2O \rightarrow HTO + HT. \quad (2)$$

The kinetics of the oxidation of tritium in a mixture with protium (H) at 25 ± 2°C was investigated in [4]. It was established that at a tritium concentration of 100-300 Ci/liter, ratio of protium to tritium 0.07-5.00, and ratio of oxygen to hydrogen isotopes 0.27-0.38, the initial rate of the reaction [d(HTO)/dt] is proportional to the concentration C_T and is determined by the function

$$\frac{d(HTO)}{dt} = KC_T(1 + bm_H) \quad (3)$$

where $K = 1.19 \cdot 10^{-4}$ min^{-1} is the rate constant of the reaction; b = 0.3 is a correction for the isotopic effect; m_H is the mole fraction of protium in the hydrogen mixture.

The rate of isotopic exchange of tritium with water vapor (H_2O) in an atmosphere of helium at a tritium concentration of 0.05-0.70 Ci/liter and a temperature 22 ± 2°C was investigated in [5] and described by the equation

TABLE 1. Characteristics and Results of Investigations

Investigated system	Concentration, Ci/liter	Time of exposure, days	Yield of HTO during exposure, %	No. of analyses during the period of exposure	Periodicity of analyses, days	Yield of HTO after seven days, %
Tritium–dry air –water vapors (air humidity 50%)	$6,3 \cdot 10^{-4}$	120	0,30±0,03	3	60; 90; 120	—
	$4,6 \cdot 10^{-3}$	120	0,47±0,05	3	60; 90; 120	—
	$1,7 \cdot 10^{-1}$	60	0,60±0,03	4	7; 14; 30; 60	0,10±0,01
	2,3	30	17,60±0,80	4	7; 14; 20; 30	3,90±0,40
	14	15	16,90±0,40	5	1; 4; 7; 11; 15	11,05±0,50
	100	0,21	0,58±0,05	2	0,042; 0,21	—
	120	7	17,30±0,20	3	1; 3; 7	17,30±0,20
	460	7	27,00±0,30	3	1; 3; 7	27,00±0,30
	600	0,21	0,87±0,10	2	0,042; 0,21	—
Tritium–argon –oxygen (20%)	$9,0 \cdot 10^{-2}$	56	0,65±0,06	4	1; 11; 22; 56	—
	$2,0 \cdot 10^{-1}$	56	0,81±0,05	4	1; 11; 22; 56	—
	7,4	14	15,10±0,50	4	1; 4; 7; 14	9,50±1,00
	19,6	28	43,30±5,70	5	1; 4; 7; 14; 28	9,60±0,80
	90	28	60,10±1,00	5	1; 4; 7; 14; 28	19,90±1,40

Translated from Atomnaya Énergiya, Vol. 38, No. 6, pp. 379-381, June, 1975. Original article submitted September 17, 1974.

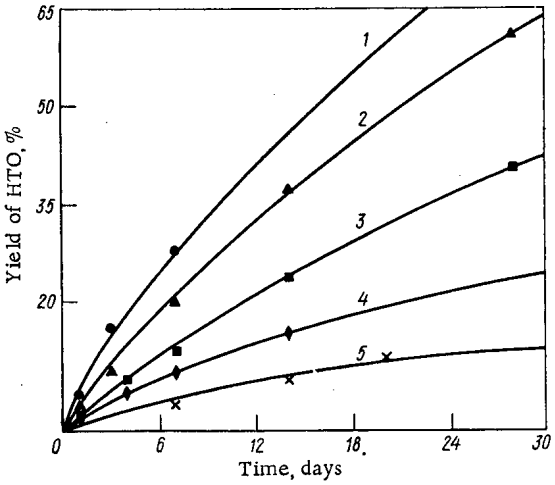

Fig. 1

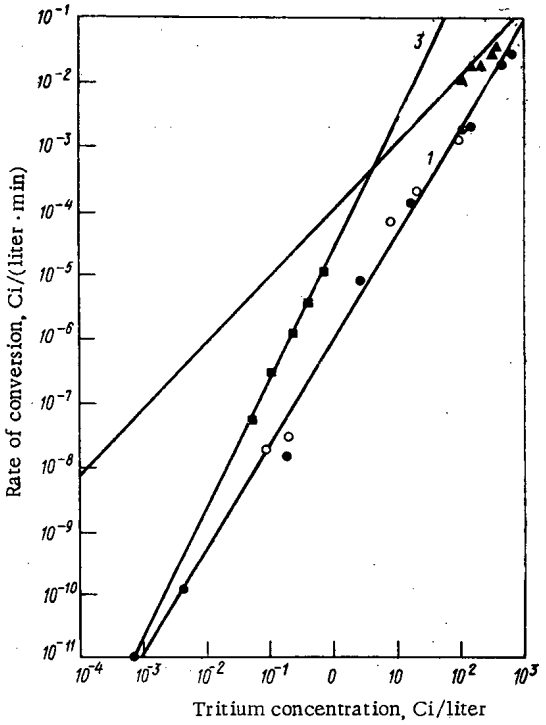

Fig. 2

Fig. 1. Dependence of the yield of HTO on the time in air (1, 5) and argon (2, 3, 4) media at various tritium concentrations (Ci/liter): 1) 460; 2) 90; 3) 19.6; 4) 7.4; 5) 2.3.

Fig. 2. Dependence of the rate of conversion of tritium to HTO on the tritium concentration: 1) experimental curve [● air; ○ argon]; 2) curves constructed according to the data of [4, 5].

$$\frac{d\,(\mathrm{HTO})}{dt} = K_1 C_T^2, \tag{4}$$

where $K_1 = 3.6 \cdot 10^{-5}$ liter/(mCi·day) [$2.5 \cdot 10^{-5}$ liter/(Ci·min)] is the rate constant of isotopic exchange. The reaction rate remains constant within the limits of water vapor densities 5.0-17.5 mg/liter; however, it drops appreciably in the presence of nitric oxide and hydrogen in the gas mixture.

We should assume that in air where oxygen and moisture are present, reactions (1) and (2) proceed simultaneously. Then the conversion of tritium to the oxide can be described by the equation

$$\frac{d\,(\mathrm{HTO})}{dt} = 1.19 \cdot 10^{-4} C_T + 2.5 \cdot 10^{-5} C_T^2. \tag{5}$$

As can be seen from this equation, when $C_T < 5$ Ci/liter, the conversion of tritium to HTO is determined by oxidation, while at $C_T > 5$ Ci/liter it is determined by isotopic exchange. However, it is suggested in [2] that in air the conversion of tritium to HTO is expressed by the function

$$\frac{d\,(\mathrm{HTO})}{dt} = (\alpha + \beta) \cdot C_T^2, \tag{6}$$

where $\alpha = 0.0062$ cm^3/mCi·h [$1.05 \cdot 10^{-4}$ liter/(Ci·min)] is the oxidation constant; $\beta = 0.0167$ cm^3/(mCi·h) [$2.80 \cdot 10^{-4}$ liter/(Ci·min)] is the isotopic exchange constant.

According to (6), oxidation and exchange are proportional to C_T^2. In this case the rate of exchange is 2.8 times as high as the rate of oxidation, which contradicts the data of [4] and function (5). Evidently the kinetics of the conversion of tritium to HTO depends substantially on the concentration of the reacting components, the composition of the gas phase, the temperature, the presence of catalysts, etc.

Since the literature data on the rates of reactions (1) and (2) have been obtained for comparatively narrow and different ranges of tritium concentrations, and gas mixtures of different compositions, by different methods, their contradictions, as well as the impossibility of using the principles obtained in the consideration of such multicomponent gas mixtures as air are quite explicable.

In this work we studied the kinetics of the conversion of tritium to HTO in air medium (the system tritium—dry air—water vapor was investigated), which is of the greatest interest, in a broad range of initial tritium concentrations, also covering the concentrations from [4, 5]. In addition, an attempt was made to evaluate the contribution of reaction (1) to the net effect of the conversion of tritium to HTO, for which purpose we also investigated the system tritium—argon—oxygen.

A glass vacuum system, consisting of a six-liter cylinder for the preparation of the gas mixture, combs with standard ground joints for the connection of the reaction vessels, systems of purification of the gases before their admission to the cylinder, and a system of evacuation and pressure control were used. The reaction vessel was a calibrated spherical flask with a volume of 0.1-0.2 liter with a cylindrical branch for the freezing-out of water and an angle stopcock with standard ground joint for connection to the comb (cylinder). Gaseous tritium (according to International Radiological Technical Specification 6-02-356-66), supplied in V/O "Izotop" glass ampoules, was used in the experiments. The tritium was transferred to the cylinder through two traps, cooled with liquid nitrogen, for drying. Air was admitted to the cylinder from the room and freed of aerosols with a filter of FPP-15 cloth, and of moisture with NaA zeolite. Grade pure argon and medicinal grade oxygen were used; the gases were purified in columns with phosphoric anhydride. The necessary amount of moisture was measured out into the cylinder by evaporating preliminary degasified distilled water.

Before preparation of the mixture, the vacuum system with flask connected (10 per filling) was degasified, washed two to three times with argon, and evacuated to $\sim 10^{-3}$ torr. The mixture was passed from the cylinder into reaction flasks, which after filling were disconnected from the system and placed for exposure for a definite time. For each of the investigated concentrations 20-30 flasks were filled (four to six at each exposure).

After the exposure, tritium and HTO in the flasks were measured separately. Part of the samples ("control") were analyzed immediately after filling. The separation of HTO from tritium was performed by absorption of HTO with distilled water, introduced into the flask. The amount of HTO formed was determined on a setup with a URB-1 ("Medik") liquid scintillator, which was calibrated with standard HTO with an error of ±10%. The amount of tritium in the flask was measured with an ionization chamber, calibrated according to tritium with a MV-2302 mass spectrometer [6]; the current in the chamber was measured with an M-95 microammeter with accuracy class 1.0.

At a tritium concentration of up to 10^{-1} Ci/liter, reaction flasks with a volume of 1.0 liter were used, while the tritium concentration was measured with a 5.0 liter ionization chamber with a direct current amplifier of the SP-1 type.

All the experiments were conducted at a temperature of 25 ± 3°C; the pressure of the gas mixture in the flasks was 600-700 torr (see Table 1).

The yield of HTO in percent of the total amount of tritium for a given time of exposure was determined according to the results of the analysis of tritium and HTO (Fig. 1). The rate of conversion of tritium to HTO was determined according to the initial portions of the kinetic curves. The dependence of the initial reaction rate on the tritium concentration is presented in Fig. 2, where curves constructed according to the data of [4, 5] are given for comparison.

An analysis of the experimental data (see Fig. 2) according to the method of least squares showed that the conversion of tritium to HTO, both in an air medium and in an atmosphere of argon, is determined by the function

$$\frac{d\,(\mathrm{HTO})}{dt} = 10^{-6} \cdot C_{\mathrm{T}}^{5/3} \quad \text{Ci/liter} \cdot \text{min}. \tag{7}$$

Since the rates of conversion of tritium and HTO are the same both in moist air and in dry argon, it can be assumed that the determining process of the conversion is radiation oxidation. As can be seen from a comparison of the literature and experimental data (see Fig. 2), for an air medium estimation of the rate of conversion according to functions (5) and (6) gives substantially elevated yields of HTO in the entire range of investigated tritium concentrations. This confirms the necessity of studying the tritium-containing gas systems used in each concrete case in resolving the question of the amount of conversion of tritium to HTO.

LITERATURE CITED

1. D. Jacobs, Re. USAEC, TID-24635 (1968).
2. O. Coffin, Health Phys., No. 10, 1083 (1967). [Cited according to Atomnaya Tekhnika za Rubezhom, No. 7, 40 (1968).]
3. G. Krebs, Radiation Hazard Resulting from Tritium Diffusion in Glove Box Operations, Los Alamos, New Mexico, Los Alamos Scientific Laboratory, University of California (1963).
4. J. Dorfman and B. Hemmer, J. Phys. Chem., 22, No. 9, 1555 (1954).
5. J. Yang, and L. Gevantman, ibid., 68, No. 1, 3115 (1964).
6. L. F. Belovodskii, V. K. Gaevoi, and V. I. Grishmanovskii, Pribory i Tekhnika Éksperimenta, No. 4, 89 (1971).

EXPERIMENTS ON THE SYNTHESIS OF NEUTRON-DEFICIENT ISOTOPES OF KURCHATOVIUM IN REACTIONS WITH ACCELERATED ^{50}Ti IONS

Yu. Ts. Oganesyan, A. G. Demin,
A. S. Il'inov, S. P. Tret'yakova,
A. A. Pleve, Yu. É. Penionzhkevich,
M. P. Ivanov, and Yu. P. Tret'yakov

UDC 539.1

During the last 20 years, 22 isotopes of heavy elements with atomic numbers Z = 102, 103, 104, and 105 have been synthesized in various laboratories [1]. From an analysis of the radioactive properties of the nuclei obtained, it follows that with increasing atomic number the lifetime of the nuclei with respect to α decay and spontaneous fission decreases.

For even—even isotopes with Z ≥ 102, just as for neutron-deficient and neutron-excess nuclei of Fermium, the basic type of decay is spontaneous fission. The lifetimes of the nuclei with respect to spontaneous fission, as can be seen from Fig. 1, depend substantially on the nucleon composition of the nuclei. The longest lifetime corresponds to a number of neutrons N = 152 and varies greatly with increasing

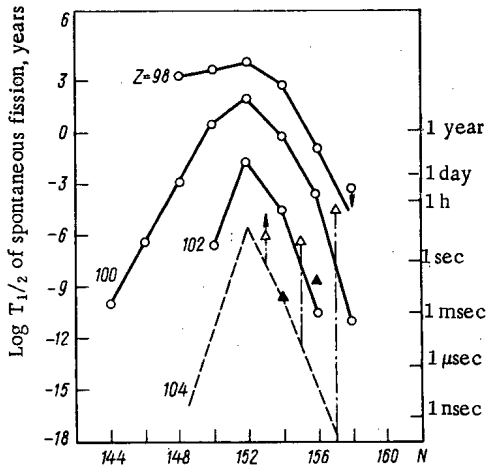

Fig. 1

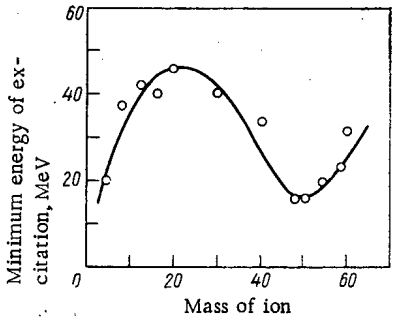

Fig. 2

Fig. 1. Systematics of the periods of spontaneous fission of elements with Z = 98, 100, 102, and 104. ○) Experimental values of the periods of spontaneous fission of even isotopes; ▲, △) known even and odd isotopes of kurchatovium, respectively; ---) extrapolation according to the data of Ghiorso et al. [6, 11] for kurchatovium isotopes.

Fig. 2. Dependence of the minimum energy of excitation of the compound nucleus ^{258}Cu, formed in various target-particle combinations, on the mass of the bombarding ion.

Translated from Atomnaya Énergiya, Vol. 38, No. 6, pp. 382-390, June, 1975. Original article submitted September 2, 1974.

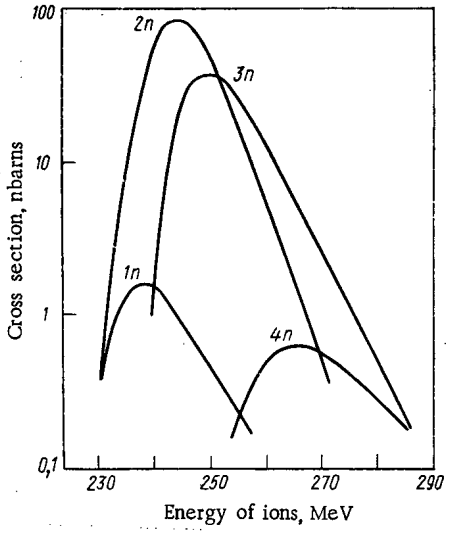

Fig. 3

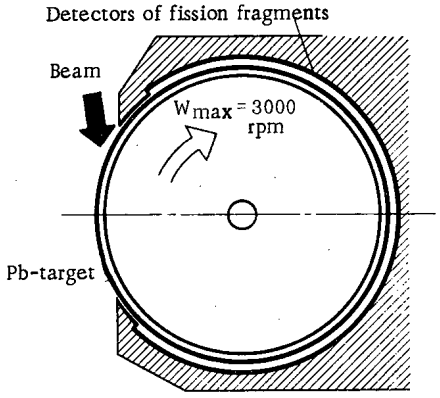

Fig. 4

Fig. 3. Calculated functions of excitation of the reactions $^{207}Pb(^{50}Ti, xn)-^{257-x}Ku$.

Fig. 4. Schematic view of an experimental device for the recording of short-lived spontaneously fissioning nuclei.

or decreasing N. For an understanding and explanation of this pattern, the region of heavy nuclei with Z > 102, where spontaneous fission may entirely determine the stability of even—even nuclei, is of the greatest interest.

However, information in this region is extremely limited. At the present time the properties of five isotopes of element 104 (two even—even nuclei) and three isotopes of element 105 are known. A spontaneously fissioning isotope of Ku (Z = 104) with mass 260 and a half-life of 0.1 sec was synthesized for the first time in Dubna [2] in the nuclear reaction $^{242}Pu(^{22}Ne, 4n)$. Then the chemical properties of kurchatovium were studied [3-5]. Later at Berkeley (United States), the α decay of odd isotopes of this element with mass 257, 259, and 261 was investigated [6-8]. In 1970 we found [9] that the isotope ^{259}Ku experiences spontaneous fission in a number of cases (13-20%) (the partial half-life $T^{SF}_{1/2} \approx$ 20-30 sec), and in [10] the periods of spontaneous fission were determined for the isotopes ^{258}Ku and ^{261}Ku, equal to 10 msec and > 10 min, respectively.

From a comparison of these data with the systematics of Ghiorso et al. [6, 11], obtained by extrapolating the properties of elements 100 and 102, it follows that the odd isotopes of element 104 have a strong prohibition of spontaneous fission ($\sim 10^7$-10^{12}), while the half-life of the even isotope ^{260}Ku exceeds the theoretical value by 10^6-10^7-fold. Such a long lifetime of ^{260}Ku was the cause of lengthy discussions between the two laboratories in Berkeley and Dubna; however, experiments on the synthesis and study of the properties of this isotope repeated in 1969 with an improved procedure confirmed the original data.

The question of the properties of heavy nuclei is important not only in the sense of the discovery of a new element and the study of its physical and chemical properties. According to the modern concepts, the barrier to the fission of heavy nuclei has a complex structure, determined to a substantial degree by shell effects. Therefore, in our opinion, it seemed extremely important to find the direct relationship between the values of the half-lives of the spontaneous fission of heavy elements and the stability of ultra-heavy nuclei in the region with Z $\approx$ 114.

From this standpoint it is necessary to investigate the properties of nuclei in a broader range of mass numbers, and in particular, to determine the periods of spontaneous fission of isotopes with N $\leq$ 152 for Z = 104.

However, such investigations involve difficulties. The nuclei of the heavy element formed in fusion reactions possess a high energy of excitation, and only a 10^{-8}-10^{-10} fraction of them can be converted to the ground state by successive emission of neutrons and γ-quanta. This leads to the fact that the cross sections of the formation of heavy nuclei are equal to 10^{-34}-10^{-32} cm^{-2}.

TABLE 1. Results of Experiments on the Synthesis of Kurchatovium

Reaction	Energy of ions in laboratory system of coordinates, MeV	Integral flux of ions, 10^{15}	Time of transfer of fission fragments to detector, sec	No. of recorded tracks of spontaneous fission	Half-life of emitter, sec	Cross section of formation of nuclei, 10^{-33} cm^2
$^{208}Pb + ^{50}Ti$	260	11	0,004	70	0,005	6
$^{207}Pb + ^{50}Ti$	260	8	1,0	12	>1	1,5
		12	0,004	53	—	
		4	0,1	17		3
		8	2,0	20	~ 4	—
$^{206}Pb + ^{50}Ti$	260	4	0,004	2	—	$\leqslant 0,3$
$^{206}Pb + ^{40}Ar$	220	9	0,002	35	0,004	3
$^{203}Tl + ^{45}Sc$	240	3	0,002	0	—	$\leqslant 0,2$
$^{205}Tl + ^{45}Sc$	240	6	0,002	0	—	$\leqslant 0,1$

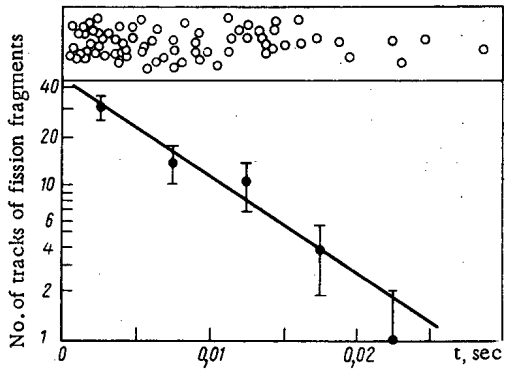

Fig. 5. Time distribution of tracks of spontaneous fission fragments in the reaction of $^{208}Pb + ^{50}Ti$ (the half-life curve was constructed with deduction of the contribution of long-lived activity with a half-life of several seconds).

On the other hand, with increasing atomic number the period of spontaneous fission decreases, especially in the region of neutron-deficient isotopes, and therefore the background from short-lived spontaneously fissioning isotopes, which are formed in reactions of multinucleon transfer, increases substantially.

The situation is substantially changed if instead of the heavy isotopes Pu, Cm, and Cf, stable nuclei of Pb or Bi are used as the target and irradiated with a beam of ions with mass $A_I > 40$ atomic units. The interaction of such nuclei was studied in our earlier work [12].

This method of synthesis was used in the present work to obtain new neutron-deficient isotopes of kurchatovium and to determine their properties.

Selection of the Reaction of Synthesis

Of all the possible target—particle combinations, in our opinion, the reaction of Pb + ^{50}Ti is the best for the synthesis of neutron-deficient isotopes of kurchatovium. Since "magic" nuclei — isotopes of lead — are used as the target, and the nucleus to be synthesized is deformed, the compound nucleus may possess a low energy of excitation. In turn, lowering the energy of excitation of the compound nucleus should lead to a decrease in the number of emitted neutrons and, consequently, to an increase in the cross sections of formation of the nuclei in the ground state [12].

Figure 2 presents the dependences of the calculated values of the minimum energy of excitation of the compound nucleus ^{258}Ku on the mass of the bombarding ion. The minimum energy of excitation is determined by the barrier to interaction B_{int} and Q of the reaction: $E^*_{min} = B_{int} + Q$, where $B_{int} = Z_I Z_T e^2/r_e \cdot (A_I^{1/3} + A_T^{1/3})$ and $Q = M_I + M_T - M_{CN}$. In the calculation of E^*_{min}, the masses of the nuclei were taken from [13], and the value of the parameter r_e was selected equal to $1.45 \cdot 10^{-13}$ cm.

From Fig. 2 it is evident that the minimum value of the energy of excitation corresponds to a mass of the bombarding particle $A_I \approx 50$ atomic units. It should be noted that the dependence presented is correct only if the parameter r_e, determining the value of the barrier to rotation B_{int}, is unchanged from light to heavier isotopes. Earlier, in the experiments of [14], it was shown that $r_e = (1.44 \pm 0.02) \cdot 10^{-13}$ cm in the case of irradiation of ^{208}Pb with ^{40}Ar and ^{52}Cr ions.

On the basis of the experimental data [12, 14] on the determination of B_{int} and the cross sections of formation of the isotopes $^{244, 246}$Fm in the reaction of $^{206, 207, 208}$Pb + ^{40}Ar, the functions of excitation of the reactions with emission of various numbers of neutrons were calculated in the irradiation of isotopes of lead with ^{50}Ti ions. The method of calculation was described in detail in [15].

As can be seen from Fig. 3, which presents as an example data for the reaction $^{207}Pb(^{50}Ti, xn)^{257-x}Ku$, the maximum cross section corresponds to the emission of two or three neutrons from the compound nucleus ^{257}Ku and decreases sharply when $x > 3$.

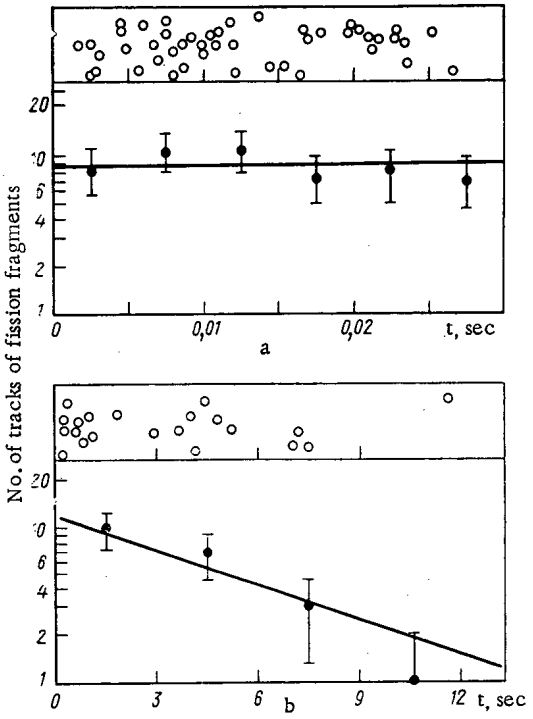

Fig. 6

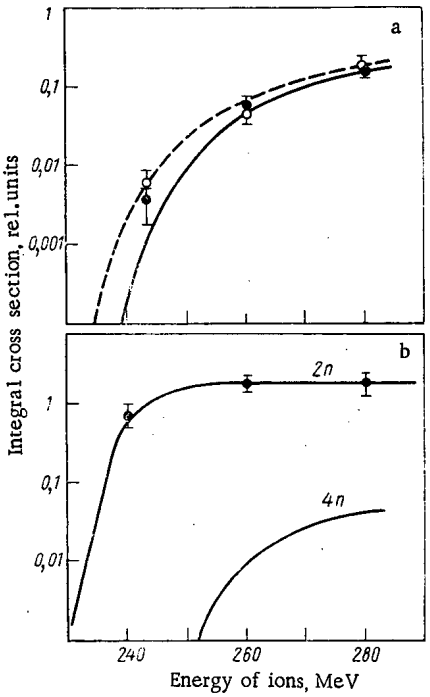

Fig. 7

Fig. 6. Distribution of tracks of fragments of spontaneous fission in the reaction of $^{207}Pb + {}^{50}Ti$: a) time cycle of measurements from 0.003 to 0.03 sec; b) from 1 to 13 sec.

Fig. 7. Integral functions of excitation (a) for the isotopes ^{151}Pm (●) and ^{204m}Pb (○), formed in the reaction $^{208m}Pb + {}^{50}Ti$: --- and ——) results of a calculation with parameter of diffuseness $d = 0.44 \cdot 10^{-13}$ and $d = 0.34 \cdot 10^{-13}$ cm, respectively (the value of the remaining parameters are the same as in [12]). Integral functions of excitation (b) for the spontaneously fissioning emitter with $T_{1/2}^{SF} \approx 5$ msec: ——) calculated values of the excitation for the reactions (^{50}Ti, 2n) and (^{50}Ti, 4n) at $d = 0.34 \cdot 10^{-13}$ cm.

It was shown earlier [12] that reactions with the emission of two neutrons are very sensitive to the value of the minimum energy of excitation of the compound nucleus. The transition from ^{48}Ti ions to ^{50}Ti ions, according to our estimates, increases the cross section of 2n-reactions approximately 100-fold. In view of this, a beam of accelerated ^{50}Ti ions was used in the experiments.

Production of Accelerated Titanium Ions

The calculated value of the barrier to interaction in the reaction $^{208}Pb + {}^{50}Ti$ is equal to 230-235 MeV in the laboratory system of coordinates. The maximum energy of the beams of accelerated ions for the 300 cm cyclotron of the Laboratory of Nuclear Research, United Institute of Nuclear Research, is determined by the ratio $E_{max} = 250\, Z_i^2 / A_I$, and for $^{50}Ti^{+7}$ and $^{50}Ti^{+4}$ is 245 and 320 MeV, respectively.

For the acceleration of ^{50}Ti ions in such a high charge state, we created a special ion source, in which the enriched isotope ^{50}Ti in the form of the metal was used as the starting material.

The intensity of the isolated beam of $^{50}Ti^{+8}$ ions was $5 \cdot 10^{10}$–10^{11} particles/sec, while the intensity of the internal beam of $^{50}Ti^{+8}$ ions was $2 \cdot 10^{11}$ particles/sec. The energy of Ti^{+7} ions is only 10-15 MeV greater than the barrier to interaction; therefore, the isolated beam was used to study the reactions proceeding with the emission of two neutrons, and the bulk of the experiments was conducted on the internal beam of the cyclotron.

Experimental Procedure

In experiments with ^{50}Ar ions [12] it was shown that when isotopes of lead are used as the target, there is practically no background associated with the spontaneous fission of side products of the reaction.

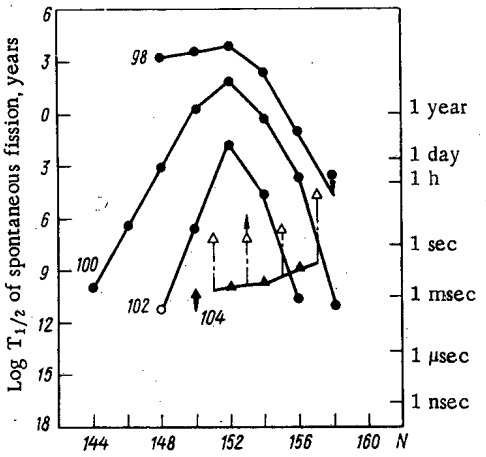

Fig. 8

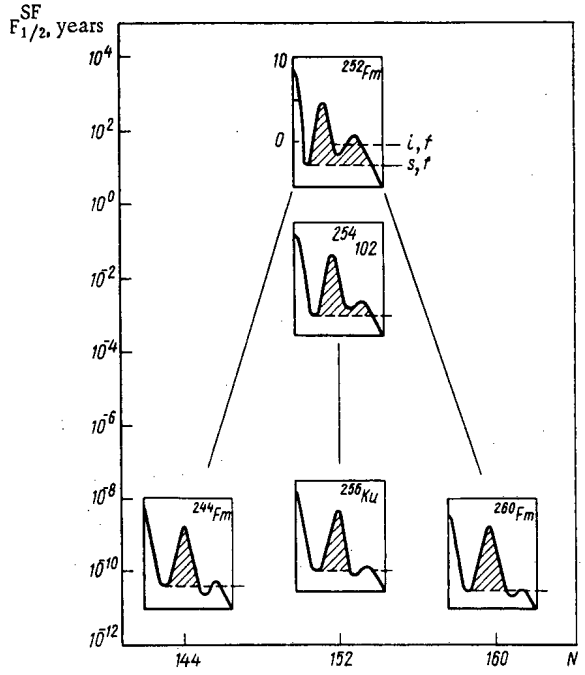

Fig. 9

Fig. 8. Systematics of the periods of spontaneous fission considering new data for the isotopes $^{250}102$, $^{255}104$, and $^{256}104$.

Fig. 9. Illustrative representation of the barriers to fission for the isotopes Fm, $^{254}102$, and ^{256}Ku. (The periods of spontaneous fission are given along the y axis.)

Therefore, for the synthesis of heavy elements by this method, a highly sensitive rapid method for the detection of nuclei according to spontaneous fission can be successfully used.

In the experiments we used the distribution of ^{208}Pb isotopes (content 97.8%, impurities ^{207}Pb 1.6% and ^{206}Pb 0.6%); ^{207}Pb (content 83.4%, impurities ^{208}Pb 14.3% and ^{206}Pb 2.3%); ^{206}Pb (content 90.4%, impurities ^{208}Pb 6.7% and ^{207}Pb 2.9%).

The experimental setup for the recording of short-lived spontaneously fissioning nuclei is schematically presented in Fig. 4. The beam of ^{50}Ti ions drops along a tangent to the surface of a hollow cylinder, oriented vertically and rotating at a maximum angular velocity of 3000 rpm. By the method of atomization, a layer of lead about 2 mg/cm^2 thick, simultaneously serving as the target and the collector of recoil nuclei, was applied on the side surface of the cylinder. As a result of the fact that the beam is incident at a small angle to the surface of the cylinder, the layer of lead is an "infinitely" thick target, in which there is an integration of the function of excitation from B_{int} to E_{max}.

The maximum energy of the internal beam of ^{50}Ti ions was selected equal to 260 MeV (see the excitation function in Fig. 3). The intensity and position of the beam of ions were monitored during the experiment with a special device, situated outside the target. The integral flux of ions that passed through the target was determined by an activation method according to the yield of the isotope ^{111}In ($T_{1/2}$ = 2.8 days), formed in the bombardment of copper with titanium ions; for these purposes, a copper target ~ 15μ thick with an area of 1 cm^2 (~1% of the total area of the lead target) was situated on the side surface of the cylinder.

Track detectors of spontaneous fission fragments of mica with a content of uranium and thorium impurities < 10^{-7} g/g were positioned around the rotating target at a distance of 2 mm. Despite the fact that the energy of the recoil is comparatively great (~ 50 MeV) and corresponds to a range in lead of ~ 6 mg/cm^2, in view of the small angle of entrance into the target these nuclei are situated close to the surface of the layer, and the efficiency of the recording of spontaneous fission fragments is about 50%.

Shields protecting the detectors from scattered ions and forced fission fragments, as well as the special method of treatment of the detectors, entirely eliminated the background at a distance of only ~2 cm from the site of incidence of the beam.

This method was tested in experiments [12] on the production of the isotopes ^{244}Fm in the reaction ^{206,207,208}Pb (^{40}Ar, xn)^{244}Fm, where it was shown that it can be successfully used for recording short-lived spontaneously fissioning emitters, if their lifetime is greater than 3 msec and the cross section of their formation exceeds 10^{-35} cm^2.

Synthesis of the Isotopes ^{256}Ku and ^{255}Ku

The isotope ^{256}Ku can be obtained in the reaction ^{208}Pb(^{50}Ti, 2n). From the systematics of the properties (see Fig. 1) it follows that the lifetime of this isotope with respect to α decay ranges from 50 to 200 msec, whereas the partial period of relatively spontaneous fission is substantially greater on account of the stabilizing action of the subshell N = 152. Therefore, in the reaction of ^{208}Pb + ^{50}Ti, we can count on the recording of spontaneous fission of the isotope ^{252}102 ($T_{1/2} \approx$ 2 sec, 30% spontaneous fission), which is formed in the α decay of the ^{256}Ku nuclei.

In the first experiment the rate of rotation of the cylinder was selected equal to 8 rpm, which permitted recording of the spontaneous fission with $T_{1/2} > 0.5$ sec. In the case of irradiation of ^{208}Pb with an integral flux of $8 \cdot 10^{15}$ ^{50}Ti ions, 12 tracks of spontaneous fission were observed, which is substantially less than the expected value. This may be evidence that either the mechanism of the fusion reaction changes substantially from ^{40}Ar ions to ^{50}Ti ions, or the properties of the isotope ^{256}Ku differ substantially from those predicted.

To test the second hypothesis, the experiments were repeated at a rate of rotation of the cylinder of 1500 rpm. At an integral flux of ^{50}Ti ions $\sim 10^{16}$ particles, 70 tracks of spontaneous fission fragments, with the time distribution presented in Fig. 5, were recorded.

Subsequent experiments were conducted with a target of ^{207}Pb at a rate of rotation of the cylinder 1500 rpm. At an integral ion flux of $\sim 1.2 \cdot 10^{16}$ particles, 53 spontaneous fission fragments were recorded (Fig. 6a). Evidently the half-life is significantly greater than the selected time value, and therefore the experiment was repeated at a lower rate of rotation (54 rpm). Here also an analogous picture of the distribution of tracks was obtained; therefore, in the third series of experiments the rate was lowered to 3.6 rpm (Fig. 6b).

Thus, it follows from the experiments that in the formation of ^{207}Pb by ^{50}Ti ions, the formation of a spontaneously fissioning emitter with a half-life of several seconds is observed.

Finally, in the last series of experiments we irradiated a target of ^{206}Pb. At an integral flux of $\sim 0.4 \cdot 10^{16}$ ions, only four tracks were recorded, half of which, taking into account the data obtained earlier, may be due to reactions on impurity isotopes ^{207}Pb and ^{206}Pb. In other words, in the combination of ^{206}Pb + ^{50}Ti, only the upper limit of formation of spontaneously fissioning nuclei can be determined.

All the experimental results are presented in Table 1. The error in the determination of the values of the cross sections, according to our estimates, do not exceed a factor of two, whereas the relative error is determined chiefly by the statistical accuracy and is ~30%.

Thus, from the aggregate of data obtained it follows that in the case of irradiation of targets of separated lead isotopes with ^{50}Ti ions, the formation of two spontaneously fissioning emitters with greatly differing half-life: about 5 msec and several seconds, is observed.

The emitter with half-life 5 msec, observed in the reaction of ^{206}Pb + ^{50}Ti, cannot be assigned to nuclei with atomic number Z < 104, since all the isotopes of element 102 are known up to N = 146 and do not possess such properties [16], while for the odd isotopes of element 103 there is a strong prohibition of spontaneous fission [17].

The maximum yield of this emitter is observed in the reaction with ^{208}Pb; the effect decreases by more than 10-fold with a target of ^{207}Pb and is practically entirely absent for ^{206}Pb.

Thus, analyzing the experimental cross sections of the reactions and the properties of the known isotopes of kurchatovium and lighter elements, it can be assumed that the observed effect is due to decay of the isotope ^{256}Ku, which is formed in the reaction ^{208}Pb(^{50}Ti, 2n)^{256}Ku.

The question of the properties of the isotope of kurchatovium with N = 152, as will be evident from the following, is of theoretical significance; therefore it is important to accurately identify the mass number of the emitter with half-life ~5 msec. Since there is a great prohibition of spontaneous fission for odd isotopes, possible candidates are the even nuclei ^{256}Ku and ^{258}Ku, which are formed in reactions with the emission of two and four neutrons, respectively.

Despite the fact that the calculated values of the cross sections of reactions with the emission of two and four neutrons differ substantially from one another (see Fig. 3), separate experiments were conducted on the measurement of the integral function of excitation for the emitter with $T_{1/2} \approx 5$ msec. Figure 7 presents the experimental values and the calculated dependences of the integral cross sections of formation of the isotope with half-life ~5 msec and the nuclei ^{151}Pm (the fission fragments of the compound nucleus) and ^{204m}Pb (products of a transfer reaction) in the irradiation of ^{208}Pb by ^{50}Ti ions. The dependences presented in Fig. 7 additionally confirm the fact that the short-lived emitter is formed in a reaction with the emission of two neutrons and is the isotope ^{256}Ku.

Comparing the yield of short-lived and long-lived activity in the reaction of ^{208}Pb + ^{50}Ti, we can conclude that the isotope ^{256}Ku in the majority of the cases experiences spontaneous fission.

It should be noted that the experimental cross section of the reaction Pb(^{50}Ti, 2n)Ku proved to be 10 times lower than the theoretical values (see Fig. 3). However, in a calculation of $\sigma(x, n)$, the empirical dependence of Sikkeland et al. [18], based on the assumption of an influence of the subshell N = 152 on the value of Γ_n/Γ_f, was used for the ratio of the partial width Γ_n/Γ_f. And yet, as will be shown later, this assumption is not substantiated for nuclei with $Z \geq 104$. The exclusion of the influence of the subshell N = 152 on the value of Γ_n/Γ_f leads to a significant decrease in the calculated cross sections, which virtually eliminates the discrepancy noted above.

The long-lived emitter with half-life about 4 sec, in all probability, is the isotope ^{255}Ku, which is formed with a maximum cross section in the reaction ^{207}Pb(^{50}Ti, 2n), and with lower probability in the reaction ^{208}Pb(^{50}Ti, 3n), and is absent in the reaction ^{206}Pb(^{50}Ti, 1n).

However, we should note that the lifetime of this emitter proved close to the lifetime of the known isotope ^{252}102, which in this combination might be obtained in the reaction of the type of ^{207}Pb(^{50}Ti, α1n)-^{252}102.

Let us consider separately the question of the probability of side processes in reactions with ions of the type of ^{40}Ar or ^{50}Ti. At a maximum energy of the bombarding ^{50}Ti ions equal to 260 MeV, the maximum energy of excitation of the compound nucleus ^{257}Ku is ~40 MeV. Estimates show that the threshold of the reaction with evaporation of an α particle and one neutron is equal to ~260 MeV. Moreover, in this region of nuclei the ratio of the partial width Γ_α/Γ_n, like Γ_p/Γ_n, is small ($\lesssim 10^{-2}$). Therefore, the contribution of the processes occurring with the evaporation of charged particles from the compound nucleus is negligible.

And yet, the process of direct emission of α particles, followed by evaporation of a neutron, as occurred in reactions with light ions of carbon, nitrogen, and oxygen, is energetically possible. However, as was shown in [19-21], the mechanism of such reactions depends substantially on the structure of the bombarding ion. In the sequence from light ions to particles of the type of ^{40}Ar and ^{50}Ti, the probability of the escape of direct α particles decreases hundreds and thousands of times.

Model experiments were conducted in which spontaneously fissioning nuclei of ^{244}Fm were obtained in reactions in the irradiation of the isotopes ^{205}Tl and ^{203}Tl with ^{45}Sc ions and of the isotopes ^{206}Pb with ^{40}Ar ions. As can be seen from Table 1, the ratio of the cross sections $\sigma(\alpha, 2n)/\sigma(2n) \lesssim 0.03$. From this it can be concluded that the probability of formation of the isotope ^{252}102 in the irradiation of ^{207}Pb with ^{50}Ti ions is negligible.

From a comparison of the cross sections of formation of the isotopes ^{255}Ku and ^{256}Ku it follows that the odd isotope ^{255}Ku has comparable values of the half-life with respect to α decay and spontaneous fission. Finally, the absence of an effect in the reactions of ^{206}Pb + ^{50}Ti may mean that the life-time of the even isotope ^{254}Ku is less than 3 msec.

DISCUSSION OF RESULTS

Let us consider the question of how the properties of the synthesized neutron-deficient isotopes of kurchatovium agree with the known data on the stability of heavy nuclei with respect to spontaneous fission.

For the isotope ^{256}Ku with N = 152, instead of the expected half-life, comprising tens and hundreds of second, the experimental value was 10^3-10^4 times smaller.

The position of this point in the systematics of spontaneous fission substantially changes the concept of the stabilizing influence of the subshell N = 152 in the transition from Z = 102 to Z = 104. The dependence of $T^{SF}_{1/2}$ for kurchatovium isotopes on the number of neutrons is evidence of a monotonic increase in the lifetime of the even—even nuclei with increasing mass, without any significant variations in the region of N = 152 (Fig. 8).

The lifetime of the odd nucleus ^{255}Ku is determined by the prohibition of spontaneous fission, which in this case is $\sim 10^3$. Now it is not surprising that the isotope ^{260}Ku has $T^{SF}_{1/2} \approx 0.1$ sec, and there is no need to assume such high prohibitions ($\sim 10^7$-10^{12}) for the other odd isotopes of kurchatovium with mass numbers 257 and 259, as was done in the form of Ghiorso et al. [6, 11]. From the systematics (see Fig. 8) it is evident that for practically all the odd isotopes of kurchatovium, the prohibition of oddness leads to an inhibition of spontaneous fission by 10^3-10^4-fold.

Since a substantial change in the half-life with respect to spontaneous fission (more than 10-fold) is observed in the sequence from the isotope ^{254}102 to the isotope ^{256}Ku, it is natural to attempt to give an at least qualitative explanation for the data obtained.

According to the modern concepts, in the region of transfermium elements the barrier to fission has a complex structure, and the stability of the nuclei with respect to spontaneous fission is determined chiefly by the contribution of the shell correction to the total energy of deformation of the nucleus.

Let us consider from this standpoint the isotopes of fermium, for which a strong influence on the half-life $T^{SF}_{1/2}$ by the subshell N = 152 has been established experimentally. When N = 152, the barrier to fission, calculated according to the method of Strutinskii [22], seems to consist of two barriers and takes the form of a two-hump curve with two minima, corresponding to the ground state and isomeric state of the nucleus. The lifetime of this nucleus with respect to spontaneous fission is determined by the integral of motion on the entire path from the ground state to a point lying beyond the second barrier (Fig. 9).

With decreasing number of neutrons (transition to lighter isotopes of fermium), the value of the second barrier will be lowered as a result of a decrease in the liquid drop energy of deformation of the nucleus, which should lead to a decrease in the periods of spontaneous fission. In the limiting case, when the ground state is higher than the second maximum, the value of $T^{SF}_{1/2}$ will be determined by the permeability only of the first barrier. It can be assumed that as a result of this circumstance the transition from ^{252}Fm to ^{244}Fm will lead to a change of approximately 10^{12}-fold in $T^{SF}_{1/2}$.

And yet, as was shown in the work of Randrup et al. [23], the possibility remains that such a situation might arise in the movement from N = 152 toward heavier isotopes of fermium. In this case the superposition of the shell correction and liquid drop energy of deformation may also lead to a substantial decrease in the second maximum and, as a result, sharply reduce the lifetime of the heavy isotopes with respect to spontaneous fission. Actually, in the sequence from ^{252}Fm to ^{258}Fm, the value of $T^{SF}_{1/2}$ changes approximately 10^{13}-fold.

Now let us fix N = 152, and we shall measure the number of protons in the nucleus. With increasing Z, the liquid drop portion of the energy of deformation will decrease, which leads to the same consequences that were observed in the case of neutron-deficient isotopes of fermium discussed above. It can be assumed that the greatest change in $T^{SF}_{1/2}$ will occur at the moment when the lifetime of the nucleus is determined chiefly by the permeability of the first barrier. The possibility remains that this situation exists in the transition from ^{252}Fm to ^{256}Ku, since the half-life with respect to spontaneous fission changes approximately 10^{12}-fold in this case.

If this assumption is correct, then further movement in the direction of large Z or variation of N at set Z should not lead to such strong changes in $T^{SF}_{1/2}$, since the value of the first barrier, as it follows from the calculations of [22], is comparatively insensitive to the nucleon composition of the nucleus. It seems to us that this viewpoint is qualitatively confirmed by the latest calculations of Pauli and Ledergerber [24] and Möller and Nix [25, 26]; however, the quantitative conclusions require a detailed theoretical analysis, considering new data with respect to the properties of isotopes of kurchatovium and heavier elements.

Such an interpretation of the experimental data means that for even—even isotopes of kurchatovium the lifetime with respect to spontaneous fission is already determined practically entirely by shell effects. This is analogous to what is expected for the region of ultraheavy elements, and it must be hoped that in

the case of movement in the direction of the twice-magnetic nucleus with Z = 114, N = 182, a sharp increase in $T_{1/2}^{SF}$ will actually be observed, as it follows from the theoretical predictions.

CONCLUSIONS

A number of conclusions can be drawn from the aggregate of experimental results.

The method of synthesis of transfermium elements in the irradiation of lead isotopes with ions with mass $A_I \geq 40$ atomic units, investigated earlier [12] for the example of the reaction Pb(^{40}Ar, xn)Fm, is also extremely effective using ^{50}Ti ions. The reactions Pb(^{40}Ar, 2n)Fm and Pb(^{50}Ti, 2n)Ku have approximately equal cross sections, which might have been expected on the basis of theoretical estimates. This permits us to hope that this method can be used successfully for the synthesis of heavier elements in the reactions induced by ^{54}Cr, ^{55}Mn, and ^{58}Fe ions.

In all probability, the substantial changes in the systematics of the half-lives for even—even isotopes of kurchatovium are associated with the structure of the barriers to fission of these nuclei. From this standpoint, it seems important to investigate the properties of more neutron-deficient isotopes of kurchatovium, using, in particular, the reactions with ^{204}Pb, and to attempt to advance into the region of elements with Z ≥ 106. On the other hand, a detailed theoretical analysis must be made of the data obtained on the basis of the modern theory of nuclear fission, which, in our opinion, will aid in a more reliable prediction of the properties of heavy and ultraheavy elements.

The authors are deeply grateful to Academician G. N. Flerov for his great support, constant aid, and valuable suggestions at all stages of this work; we should like to thank V. M. Plotko and N. A. Danilova for their great contribution to the development of the experimental method and their active participation in the experiments, as well as K. I. Merkin and T. I. Rybakov for their painstaking work on the examination of a large number of detectors of fission fragments. The authors are grateful to the operating group of the U-300 accelerator, supervised by A. N. Filipson, for producing intense and stable beams of accelerated ions. The enriched isotope ^{50}Ti was kindly provided by the State Isotope Reserve of the USSR, and the authors are grateful to V. P. Bochin, V. S. Romanov, and S. A. Sel'yanov for aid in the preparation of samples of this isotope for the ion source.

LITERATURE CITED

1. G. N. Flerov and I. Zvara, Report of the United Institute of Nuclear Research D7-6013 [in Russian], Dubna (1971).
2. G. N. Flerov et al., At. Énerg., 17, No. 4, 310 (1964); Phys. Letters, 13, 73 (1964).
3. I. Zvara et al., Report of the United Institute of Nuclear Research P7-3783 [in Russian], Dubna (1968); Radiokhimiya, 11, 163 (1969).
4. I. Zvara et al., Report of the United Institute of Nuclear Research D7-4542 [in Russian], Dubna (1969); Radiokhimiya, 12, 565 (1970); J. Inorg. and Nucl. Chem., 32, 1885 (1970).
5. I. Zvara et al., Report of the United Institute of Nuclear Research D12-5845 [in Russian], Dubna (1971); J. Inorg. and Nucl. Chem. Letters, 7, 1109 (1971).
6. A. Ghiorso, in: Proc. R. A. Welch Found. Conf. on Chemical Research, XIII. The Transuranium Elements. The Mendeleev Centennial, Houston, Texas, 17-19 November (1949), p. 107.
7. A. Ghiorso et al., Phys. Rev. Letters, 22, 1317 (1949).
8. A. Ghiorso et al., Phys. Letters, 32B, 95 (1970).
9. Yu. Ts. Oganesyan et al., At. Énerg., 28, No. 5, 393 (1970).
10. M. J. Nurmia, Nuclear Chemistry Annual Report LBP-666, Berkeley (1971), p. 42.
11. A. Ghiorso and T. Sikkeland, Phys. Today, 20, No. 9, 25 (1967).
12. Yu. Ts. Oganesyan et al., Preprint of the United Institute of Nuclear Research D7-8194 [in Russian], Dubna (1974).
13. W. Myers and W. Swiatecki, in: Proc. Intern. Symp., "Why and How Should We Investigate Nuclides for the Stability Line," Lysekil, Sweden (1966); Almquist and Wiksell, Stockholm (1968).
14. Yu. Ts. Oganesyan et al., Preprint of the United Institute of Nuclear Research P7-7863 [in Russian], Dubna (1974).
15. A. S. Il'inov, Report of the United Institute of Nuclear Research P7-7108 [in Russian], Dubna (1973).
16. G. N. Flerov, At. Énerg., 24, No. 1, 5 (1968); Ann. Phys., 2, 311 (1967).
17. G. N. Flerov et al., Report of the United Institute of Nuclear Research P7-4932 [in Russian], Dubna (1970).

18. T. Sikkeland, A. Ghiorso, and M. Nurmia, Phys. Rev., 172, 1232 (1968).
19. T. Galin et al., Preprint IPNO -RC-73-03, Orsay (1973).
20. L. Moretto et al., Preprint LBP-1966, Berkeley (1973).
21. A. G. Artyukh et al., Report of the United Institute of Nuclear Research P7-7189 [in Russian], Dubna (1973).
22. M. Brack et al., Rev. Mod. Phys., 44, 320 (1972).
23. T. Randrup et al., Nucl. Phys., A217, 221 (1973).
24. H. Pauli and T. Ledergerber, in: Proc. 3rd. Symp. on Physics and Chemistry of Fission, Rochester, Paper IAEA-SM-174/202 (1973).
25. P. Möller and J. Nix, ibid., Paper IAEA-SM-174/202 (1973).
26. P. Möller and J. Nix, Preprint LA-UR-74-417, Los Alamos (1974).

PROBLEM OF ENVIRONMENTAL PROTECTION IN THE OPERATION OF NUCLEAR POWER STATIONS*

N. G. Gusev

UDC 551.510.72

Protection of population and environment in the design and operation of nuclear industrial units is becoming an important contemporary social problem. This review considers the need for the distribution of established maximum doses over radiation sources and the need for estimates of collective and population doses from all forms of nuclear energy.

Requirement for Distribution of Maximum Population Doses

Scientists of all countries have concentrated their attention on the problem of protection against ionizing radiation from the very first steps in the peaceful use of atomic energy. As a result, the safest branch of industry for personnel and population — nuclear power — was created in a short time.

The international Commission on Radiological Protection (ICRP) established maximum permissible doses (MPD) which are considered safe for the occupational worker and the general population. National regulations were based on these recommendations. In planning units for the nuclear industry, however, the application of these regulations is complicated by a number of factors arising out of the extensive introduction of nuclear energy into many fields of human activity. If one assumes that by the year 2000 the

*Reviews published in this issue are revised texts of papers read at the plenary session of the All-Union Scientific Conference on Protection against Ionizing Radiation from Nuclear Installations (Moscow, 17-19 December, 1974).

TABLE 1. Distribution of Maximum Population Dose over Radiation Sources, % of Total Maximum Dose

Radiation source	Gaseous and aerosol wastes	Liquid and solid wastes	Sum
Water-cooled, water-moderated reactors (VVÉR)	4	2	6
Single-loop reactors (RBMK)	5	3	8
Gas-cooled reactors	2	1	3
Thermal nuclear power stations	3	1	4
Fast reactors	2	1	3
Experimental reactors	3	2	5
Other types of reactors	4	2	6
Fuel reprocessing plants	10	8	18
Ores, hydrometallurgy, fuel elements	2	3	5
Radiochemistry, irradiators	1	1	2
Burial grounds for liquid and solid waste	1	3	4
Structural materials	–	–	5
Agricultural fertilizers	–	–	4
Accelerators, electron-beam tubes	–	–	1
Television sets	–	–	1
Reserve for other sources	–	–	25

Translated from Atomnaya Énergiya, Vol. 38, No. 6, pp. 391-397, June, 1975. Original article submitted January 8, 1975.

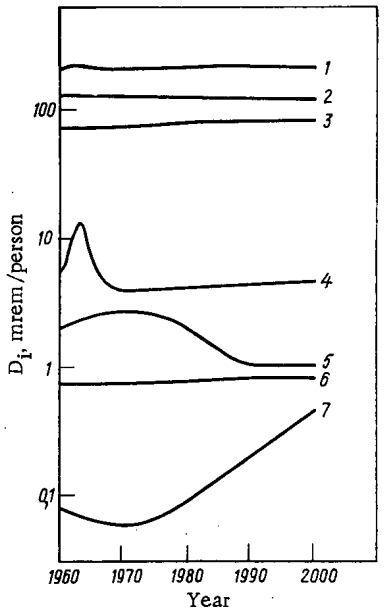

Fig. 1. Mean annual whole-body dose (USA): 1) total dose; 2) natural radiation; 3) medical procedures; 4) global fallout; 5) various sources; 6) occupational irradiation; 7) nuclear power stations and other sources of environmental contamination.

TABLE 2. Maximum Annual Doses, rem

Category	Critical-organ group			
	I	II	III	IV
A. Staff personnel	5	15	30	75
B. Individuals in the general population	0,5	1,5	3*	7,5
C. General population	0,17	0,5	1	—

*For thyroid gland in children, MPD = 1.5 rem/yr.

electrical power from nuclear power stations over the entire world will amount to 3000 GW, then from a rough estimate there will be generated in that period from nuclear power alone (in billions of curies) a mixture of fission products amounting to ~40,000 (no holding time) or 600 (after one year's holding time) including the long-lived fission products (no holding time): ^{85}Kr, 3; ^{89}Sr, 400; ^{90}Sr, 30; ^{137}Cs, 35; ^{131}I, 250; ^{129}I, 10^{-5}, etc. A large amount of long-lived isotopes (^{3}H, ^{14}C, ^{54}Mn, ^{60}Co, ^{134}Cs) and transuranic elements will be formed. There will be an increase in the number of other sources of artificial radiation and an ever increasing number of people will be subject to their effects. Thus, of the two main principles for protection against radiation promulgated by the ICRP — maintaining radiation doses at the lowest possible level (allowing for technological and economic considerations) and a reduction in the number of irradiated individuals — only the first is actually achievable.

In this review, however, we raise the question not of further reduction in dose but of the need for distribution of presently established MPD for the population with consideration of the partial contribution from the separate kinds of radiation sources so that the total dose does not exceed the established maximum.

An analysis was made of a large number of reports on actual and predicted discharges, on levels of environmental contamination, on exposure of the general population to various sources of ionizing radiations, and on methods and approaches to the evaluation of population doses. Part of this material appears in [1-17]. Based on the analysis, an attempt is made in this review to pick out the most important radiation sources (Table 1). The list of radiation sources given in Table 1 includes only the portion susceptible to quantitative analysis.

Particularly complicated is the solution of the problem of population exposure for medical application of x rays, mainly in x-ray diagnostics and stomatological procedures. According to [1], the mean value of the genetically significant dose (GSD) from diagnostic procedures amounts to 20 mrad/yr. Since the GSD is a weighted mean value including the relative birth rate and relative exposure for individuals up to 30 years of age, the actual doses to the gonads, and even more to the bone marrow or abdominal region, will be considerably higher. [By definition [1],

$$\mathrm{GSD} = \frac{\sum_j \sum_k (N^F_{j,k} W^F_{j,k} D^F_{j,k} + N^M_{j,k} W^M_{j,k} D^M_{j,k})}{\sum_k (N^F_k W^F_k + N^M_k W^M_k)}$$

TABLE 3. Maximum Doses Recommended for Individuals, mrem /yr

Group	Isotope	Critical-organ group		
		I	II	III
K	Global genetically significant isotopes: ^{3}H, ^{35}S, ^{85}Kr, ^{133}Xe, ^{134}Cs, ^{137}Cs	100	–	–
L	Global somatically significant isotopes: ^{14}C, ^{129}I, ^{131}I, ^{89}Sr, ^{90}Sr, ^{144}Ce, $^{238-241}Pu$, ^{241}Am	–	400	900
M	Local isotopes* propagated over a radius > 10 km	170	500	1000
N	The same for a radius < 10 km	500	1500	3000†

*We arbitrarily call isotopes not in Groups K and L local.

†For the thyroid gland in children, MPD = 1500 mrem/yr.

where j and k are the type of irradiation and age; F and M denote female and male; N_j is the number of individuals receiving the dose D_j rad/yr to the gonads; W is the expected number of children per person. All calculations are carried out up to 30 years of age.]

The individual radiation doses for the population of the United States from various radiation sources [2] are shown in Fig. 1 as estimated for the period 1960-2000. The comparison was made with respect to whole-body doses except for the dose from medical procedures. In the calculation of the latter, the somatic dose per capita resulting from irradiation of the abdominal region (abdominal dose) was used as the basis. It is clear that this dose is about 90% of the total dose from artificial sources of irradiation and is at least 35% of the dose from all sources, including the dose from natural radiation. Being 2-3 times less than the abdominal dose, the GSD exceeds the dose from any other artificial radiation sources.

It is necessary to plan MPD distribution with all radiation sources included and to pay particular attention to the acceptance of technical and organizational solutions for the reduction of population exposure during medical procedures. This form of radiation effect is not included in Table 1 but it must be taken into account (just like exposure from contamination resulting from nuclear explosions) when considering the social aspects of the use of nuclear energy.

There are also other sources which do not appear in Table 1. Among them are, for example, discharges of natural radioactive materials introduced into the atmosphere by thermal and electric power stations operating with mineral fuel [9, 17], nuclear explosion for peaceful purposes, nuclear accidents, exposure in aviation and astronautics when transporting nuclear fuel, etc. However, the reserve set aside for them and also for new sources (25%) does not include the dose from medical procedures.

There are standards recommended by the ICRP and accepted in MRB-69 (Table 2).

The value MPD = 0.17 rem/yr for the general population (Group 1 critical organs) corresponds to a GDS=5 rem in 30 years. Given below is the recommended distribution of this maximum dose in rem/per 30 years:

Staff 1.0
Individuals..... 0.5
Population 2
Reserve.... ..... 1.5

The GSD for the population is distributed in the following manner: 0.5 and 1.5 rem respectively from external and internal irradiation.

There is no distribution of the maximum somatically significant dose (SSD) with respect to the various population categories. Evidently, the ICRP will make recommendations in time with respect to this problem.

New difficulties arise in the development of standards with respect to irradiation. An immediate one is the concept of "global" isotopes. This term arose after it became known that because of nuclear explosions, global contamination of the biosphere (including the entire animal and vegetable worlds, the

atmosphere, and the hydrosphere) by such artificial isotopes as ^{3}H, ^{14}C, ^{85}Kr, ^{89}Sr, ^{90}Sr, and ^{137}Cs ocurred. However, in nuclear power, ^{129}I is usually still assigned to the class of global isotopes although the propagation of this isotope over considerable distances by atmospheric flow is unlikely because of the high weight ratio (6 kg/Ci). Nevertheless, a number of other isotopes which are present in atmospheric discharges or liquid wastes from nuclear units should be included in the class of global isotopes under conditions where there is a high density of nuclear-industry sources. Besides radiological properties (particularly high radiotoxicity), one should consider the total number of isotopes produced in an entire technical cycle, the fraction reaching the environment, the physical and physicochemical characteristics of the isotopes, the capability of actively participating in biological processes (active metabolism), the possibility of accumulation in soil or other media, the creation of an intensified γ-ray field at a given locality, etc. The most important criterion for assigning one or another isotope (or source) to the global category is a relatively large contribution to the collective or population dose. It is also necessary to take into account the well-known requirement that for presently established MPD occupational workers make up no more than 1.7%, and individuals in the population no more than 3.3%, of the entire population.

Table 3 gives MPD corresponding to 100% recommended for individuals in a population and also the isotopes which should be considered global. The MPD for Group K isotopes (100 instead of 117 mrem) is taken from the GSD distribution given above where a genetically significant MPD of 3.5 rem in 30 years is assigned to all categories; the MPD for Group L is taken from Table 2 after subtraction of a dose of 100 mrem/yr resulting from genetically significant isotopes; the MPD for Groups M and N is also taken from Table 2 for categories B and C respectively depending on the distance over which the isotopes may be propagated (usually, the greater the distance the greater the contribution to the collective dose). When using Tables 1 or 3 in practice, one applies the generally accepted rule that the MPD to the entire body or to individual groups of organs from a sum of isotopes (or from several types of ionizing radiation) must not exceed the MPD from a single isotope.

Among other controversial questions are the uncertainty of including the contribution to the MPD from radioactive wastes of other nuclear power stations or, generally, other nuclear industrial units, the proper selection of isotopes belonging to the global group particularly if the problem involves liquid wastes, the uncertainty of dose prediction under accident situations, the well-known difficulties in predicting the development of nuclear industry and particularly the appearance of new sources of radiation, etc.

We note in conclusion that the USAEC, as a supplement to the basic standards, published a circular in 1971 [18] in which the annual MPD from radioactive wastes of newly planned water-cooled reactors was recommended to be approximately 1/100 of the MPD established for the sum of all sources, namely 5 mrem (instead of 500 mrem) for individuals in the population living at the boundary of the protection zone (roughly 0.5 km) and 1 mrem (instead of 170 mrem) as the mean annual dose for the general population. An extensive discussion of this concept of the USAEC is given in [6-8].

Analysis of actual gaseous, aerosol, and liquid wastes of a nuclear power station and also of actual and predicted doses shows that the proposed distribution of maximum doses does not create any economic or technical problems for nuclear power stations since the actual (calculated) doses are considerably lower than those proposed.

Need for Evaluation of Population Dose

The population dose is a measure of the general irradiation of the whole body, or of a given organ, for a group (population) as a whole. If the number of people receiving a radiation dose in the range from D to D + dD is N(D)dD, then the population dose D_p is defined by [19]

$$D_p = \int DN(D)\,dD, \tag{1}$$

where the integration is carried out within the limits of the general distribution of dose for the entire population. If one is talking of a portion of the population, the term "collective dose" is used.

The population dose can also be defined by a summation of the individual doses $D_{i,j}$ over all groups of irradiated people N_j, i.e.,

$$D_p = \sum_j N_j D_{i,j}, \tag{2}$$

where j is the level of irradiation and the letter i indicates that the specified quantity (D_i, $\bar{D}_i$, G_i) refers to an individual. Sometimes one also uses the term "average individual dose" $\bar{D}_i$,

$$\bar{D}_i = D_p P, \tag{3}$$

where $p = \sum_j N_j$ is the number of people in the population.

At the present time there are various mathematical models for the quantitative evaluation of individual and population doses resulting from radioactive wastes of nuclear units. This paper briefly discusses the model developed in [20-23].

Calculation of the individual dose D_i from gaseous and aerosol discharges is conveniently performed by means of the expression

$$D_i = \bar{\mathcal{P}}\,[(\text{rem/sec})/(\text{Ci/m}^3)]\, G_i\,[\text{sec/m}^3]\, Q\,[\text{Ci}]. \tag{4}$$

Here, Q is the discharge of the isotope; C_i is the "meteorological dilution factor" which is numerically equal to the ratio between the atmospheric concentration of the isotope and the amount of isotopic discharge per unit time; $\bar{\mathcal{P}}$ is a dosimetric conversion factor corresponding to the dose rate for unit atmospheric concentration of the isotope. It should be noted that the determination of the dosimetric conversion factor is a subject for serious study since it must take into account all paths for isotopic effects on humans (inhalation, food chain, γ-ray fields from radioactive clouds or soil, etc.). Its value may vary very widely for a single given isotope. Numerical data for the factor $\bar{\mathcal{P}}$ is given in [6, 21, 24].

Unfortunately, there is no uniformity of opinion on the choice of a model for the determination of the factor G_i. Thus in foreign practice, calculations of G_i are based on the Gaussian model of Pasquill and Gifford [25, 26], which is recommended by IAEA [27]. In our country, other methods are used (for example, see the review [28]). Strictly speaking, Eq. (4) for the individual dose D_i is valid for the calculation of doses from gaseous and aerosol discharges for any paths of action except those cases where the contaminated products travel into other regions. A similar formula for the population dose was produced in the form [20, 21]

$$D_p = \bar{\mathcal{P}}\left[\frac{\text{rem/sec}}{\text{Ci/m}^3}\right] \bar{\rho}\,[\text{persons/m}^2]\, G_p\,[\text{sec/m}]\, Q\,[\text{Ci}]. \tag{5}$$

Here $\bar{\rho}$ is the average population density for a given population; G_p is the so-called population dilution factor, which is obtained by integration of the individual dilution factor G_i over the entire area. It can be represented in the following form,

$$G_p = \sqrt{\frac{2}{\pi}} \int_0^\infty \frac{F(t)}{\sigma_z(t)} \exp\left[-\frac{1}{2}\frac{H_{ef}^2}{\sigma_z^2(t)}\right] dt, \tag{6}$$

where F(t) is a dimensionless function which takes into account depletion of the plume because of radioactive decay and deposition of isotopes on the soil during the time t; H_{ef} is the effective height of the discharge.

In the more complicated case, for example, where the products contaminated at the location of a nuclear power station travel into other regions, the contribution to the population dose can be determined from

$$D_p = \sum_j D_c N_j I_j = D_c I_m, \tag{7}$$

where D_c is a normalization factor numerically equal to the integral dose per unit activity entering the body, rem/Ci/person;* I_j is the intake of a given isotope with food into the bodies of a group of N_j people (here j refers to the amount of the individual intake); $I_m = \sum_j N_j I_j$ is the total intake of the isotope into the bodies of all individuals, Ci.

In the simplest case (where one neglects radioactive decay, variation of isotopic content in processing of foods, etc.), I_m can be replaced by A_m — the total content of an isotope in all contaminated intake products, Ci:

*The integral dose or dose commitment is given in general form (for any amount of isotope entering the body) by the expression $D_c = \int_0^\infty \dot{D}(t)dt$, rad, or $D_c = \int_0^\infty \dot{H}(t)dt$, rem, where $\dot{D}(t)$ and $\dot{H}(t)$ are the absorbed-dose rate and the dose-equivalent rate.

$$I_m \approx A_m. \tag{8}$$

One of the purposes of the population dose is the determination of the public risk in using nuclear energy. In this instance, a linear (and not a threshold) dose—effect dependence is used. Then when calculating the population dose from contaminated products by Eq. (7), or with the approximation (8) included, there is no need to know the distribution of individual doses, the number of individuals, or the locality in which they live. It is only important to know what the total amount I_m of an isotope is in contaminated source products during the time of their consumption. In order to include the various metabolic paths of action, Eq. (7) can be rewritten in the following form [22]

$$D_p = D_c K_1 K_2 K_3 Q. \tag{9}$$

Here, K_1 is the fraction of discharged isotopes deposited on fields or pastures; K_2 is the fraction of the isotopes from the discharge deposited on the soil which is transferred into the edible portion of plants; K_3 is the ratio between the cumulative content of the isotope in the food intake of the population and its cumulative content in the edible portion of cultivated plants or forage at the time of harvesting or at the time cattle are out to pasture. The factor K_3 takes into account decay and removal of an isotope during transportation, processing and storage of the products as well as its "loss" through migration in the bodies of animals.

These dimensionless coefficients are defined by the relations

$$K_1 = G_p v_g \nu; \tag{10}$$

$$K_2 = \eta_1 K_4 + \eta_2, \tag{11}$$

where

$$K_4 = C\left[\frac{(\text{Ci/kg})\ \text{yr}}{\text{Ci/m}^2}\right] w\left[\frac{\text{kg/yr}}{\text{m}^2}\right] \tag{12}$$

is the fraction of singly deposited activity in the soil which is transported into the edible portion of a given type of plant grown during the time of complete removal of the isotope from the vegetative layer of the soil; v_g is the rate of deposition, m/sec.

For dairy cattle out to pasture,

$$K_3 = \frac{T_B\ [\text{days/yr}]}{365\ [\text{days/yr}]} \bar{\rho}_k\ [\text{cows/m}^2]\ \bar{S}\ [\text{m}^2/(\text{cows-days})]\quad \frac{T_{ef}\ [\text{days}]}{0.693} K_k; \tag{13}$$

for farm animals,

$$K_3 = \sum_f \frac{1}{\lambda T_f} [1 - \exp(-\lambda T_f)]\ K_r \sum_l \xi_{r,l} \exp(-\lambda T_l); \tag{14}$$

for products of plant origin,

$$K_f = \sum_p \frac{1}{\lambda T_p} [1 - \exp(-\lambda T_f)]. \tag{15}$$

Here, ν is the fraction of the area occupied by the corresponding agricultural land; η_1 and η_2 are respectively the fractions of all deposited contaminants transported into the edible portions of plants through the roots and leaves; w is the agricultural productivity; C is the total content of an isotope in the edible portion of a plant per kg weight for a one-time contamination of 1 m^2 of soil surface by an activity of 1 Ci; $\bar{\rho}_k$ is the average density of dairy cattle in the contaminated area; $\bar{S}$ is the area of pasture from which a cow eats grass in a day; T_{ef} is the time for half-removal of an isotope from the edible portion of grass; K_r is the fraction of an isotope absorbed from forage by animals of the r-th type which is transferred into products obtained from these animals (for cows, $K_r = K_k$); $\xi_{r,l}$ is the fraction of all products yielded by the r-th type of animal which is processed into primary food products; T_p and T_f are warehouse storage times for plant products and forage; T_l is the time consumed in processing and transport of the primary form of food products from cattle; T_B is the time cattle are out to pasture; λ is the decay constant for a given isotope.

At the present time, the input parameters for this model are being refined and a computer program is being written. Note that in contrast to Eqs. (1) and (2) where it is necessary to know individual exposure doses, knowledge of population density or of the number of individuals in a population is not needed for the calculation of the population dose from contaminated products when using Eqs. (7)-(15); one only needs to know the amount of isotope present in contaminated food at the time of consumption.

Of the other mathematical models for calculating population and individual doses from radioactive wastes, one should single out the model developed, and already used in practice, by US scientists [10]. Based on this model, the HERMES computer program was written in BASIC; this program encompasses all possible paths of action for radioactive materials in the environment and is intended to solve such problems as the potential development of nuclear power in the US up to the year 2000, optimal selection of sites for nuclear units, escape and propagation of radioactive materials and their resultant concentrations in air, water, soil, and bottom sediments, concentrations in food products, and, finally, radiation doses from radioactive materials entering the body with air, water, and food products and from external radiation in air, water, or soil. Results obtained by the use of this and other programs have been presented [2, 6, 16, 17].

Population or collective doses are a required social criterion in the problem of radiation safety for the population and in protection of the environment since, based on their evaluation, one can solve the problem of the fundamental partial distribution of MPD within a population with respect to radiation sources in order to assure consistency of established maximum doses from all types of nuclear energy used in the activities of society; one can predict population exposure for further development of the nuclear industry and on this basis determine risk factors for the public from the contributions to the population dose of individual radiation sources. Since the risk concept is based on the assumption of a linear dose—effect relation, the public risk factor R_p can be defined by

$$R_p = \overline{R}_i \text{ [damage/(rem-person)]} \; N \text{ [persons/population] [rem]} \; \overline{D}_i \text{ [rem]} = \overline{R}_i D_p. \qquad (16)$$

Here, $\overline{R}_i$ is the total individual risk factor including somatic and genetic effects (according to ICRP data, $\overline{R}_i = 10^{-4}$ for chronic irradiation). More detailed discussions of risk factors can be found in [2, 3, 6, 11-14, 16, 17, 28-30].

The questions touched on in this review require extensive discussion and active participation by specialists in various fields. They must be solved in planning for the development of the nuclear industry of the future in order to ensure protection of all segments of the population against ionizing radiation and protection of the environment against contamination by radioactive materials.

LITERATURE CITED

1. United Nations Scientific Committee on the Effects of Atomic Radiation, UN, New York (1972).
2. Estimates of Ionizing Radiation Doses in the United States, 1960-2000. US Environmental Protection Agency, Washington (1972).
3. The Potential Radiological Implications of Nuclear Facilities on the Upper Mississippi River Basin in the Year 2000, USAEC (1973).
4. Natural Radiation Exposure in the United States, US Environmental Protection Agency, Washington (1972).
5. Report on Releases of Radioactivity in Effluents and Solid Waste from Nuclear Power Plants for 1972, USAEC, Washington (1973).
6. USAEC, Final Environmental Statement Concerning Proposed Rule Making Action: Numerical Guides for Design Objectives and Limiting Conditions for Operation to Meet the Criterion:"As Low as Practicable for Radioactive Material on Light-Water-Cooled Nuclear Power Reactor Effluents," Vol. 1-3, WASH-1258 (1973).
7. G. Whipple, Third Intern. Congr. of the Intern. Radiation Protection Association, Washington, 9-14 Sept., 1973, Rep. 156.
8. A. Hull, Nucl. News, 11, 53 (1972).
9. P. Pellerin, in: Proc. IAEA Symp. on Environmental Surveillance around Nuclear Installations, Warsaw, 5-9 Nov., 1973, Rep. SM-180/76.
10. J. Soldat et al., in: Proc. IAEA Symp. on Environmental Behavior of Radionuclides Released in the Nuclear Industry, Aix-en-Provence, France, 14-18 May, 1972, Rep. SM-172/82.
11. The Effect on Populations of Exposure to Low Levels of Ionizing Radiation, BEIR Rep., Washington, D. C., November, 1972.
12. C. Comar, Third Intern. Congr. of the Intern. Radiation Protection Association, Washington, 9-14 Sept., 1973, Rep. 1.
13. J. Crow, ibid., Rep. 2.
14. A. Upton, ibid., Rep. 3.
15. A. Hull, ibid., Rep. 158.

16. Environmental Radiation Dose Commitment: An Application to the Nuclear Power Industry, USA EPA-520/4-73-002, Washington (1974).
17. Reactor Safety Study. An Assessment of Accident Risks in US Commercial Nuclear Power Plants, USAEC, Washington (1974).
18. Licensing of Protection and Utilization Facilities, US-10-CFR-50, Federal Register, 36, No. 111 (1971).
19. Bo. Lindell, Proc. IAEA Symp. on Environmental Surveillance around Nuclear Installations, Warsaw, 5-9 Nov., 1973, Rep. SM-180/77.
20. N. G. Gusev et al., Third Intern. Congr. of the Intern. Radiation Protection Association, Washington, 9-14 Sept., 1973, Rep. 157.
21. N. G. Gusev and V. A. Belyaev, Proc. IAEA Symp. on Environmental Surveillance around Nuclear Installations, Warsaw, 5-9, Nov., 1973, Rep. 82.
22. V. A. Belyaev, in: Experience in Operation of Nuclear Power Stations and Path for Future Development of Nuclear Power [in Russian], Vol. II, Izd. FÉI, Obninsk (1974), p. 355.
23. V. A. Belyaev, in: International Conference on Physical Aspects of Atmospheric Contamination [in Russian], Vilnius, 18-20 June, 1974, p. 176.
24. P. Bryant, Proc. IAEA Symp. on Environmental Surveillance around Nuclear Installations, Warsaw, 5-9 Nov., 1973, Rep. 12.
25. F. Pasquill, Meteorolog. Mag., 90, 33 (1961).
26. F. Gifford, J. Appl. Meteorolog., 6, 644 (1967).
27. Application of Meteorology to Safety at Nuclear Plants, Safety Series, No. 29, IAEA, Vienna (1968).
28. N. E. Artemova, At. Énerg., 36, No. 1, 32 (1974).
29. Yu. I. Moskalev et al., Concept of Biological Risk for the Effect of Ionizing Radiation [in Russian], Atomizdat, Moscow (1973).
30. Radiosensitivity and Spatial Distribution of Dose (ICRP Publication 14) [Russian translation], Atomizdat, Moscow (1974).
31. Recent Advances in Nuclear Medicine, New York—London (1974).

CONTEMPORARY TRENDS IN EXPERIMENTAL SHIELDING PHYSICS RESEARCH

V. P. Mashkovich and S. G. Tsypin

UDC 621.039-78

The contribution of experimental research to the solution of problems in the physics of shielding against radiations has been decreasing in the last few years in comparison with theoretical and computational research. This change can be traced, for example, in [1, 2]. Thus 60% of the papers in the 1969 Symposium were devoted to calculational research, while in 1974 the number was 85%.

Moreover, the limitations of theoretical methods require experimental confirmation of the computational methods and the set of constants assumed. At the present time a number of problems cannot be solved by computational means because of limitations of the methods.

Contemporary experimental research in shielding physics is characterized by: 1) differentiation of the information obtained; 2) more and more attention to complex geometries (multidimensional and heterogeneous shields); 3) shift of some of the best understood parts of shielding to engineering practice.

All such experimental research can be divided into two groups: research on verifying computational methods and sets of interaction constants, which we call reference point research; mock-up experiments for solving problems which at the present time cannot be solved by computational means because of limitations in the computational methods or difficulties of the model representation. With the development of reference point experiments the statement that "calculation gives the necessary information — experiment the reference point" is becoming more and more valid.

The following are the most interesting reference point experiments on which experimentalists should concentrate their attention.

1) Basic experiments (benchmark type experiments). They should be performed under "clean," standard, very elementary conditions. At the present time it is desirable to perform basic experiments in multidimensional geometries.

2) Simulated experiments on actual nuclear-industrial installations such as reactors and accelerators to estimate the quality of the computational techniques under actual conditions. These measurements enable one to correct the methods and to introduce correction factors into the results of the calculations.

3) Full-scale experiments on actual nuclear-industrial installations. These experiments test the computational methods for solving the most complicated problems of making real shields. Full-scale experiments become much more complicated with increasing dimensionality of the geometry. This generally requires idealizing the problem, which in turn requires careful experimental testing of the admissibility of the assumed idealization and a determination of the errors introduced by such an idealization.

The main trends in radiation shielding research at the present time are listed below.

1. The Development of Theoretical Methods and Computer Programs for Calculating Distributions of Ionizing Radiations. In recent years special attention has been paid to the development of the Monte-Carlo method and the method of discrete ordinates. The complex of one-dimensional ROZ programs and the multi-group RADUGA program for two-dimensional reactor shield calculations form a good basis for solving many shielding physics problems. The MD and MDA methods are successful modifications of the

Translated from Atomnaya Énergiya, Vol. 38, No. 6, pp. 398-400, June, 1975. Original article submitted January 8, 1975.

Monte-Carlo method for calculating radiation fields. By using these methods radiation fields can be successfully predicted at large distances from sources, even at earth—air and vacuum—air boundaries.

It is gratifying that programs have appeared which satisfactorily predict distributions of high-energy particles and electrons. Computer programs have been developed for calculating radiation fields in inhomogeneous media such as shields with multisectional channels and voids, and for nonstationary problems.

2. Accumulation of Experimental and Computational Information on the Shaping of Radiation Fields in Shields. Specialized facilities have been built to study shields. A large amount of work has been done in building various experimental arrangements at reactors and charged particle accelerators. Converters for neutrons of various energies are interesting and seem promising for experimental research on reactor problems.

Gamma ray distributions have been investigated. A number of studies have been made of the spatial, angular, and energy distributions of gamma radiation for one-dimensional shield geometry. Interesting work has been done on the time dependence of radiation fields from pulsed gamma sources, and on deep penetration problems, mainly for elementary sources. Studies have been made of neutron and capture gamma distributions. Extensive information has been accumulated on the shaping of distributions of neutrons of various energies, including intermediate energies, and on capture gamma radiation in various media.

Gamma and neutron distributions have been studied in air and at earth—air and vacuum—air boundaries. These studies are distinguished by the systematic nature of the data and the performance of experiments at large distances from sources of various energies, including low-energy gamma sources.

Research on shielding high-energy particle accelerators has progressed considerably. The differential and integral characteristics of electrons beyond thick barriers have been studied intensively.

The study of albedos of gamma rays and neutrons from isotopic and reactor sources is largely complete. The problems of determining the characteristics of quasialbedo radiation have been studied to a lesser degree.

The penetration of radiations through shield inhomogeneities has been investigated: computational methods based on the use of constants for the macroscopic interaction of radiation with matter are well developed. Channels of basic shapes for radiations of various types and energies including intermediate neutrons have been examined. Great efforts have been directed toward the study of the shielding characteristics and radiation resistance of various concretes and structural materials which appear promising for use in shields.

3. Studies of Nuclear Constants. Interesting work has recently been done on the preparation of group constants and constants for calculations by the Monte-Carlo method. Many experimental investigations of the blocking of the resonance structure of the total group cross sections have been made. Interesting studies have been made of the choice of nuclear constants for calculating secondary radiation, and the effect of variations in the cross sections on neutron spectra. The problem of determining the nuclear constants for the interaction of heavy charged particles with matter has been studied seriously.

4. Study of Shields of Actual Nuclear-Industrial Installations. The specialists have paid a great deal of attention to reactor shields, to problems of the radiation safety of atomic power plants, the effectiveness of the biological shielding, the study of radiation fields in atomic power plant rooms, the radiation shield for refueling, and the prediction of the radiation shields required for maintenance and preventive inspections.

A number of problems in the physics of radiation shielding can now be considered essentially solved. Various specialized test stands and facilities have been built and widely used in the Soviet Union. Thus a large amount of important practical information has been obtained on an arrangement in the B-2 beam of the BR-5 reactor [3], on a fission neutron converter [4] and an intermediate neutron converter [5] of the BR-5 reactor, on test stands at the VVR-50 [6], the OR-M [6], and the RFZ [3].

We list the main problems for further theoretical and computational research in the physics of shielding against ionizing radiations from nuclear-industrial installations.

1. The creation of complex efficient computer programs for calculating problems in the physics of radiation shielding by using tested algorithms and programs for calculating radiation transport. Particular attention should be paid to the writing of programs for multidimensional geometries close to shields around actual nuclear-industrial installations.

2. The development of shield optimization programs which take account of primary and secondary radiations. It is clear that these problems cannot be solved without programs which combine various methods within the framework of a single program, in particular the Monte-Carlo and discrete ordinates methods.
3. The development of new semiempirical methods and concepts for calculating biological shields and predicting radiation fields in a shield and in the space surrounding it. These are convenient for performing engineering calculations and making estimates.
4. Investigations of macroscopic shielding constants for the interaction of radiations with matter, taking account of deep-penetration problems, and microscopic nuclear interaction constants.

We list the problems to be considered in completing these investigations.

Among the problems of shielding against ionizing radiations requiring further experimental research are:

1. New experimental test stands and facilities using well-known radiation sources similar to those of actual nuclear-industrial installations should be built for basic and simulated experiments.
2. Performing basic experiments to test the validity of computational methods and the sets of constants used for the interaction of radiations with matter.
3. Conducting full-scale experiments on actual nuclear-industrial installations to improve the computational methods and the design of biological shields. Special conditions must be provided for such studies.
4. Performing basic experimental research on the penetration of radiations through heterogeneous shields, the propagation of secondary and scattered radiations in media, the study of the energy and dose compositions of radiations of different forms in shields, the problems of deep penetration, and the problems of shield optimization. The simulated and full-scale experiments should include a study of the penetration of radiations through shield inhomogeneities.
5. The development and study of the properties of new, inexpensive, and promising heat- and radiation-resistant shielding materials with good shielding, physical, and chemical characteristics.

The important problems of radiation shielding include a study of ways of increasing the effectiveness and decreasing the cost of biological shields, the reliability of the shields around nuclear-industrial installations, the solution of the problem of decreasing the radiation dose to atomic power plant personnel during repair work, preventive inspections, etc.

The problems listed in one degree or another are involved in the shielding of various nuclear-industrial installations — sources of ionizing radiations — and should be studied as they apply to nuclear reactors of various classes and purposes, charged particle accelerators, irradiation facilities, devices and apparatus with sources of ionizing radiation, etc.

It is satisfying to note that a large group of specialists in our country is working on the problems of radiation safety. We look to this group for solutions of the problems posed.

LITERATURE CITED

1. Problems in Shielding against Penetrating Radiations from Reactor Installations. Collection. Vols. 1-7 [in Russian], SÉV, Melekass (1969).
2. Abstracts of papers "Problems in the Physics of Shielding Atomic Power Plant Reactors" [in Russian], SÉV, Moscow (1974).
3. Yu. A. Kazanskii et al., Physical Research in Reactor Shielding [in Russian], Atomizdat, Moscow (1966).
4. V. P. Mashkovich et al., Atomnaya Énergiya, 2, 125 (1967).
5. A. D. Lipunov et al., Atomnaya Énergiya, 6, 549 (1967).
6. V. G. Maleev et al., Paper presented at the first conference of specialists on problems of shielding atomic power plants "Problems in the Physics of Shielding Atomic Power Plant Reactors" [in Russian], Moscow (1974).

NUMERICAL SOLUTIONS OF THE KINETIC EQUATION FOR REACTOR SHIELDING PROBLEMS

T. A. Germogenova

UDC 621.039.51.12: 621.039.538

In recent years engineering calculations of shielding physics problems are being supplemented more and more by transport theory computations. These furnish detailed accurate information on the spatial, angular, and energy distributions of radiation fields in a reactor and shield. Radiation transport in a shield is treated mathematically either by using the Monte Carlo method or by solving multigroup systems which approximate the kinetic equation for radiation transport. Many numerical methods have been developed for solving such systems. The present paper reviews these methods.

1. As a rule different degrees of accuracy and detail are required in describing radiation fields in different parts of a shield and reactor. In a reactor the most important quantities are integral characteristics such as k_{eff}, the breeding ratio, the spectral distribution of fluxes etc., while for a shield it is also frequently necessary to know the angular distributions of the radiation fluxes.

By using the theorem on the equivalence of the solution of a boundary value problem for the multigroup transport equations in the complete reactor-shield system and its solution for individual regions of this system with corresponding boundary conditions [1], it is possible to reduce the original problem for a large complex system to a somewhat simpler one. For individual regions of the shield such a boundary value problem has the form

$$\frac{\partial \mathbf{F}_n}{\partial \Omega} + \hat{\Sigma}_n \mathbf{F}_n = \hat{\Sigma}_{n \to n} \mathbf{F}_n + \mathbf{q}_n; \tag{1}$$

$$\frac{\partial \mathbf{F}_\gamma}{\partial \Omega} + \hat{\Sigma}_\gamma \mathbf{F}_\gamma = \hat{\Sigma}_{\gamma \to \gamma} \mathbf{F}_\gamma + \hat{\Sigma}_{n \to \gamma} \mathbf{F}_n + \bar{\mathbf{q}}_\gamma; \tag{2}$$

$$\mathbf{F}_n|_{\text{in}} = \hat{R}_n [\mathbf{F}_n|_{\text{out}}] + \varphi_n, \quad \mathbf{F}_\gamma|_{\text{in}} = \hat{R}_\gamma [\mathbf{F}_\gamma|_{\text{out}}] + \hat{R}_{n\gamma} [\mathbf{F}_n|_{\text{out}}] + \varphi_\gamma.$$

Here $\mathbf{F}_n$ and $\mathbf{F}_\gamma$ are vector functions whose components describe the spatial and angular distributions of fluxes in the corresponding groups; $\hat{\Sigma}_n$ and $\hat{\Sigma}_\gamma$ are diagonal matrices with elements $\Sigma_i(\mathbf{r})$ corresponding to the total cross sections for the interaction of radiation with matter; $\hat{\Sigma}_{n \to n}$, $\hat{\Sigma}_{n \to \gamma}$, and $\hat{\Sigma}_{\gamma \to \gamma}$ are triangular matrices with elements corresponding to the integral scattering operators:

$$(\hat{\Sigma}\mathbf{F})_i = \sum_{j=1}^{Q} \int \Sigma_{ij}(\mathbf{r}, \mu_s)\, \mathbf{F}(\mathbf{r}, \Omega')\, d\Omega', \quad \mu_s = \Omega\Omega'.$$

The functions $\Sigma_i(\mathbf{r})$ and $\Sigma_{ij}(\mathbf{r}, \mu_s)$ are piecewise constant functions of $\mathbf{r}$. The elements of the matrices $\mathbf{R}$ in (2) are integral reflection coefficients (albedos), and the functions φ_n and φ_γ describe the radiation incident on the outer surface of the volume under consideration.

At the present time we are concerned mainly with numerical solutions of one- and two-dimensional forward and adjoint problems. The algorithms and programs developed for solving such problems and combinations of them by Monte Carlo methods, with perturbation theory for taking account of three-dimensional effects, suffice for a broad circle of practical shielding physics problems.

2. Any numerical method for solving the multigroup system of equations (1) has two aspects: a method for approximating the problem, and a method for solving the high-order linear algebraic system arising in the approximation.

A successful approximation can be achieved only by understanding and taking correct account of the qualitative behavior and the singularities of the solution related to the discontinuities of the coefficients

Translated from Atomnaya Énergiya, Vol. 38, No. 6, pp. 401-405, June, 1975. Original article submitted January 8, 1975.

TABLE 1. Singularities of First Iterations in Problems with Concentrated Sources

Iteration	Source: point monodirectional, $\delta(\Omega-\Omega_0)\,\delta(r-r_0)$	point distributed, $\delta(r-r_0)$	line monodirectional, $\delta(\Omega-\Omega)\,\delta(x)\,\delta(y)$	line distributed, $\delta(x)\,\delta(y)$	plane monodirectional, $\delta(\Omega-\Omega_0)\,\delta(z)$	plane distributed, $\delta(z)$
0	$\delta(\Omega-\Omega_0)\times\delta\left(\frac{r-r_0}{\lvert r-r_0\rvert}-\Omega_0\right)$	$\frac{\delta\left(\frac{r-r_0}{\lvert r-r_0\rvert}-\Omega\right)}{\lvert r-r_0\rvert^2}$	$\frac{\delta(\varphi-\varphi_0)\,\delta(\Omega-\Omega_0)}{\sqrt{x^2+y^2}}$	$\frac{\delta(\varphi-\varphi_\Omega)}{\sqrt{x^2+y^2}}$	$\frac{e^{-\frac{z}{\Omega e_z}}\,\delta(\Omega-\Omega_0)}{\Omega e_z}$	$\frac{e^{-\frac{z}{\Omega e_z}}}{\Omega e_z}$
1	$\frac{\delta(\varphi-\varphi_0)}{\sqrt{\lvert r-r_0\rvert^2-(r-r_0,\,\Omega_0)^2}}$	$[\lvert r-r_0\rvert^2-(r-r_0,\,\Omega)^2]^{-1/2}$	$\frac{1}{(\varphi-\varphi_0)\sqrt{x^2+y^2}}$	$\ln[(\varphi-\varphi_\Omega)\sqrt{x^2+y^2}]$	—	—
2	$\ln\frac{\varphi-\varphi_0}{\sqrt{\lvert r-r_0\rvert^2-(r-r_0,\,\Omega_0)^2}}$	$\ln[\lvert r-r_0\rvert^2-(r-r_0,\,\Omega)^2]$	$\ln[(\varphi-\varphi_0)\sqrt{x^2+y^2}]$	—	—	—

in system (1) and the functions describing the radiation sources. These singularities of the solution cause oscillations in finite-difference methods.

Discontinuities in the functions φ and q are preserved only in the distribution of the unscattered part of the radiation; the intensity of the scattered radiation is a smooth function. The singularities in the intensity of the scattered radiation of the first few orders in problems with lumped sources [2] are given in Table 1. Obviously the analytic elimination of the most essential singularities in such problems is most effective.

Discontinuities in derivatives and in the solution itself arising from discontinuities in the coefficients of the multigroup system (1) are more complicated. At boundaries separating different materials these discontinuities are retained in the scattered radiation of all orders. Along straight lines tangent to the boundaries the spatial and angular derivatives of the solution have singularities. If the curvature of the surface is zero discontinuities in the solution itself arise along the corresponding tangents [3].

The analytical results obtained in the asymptotic study of a number of model problems play an important role in the development of computational methods in transport theory. Although such problems are far from real, studying them on the one hand gives a qualitative idea of the solution, and on the other hand enables one to construct tests to appraise the computational algorithms and check programs. This is very complicated in real programs. Solutions of problems for infinite and semiinfinite media are widely used for this purpose [4-6]. Recently certain successes have been achieved in constructing asymptotic formulas in one- and two-dimensional one-group problems for bounded media.

In problems on the penetration of radiation through plane homogeneous and inhomogeneous layers of finite thickness formulas have been found for the reflection and penetration of radiation and the conditions inside the layer far from the boundaries. These formulas contain a number of one-dimensional functions and parameters determined by the scattering indicatrix and the value of $\lambda = \Sigma_s/\Sigma_t$ [7-9]. These functions and parameters are found from the numerical solution of one-dimensional integral equations. The accuracy of the asymptotic formulas is adequate for a wide range of problems for layers several mean free paths in thickness and increase rapidly with increasing layer thickness.

Some analytical results have been obtained recently in studies of two-dimensional one-group problems. Thus in the problem of a point source in a sufficiently thick slab the Wigner effect in the angular distributions arising from multiple scattering was estimated. As a result of this effect a detector moved along the surface of a slab records the maximum of the radiation intensity in a direction which does not coincide with the direction of the source. There is a peculiar refraction of the radiation as a result of multiple scattering. Theoretical estimates have been confirmed by a number of numerical calculations (L. P. Bass et al.).

Lam and Leonard [10] have investigated certain properties of radiation fields in multidimensional models and have analyzed in detail the solution of the transport equation in the neighborhood of a boundary surface of complex shape on the basis of the Milne problem for four-space.

3. In one-dimensional problems, particularly in problems with plane geometry, qualitative ideas of local properties of the solution and its asymptotic behavior are widely used in an algebraic approximation of the problem, both in finite-difference methods and in various semianalytic treatments. In the latter,

auxiliary functions and parameters are ordinarily determined by using variational functionals of the problem or various averages. The most used methods (discrete ordinates, spherical harmonics, Carlson, synthetic etc.) are described in well-known monographs and summary articles [10-11]. However, the more complicated the problem posed, i.e. the greater the demand for accuracy and detail in the information on the flux distributions, the more complicated the geometrical and physical models, and correspondingly the simpler the approximation methods that have to be used. Thus in determining the differential distributions of neutrons and gamma rays in plane heterogeneous shields the method of discrete ordinates is the most reliable, while in curvilinear one- and two-dimensional geometries the method of characteristics with linear interpolation in which the singularities of the solution are taken into account in a natural way [12-14] is preferred. The method of characteristics is stable for any ratio of stops, but because of linear interpolation it is only first order accurate.

The S_N and DS_N methods, based on the use of balance relations in the cells of the mesh, are second-order accurate for smooth solutions and are generally simpler to use. As a rule they lead to instabilities in the calculations, particularly often to oscillations in the angular distributions [15-17]. Various methods have been proposed by a number of authors for eliminating the oscillations in quantities integral in the angular variable. Among such methods we note the introduction of fictitious sources into the DS_N equations approximating problem (1) and (2) to ensure that these equations are equivalent to the method of spherical harmonics (DOPL method [18, 19]), and the use of variational principles to formulate various schemes, in particular the method of finite elements [20].

It seems to us that in complex problems it is most expedient first to remove the singularities in the solution, and to choose the form of approximation, in particular the shapes and sizes of the mesh cells, in accord with the behavior of the solution, and then to use composite schemes which are first-order accurate (the type used in the method of characteristics) along the "singular" straight lines with balance methods in the regions where the solutions are smooth. Examples of such composite schemes are the BOX method [21], the methods proposed in [22], and a combination of the "rhombic" scheme (second order) with the "step" scheme (first order) [23].

While the theory of the method of characteristics is rather simple, estimates of the stability and convergence of balance methods, and even more of combinations of different methods, are only in the initial stage. As a rule authors make very rigid assumptions about the differential properties of the solutions. These assumptions are not satisfied in real transport theory problems. However, we have accumulated considerable experience with numerical solutions of various boundary problems of the type (1), (2).

4. As a result of approximation the original problems (1) and (2) are reduced to inhomogeneous linear systems, generally of very high order p. In one-group one-dimensional problems $p \approx 10^3$-10^4, and in two-dimensional problems $p \approx 10^5$-10^7. An iterative method is generally used to solve such systems. In its primitive form this method, which corresponds to successively taking account of the fluxes of unscattered, singly scattered, doubly scattered etc. radiation, has been significantly improved in recent years by the introduction of various methods for accelerating the convergence. Such methods are particularly important for large regions where the simple iterative method converges very slowly. The most effective methods alternate simple iteration with solutions of equations of lower dimensionality for average quantities appearing as correction factors (quasidiffusion and flux average methods [7]) or components (KR methods [11]). The equations for these quantities are obtained by averaging over the angular variables of problem (1) and (2), or by using appropriate variational functionals.

The proper choice of the parameters defining the mesh size and the duration of the iterative process plays a fundamental role in the solution of practical problems. In shielding physics problems these parameters depend strongly on the class of problems, i.e. on the physical and geometrical models and on the required accuracy in the differential distributions. As a rule the choice of parameters is based on intuitive considerations. Recently, however, papers have appeared in which attempts were made to change from intuition to quantitative rules. Thus V. A. Utkin examined a class of iron—water slab shields and studied in detail the nature of the convergence of methods such as the method of discrete ordinates. Problems of the accuracy of the $2P_N$ approximations in one-velocity problems with various indicatrixes are discussed in [24].

5. We have written two complexes of computer programs to solve the multigroup systems (1) and (2): ROZ to calculate one-dimensional transport theory problems, and RADUGA to solve the two-dimensional transport equations in axisymmetric systems. A large staff participated in the development of these complexes.

The methods of solution were chosen to yield high accuracy and detailed information on the spatial, energy, and angular distributions of radiations. The algorithms used are based on the method of discrete ordinates in plane geometry and the method of characteristics with interpolation in curvilinear geometries. The finite-difference equations were solved by an iterative method with acceleration of convergence in one-dimensional problems by the method of flux averages, and in two-dimensional problems by a quasi-diffusion procedure.

Among the one-dimensional programs the ROZ-6 program has the broadest possibilities. It enables one to treat various forward and adjoint problems: to calculate various functionals, derivatives of solutions with respect to parameters, etc.

The apparatus of adjoint solutions can be used to lower the geometric dimensions of a problem to dimensions determined by the properties of the medium and the character of the required functionals, independently of the form of the source. Thus a two-dimensional problem on determining the sensitivity of a spherical detector is equivalent to a one-dimensional adjoint problem of a point isotropic source at the center of the sphere.

This problem was solved by using a spherical variant of the ROZ-1 program [25].

In contrast with the universal ROZ-6 program, which is suitable for solving a very broad class of shielding physics problems, the ROZ-7 and ROZ-8 programs were designed to solve special problems. The ROZ-7 program (M. V. Vyrskii) was written to calculate multilayer slab shields in the age-diffusion approximation with a very large number of nodes in the energy variable. The ROZ-8 program (N. V. Konovalov) was used to calculate asymptotic parameters and functions and the resulting distributions of radiation in thick multilayer slab shields in the one-velocity approximation with very broad assumptions about the scattering and absorption characteristics.

The complex of RADUGA programs was written as a modulator system for a BÉSM-6 computer to generate programs for solving axisymmetric problems of the type (1) and (2) in heterogeneous cylindrical regions for arbitrary irradiation conditions and internal source distributions. The variety of geometrical models, source shapes, types of boundary conditions, and elementary types of interaction of radiation with matter necessitate extremely complex and diverse algorithms for calculating radiation fields in such systems. The algorithms are combinations of independent elementary parts of basic elements. A specified set of basic elements determines the content of the algorithm, and the memory parameters fix its scale. The important features ensuring high efficiency of specific programs are the hierarchy of equations for taking account of various qualitative properties of the solution at various levels, and an algorithm for the storage of parameters making possible a wide variation in mesh size.

The RADUGA systems uses a library of basic elements and a library of input parameters and mathematical information for the BÉSM-6 computer [26]. The ROZ and RADUGA complexes were used in solving many shielding-physics problems. The results of a number of calculations have been reported in the literature. An important feature in preparing for calculations is the specification of group constants determining the coefficients in problem (1), (2). The well-known ARAMAKO [27] and OBRAZ [28] programs for calculating constants are being added to the ROZ and RADUGA complexes.

LITERATURE CITED

1. T. A. Germogenova et al., Neutron Albedo [in Russian], Atomizdat, Moscow (1973).
2. T. A. Germogenova, Preprint No. 23 [in Russian], Institute of Applied Mathematics, AN SSSR (1971).
3. T. A. Germogenova, Dokl. Akad. Nauk SSSR, 187, 18 (1969).
4. M. Maslennikov, Atomic Energy Rev., 5, 59 (1967).
5. K. Case and P. Zweifel, Linear Transport Theory, Addison—Wesley, Reading (1967).
6. V. V. Sobolev, The Scattering of Light in Planetary Atmospheres [in Russian], Nauka, Moscow (1972).
7. T. A. Germogenova et al., The Transport of Fast Neutrons in Slab Shields [in Russian], Atomizdat, Moscow (1971).
8. T. A. Germogenova and N. V. Konovalov, Zh. Vychisl. Mat. i Mat. Fiz., 14, 928 (1974).
9. N. V. Konovalov, Preprint No. 65 [in Russian], Institute of Applied Mathematics; AN SSSR (1974).
10. S. Lam and A. Leonard, Transport Theory and Statistical Physics, Vol. 3, No. 1 (1973).
11. G. I. Marchuk and V. I. Lebedev, Numerical Methods in the Theory of Neutron Transport [in Russian], Atomizdat, Moscow (1972).
12. Handbook on Radiation Shielding for Engineers [in Russian], Vol. 1, Atomizdat, Moscow (1972), p. 84.

13. T. A. Germogenova and L. P. Bass, in: Problems in the Physics of Reactor Shielding [in Russian], No. 3, Atomizdat, Moscow (1969), p. 69.
14. K. Takenchi and A. Jamaji, in: Proceedings of the Fourth International Conference on Reactor Shielding, Vol. 2, Paris (1972), p. 339.
15. V. Hankin et al., JQSRT, 11, 949 (1971).
16. K. Lathrop, Nucl. Sci. and Engn., 45, No. 3 (1971).
17. W. Reed, Nucl. Sci. and Engng., 46, 309 (1971).
18. J. Jung et al., Nucl. Sci. and Engng., 49, 1 (1972).
19. J. Jung et al., Nucl. Sci and Engng., 53, 355 (1974).
20. W. Miller et al., Nucl. Sci. and Engng., 52, 12 (1973).
21. J. Arkuszewski et al., Nucl. Sci. and Engng., 49, 20 (1972).
22. V. Ya. Gol'din et al., Zh. Vychisl. Mat. i Mat. Fiz., 5, No. 5 (1965).
23. K. Lathrop, J. Comput. Phys., 4, 475 (1969).
24. Sh. S. Nikolaishvili and V. P. Polivanskii, in: Problems in the Physics of Reactor Shielding [in Russian], No. 5, Atomizdat, Moscow, p. 47; Yu. K. Shchekin, Izv. AN BSSR, Ser. Fiz. i Énerget., No. 2 (1971).
25. V. A. Utkin, in: Problems in the Physics of Reactor Shielding [in Russian], No. 6, Atomizdat (1974), p. 150.
26. L. P. Bass et al., Preprint No. 11 [in Russian], Institute of Applied Mathematics, AN SSSR (1973).
27. V. F. Khokhlov et al., in: Nuclear Constants [in Russian], No. 8, Part 3, TsNII Atominform (1972), p. 3.
28. V. F. Khokhlov et al., Nuclear Constants [in Russian], No. 8, Part 4, TsNII Atominform (1972), p. 154.

BOOK REVIEWS

Yu. A. Egorova (editor)

PROBLEMS OF THE PHYSICS OF REACTOR SHIELDING*

Reviewed by B. R. Bergel'son

It is more than 10 years since the collection "Problems of the Physics of Reactor Shielding" was published. In it questions are reflected concerning the problems of shielding nuclear-technological installations from radioactive radiations. The data contained in the six issues of the collection are obviously of interest to engineers and scientific workers working in the most diverse branches of science and technology. In four sections of the sixth edition, more than 30 papers are assembled.

In the first section, devoted to the theory of radiation transfer and methods of calculating shielding, the papers of a team fruitfully working under the direction of T. A. Germogenova are traditionally presented. Among them, the most interesting is a paper in which the advantages are discussed of a method of subgroups for calculating the resonance structure of the neutron cross-sections. In the two papers by V. G. Zolotukhin et al., the possibilities of the Monte Carlo method are shown for calculations of the radiation field at large distances from the source and during the passage of γ-radiation through curved channels. Two papers are devoted to practical methods of calculation and to the problem of shielding optimization. A nonstandard approach to the problem is demonstrated in the paper by É. E. Petrov and B. L. Shemetko, in which the authors used the device of small perturbation theory in order to determine the radiation scattered by screens of small thickness.

In the second section, the results of the experimental investigation of different shields are recounted and in the third section, a paper with a methodological leaning. Amongst these papers may be mentioned the paper by A. L. Barinov et al., concerning the results of a detailed measurement of the absolute fluxes and spectra of the fast neutrons in front of and behind the hull of the VVÉR-440 reactor and the paper by V. I. Avaev and E. P. Efimov, devoted to the inadequately developed problem of determining radiation energy releases in metal structures in those cases when the γ-emission spectrum is formed in the surrounding light medium. The paper by V. V. Bolyatko et al. is interesting, in which the passage of neutrons of intermediate energy through shielding with inhomogeneities is investigated.

In the fourth section of the collection, there are three papers devoted to an investigation of concretes as materials for the biological shield of reactors.

Usually, in experimental papers devoted to the measurement of the spectrum of radiation which has passed through shielding screens, the conditions of the experiment are not discussed completely: the geometry, source and detector characteristics. This complicates or even makes impossible the use of the results of the experiment by a wide circle of readers for solving other problems and for verifying computational programs.

These publications frequently are found to be useful mainly only for a small circle of workers. In this sense, some experimental papers described in this collection are no exception.

At the recently constituted All-Union Conference on Shielding from Ionizing Radiations, many participants spoke of the necessity for carrying out so-called test-experiments, according to the results of which comparisons of the numerous computational programs might be undertaken. It can be hoped that, in the near future, these experiments will be carried out and their results, with a detailed description of the experimental conditions, will be published in subsequent issues of the collection.

*Atomizdat, Moscow, 1974.

Translated from Atomnaya Énergiya, Vol. 38, No. 6, p. 405, June, 1975.

In conclusion, the editorial board of the collection, during preparations for the publication of new issues may desire to attract a wider circle of authors, by informing them beforehand of the issues being prepared.

ARTICLES

PROBLEMS OF SECONDARY GAMMA RADIATION IN REACTOR SHIELDS

A. A. Abagyan, T. A. Germogenova,
A. A. Dubinin, V. I. Zhuravlev,
V. A. Klimanov, E. I. Kostin,
V. P. Mashkovich, V. K. Sakharov,
and V. A. Utkin

UDC 621.039.534.7

A nuclear reactor shield is a complex system of materials of low atomic numbers to attenuate neutrons, and materials of high atomic numbers to attenuate gamma rays. Both heterogeneous and homogeneous mixtures of heavy and light materials occur in a real shield. To minimize the total shield weight the heavy component of the shield must be placed close to the core. As a rule the shielding layers close to the core consist of metal neutron shields, which leads to the production of intense secondary gamma radiation.

The radiation environment outside a reactor shield is frequently determined completely by secondary gamma radiation. Knowledge of the characteristics and rules of its propagation in a medium enable one to

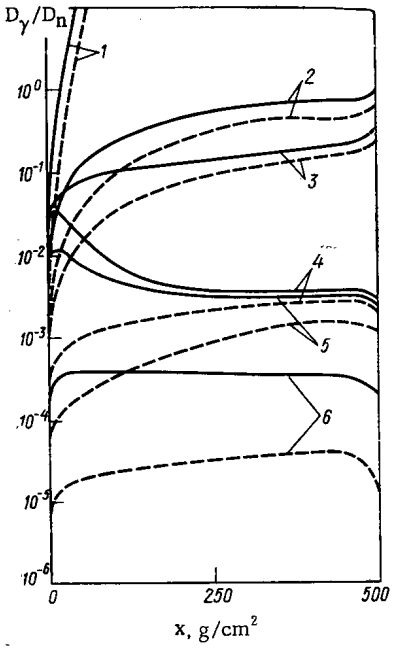

Fig. 1

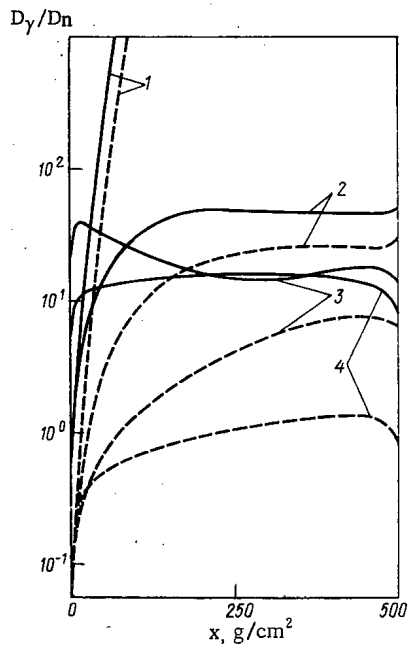

Fig. 2

Fig. 1. Relative doses of capture gamma radiation: ----) neutron source with a fission spectrum; ——) neutron source with a fission spectrum for E > 2.5 MeV and a 1/E spectrum for E < 2.5 MeV; 1) water; 2) zirconium hydride; 3) concrete; 4) tungsten; 5) iron; 6) lead.

Fig. 2. Relative heat deposition of capture gamma radiation (notation same as in Fig. 1): 1) water, 2) zirconium hydride; 3) iron; 4) lead.

Translated from Atomnaya Énergiya, Vol. 38, No. 6, pp. 406-409, June, 1975. Original article submitted January 8, 1975.

TABLE 1. Shield Thickness for which $D_\gamma = D_n$ for a Neutron Source with a Fission Spectrum

Material	l_D, cm
H	50
LiH	67
H_2O	36
H_2O + 1 wt. % B	54
C	90
C + 1 wt. % B	100

choose the optimum location of shielding layers close to the core and in more distant regions. Therefore the study of the characteristics of secondary gamma radiation is very important in the reactor shielding problem.

This problem has been the subject of considerable experimental and theoretical research. However, most of the papers, the basic results of which are described in [1, 2], do not describe the fields of secondary gamma radiation over the whole range of energies, and therefore the published data cannot always be used in calculations.

The purpose of the present article is to present a systematic investigation of certain general principles of the production, escape, and propagation of secondary gamma radiation in a shield on the basis of experimental and computational data on the differential and integral characteristics of secondary gamma radiation in a broad selection of shielding materials for various neutron spectra. The calculations were peformed with the ROZ-5 program [3, 4]. The neutron flux density in the q-th energy group $\Phi_n^q(x, \mu)$ and the gamma flux density in the i-th energy group $\Phi_\gamma^i(x, \mu)$ are determined as functions of the coordinate x and the angle $\theta = \cos^{-1}\mu$ for plane one-dimensional geometry and azimuthal symmetry by the system of equations

$$\mu \frac{\partial \Phi_n^q}{\partial x} + \Sigma_t'^q(x)\,\Phi_n^q(x, \mu) = \sum_{p=1}^{Q} \int_{-1}^{+1} d\mu' \Phi_n^p(x, \mu')\, g_n^{p \to q}(x, \mu' \to \mu);$$

$$\mu \frac{\partial \Phi_\gamma^i}{\partial x} \mu_\gamma^i(x)\,\Phi_\gamma^i(x, \mu) = \sum_{j=1}^{I}{}' \int_{-1}^{+1} d\mu' \Phi_\gamma^j(x, \mu')\, q_\gamma^{j \to i}(x, \mu' \to \mu)$$

$$+ \sum_{q=1}^{Q}{}' S^{q \to i}(x) \int_{-1}^{+1} d\mu' \Phi_n^q(x, \mu')$$

with the boundary conditions

$$\begin{cases} \Phi_n^q(x, \mu) = \Phi_{n_0}^q(\mu) \\ \Phi_\gamma^i(x, \mu) = \Phi_{\gamma_0}^i(\mu) \end{cases} \quad \text{for} \quad x = 0 \text{ and } \mu > 0;$$

$$\begin{cases} \Phi_n^q(x, \mu) = 0 \\ \Phi_\gamma^i(x, \mu) = 0 \end{cases} \quad \text{for} \quad x = H \text{ and } \mu < 0.$$

Here Σ_t^q and μ_γ^i are the group averaged macroscopic cross sections for the interaction of neutrons and gamma rays with matter; $g^{p \to q}$ and $g^{j \to i}$ are the neutron and gamma ray scattering indicatrixes; $S^{q \to i}$ is the yield of gamma rays of group i in the interaction of neutrons of group q with matter. The ROZ-5 program solves the equations presented by the method of characteristics. The finite difference equations are solved by an iterative technique using the method of nonlinear acceleration of convergence [5]. A comparison of the calculated and experimental results showed that the ROZ-5 program gives adequate accuracy. The maximum divergences are 25% in the integral and about 40% in the differential characteristics of the radiation field [6].

In the present paper we consider the relative characteristics of capture gamma rays beyond shielding layers of various materials, defined as the ratio of the functionals resulting from capture gamma rays to the functionals resulting from neutrons. For heavy shields those characteristics are practically independent of the angular distribution of neutrons at the inside of the shield for a broad class of azimuthally symmetric angular distributions of the neutron sources, and therefore the basic information was obtained for infinite plane monodirectional sources.

Abagyan et al. [5] investigated the effect on the fluxes of secondary gamma radiation in a tungsten slab shield of taking account of the dependence of the capture gamma spectrum on the energy of the absorbed neutrons. They found that the relative characteristics of capture gamma rays differ by 30-40% from the values calculated by using the spectrum of gamma rays accompanying thermal neutron capture for all neutron groups. In addition the analysis of the original data showed that the total gamma energy emitted in the radiative capture of neutrons with energies in the range 10-100 keV differed by just such an amount from the energy of the gamma rays emitted in the radiative capture of thermal neutrons. It can

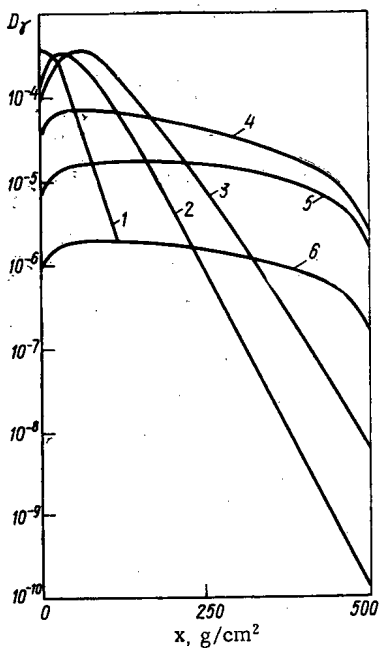

Fig. 3

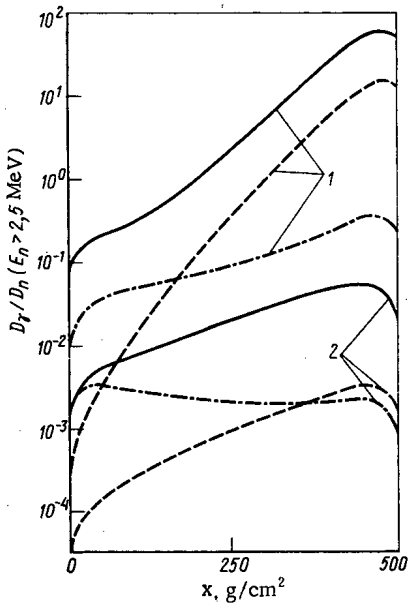

Fig. 4

Fig. 3. Doses of capture gamma radiation from the irradiation of a slab by a unit current of neutrons having a fission spectrum. The notation on the curves is the same as in Fig. 1.

Fig. 4. Relative doses of secondary gamma radiation: ----) capture gamma radiation from a neutron source with a fission spectrum; ——) capture gamma radiation from a neutron source having a fission spectrum for E > 2.5 MeV and a 1/E spectrum for E < 2.5 MeV; -·-·-) gamma radiation accompanying the inelastic scattering of neutrons from a source having a fission spectrum; 1) iron; 2) lead.

be assumed that the main inaccuracies in the calculation of the integral characteristics of capture gamma radiation at the exit from a layer of heavy shielding material are due to the error in taking account of the contribution to the capture gamma radiation of the various isotopes of a mixture of isotopes.

The rules for the production and escape of capture gamma radiation are of a completely different character for light and heavy shield materials. Light shielding materials are typically characterized by a strong dependence of the relative characteristics of the capture gamma rays on the neutron spectrum at the inside of the shield. The relative characteristics in the first approximation are inversely proportional to the fraction of fast neutrons in the source spectrum. All the relative characteristics of capture gamma rays (relative dose, flux, heat deposition) increase exponentially with the increase in thickness of a layer of light shielding material and for a certain thickness l become larger than unity. Naturally this thickness depends on the form of the functional, the shielding material, and the neutron spectrum at the inside of the shield. It is smaller the softer the neutron source spectrum.

Table 1 lists values of the thickness of the layer of light shielding material l_D for which the capture gamma dose rate is equal to the neutron dose rate just outside a slab irradiated by neutrons having a fission spectrum.

The fission spectrum is one of the hardest spectra encountered in reactor shielding calculations, and light materials, which effectively attenuate the neutron flux, have little effect on the gamma radiation. Therefore the values of l_D listed in the table determine approximately the maximum thickness of the outermost shielding layer of light material.

In heavy materials, in contrast with light materials, the neutron spectrum is not established until the layer is thick, and the gamma radiation is strongly attenuated by the material. These features of heavy materials cause all the relative characteristics of the capture gamma rays in media with a large atomic weight either to decrease with the thickness of the shielding layer (for a soft initial neutron spectrum) or

to increase with the thickness of the shielding layer (for a hard initial neutron spectrum) but much more slowly in comparison with the corresponding characteristics for light media. A peculiarity of the relative characteristics (Figs. 1 and 2) is the convergence of their values corresponding to different neutron source spectra as the layer thickness is increased. This convergence is different for different materials and is determined largely by the value of the radiative capture cross section.

Materials having both heavy and hydrogen nuclei in their composition (metal hydrides, concretes) are similar to light shielding materials from the point of view of shaping the neutron spectrum, but unlike light materials they have large gamma absorption cross sections. The transport of gamma radiation in these materials is similar to that in heavy materials, and the gamma field at any point in the medium is determined largely by the gamma sources in the immediate vicinity. It is typical of heavy hydrogenous materials that the realtive characteristics of capture gamma radiation increase with the layer thickness for all types of neutron spectra at the inside of the shield, but this increase is appreciably slower than in light shielding materials.

An analysis of the relative (Figs. 1 and 2) and absolute (Fig. 3) values of the characteristics of capture gamma radiation for various shielding materials leads to the conclusion that the best materials from the point of view of minimum escape of capture gamma radiation are heavy hydrogeneous materials. Lead is the best of the heavy nonhydrogeneous materials. The choice of any other material for a heavy shield is determined by the neutron spectrum at the inside of the shielding layer and the required thickness of this layer.

Studies were also made of the contribution to the various functionals of secondary gamma radiation from the inelastic scattering of neutrons in iron and lead. As can be seen from Fig. 4 this radiation makes an appreciable contribution to the characteristics only for hard initial neutron spectra and thin shielding layers. However, in sufficiently thick layers of materials such as lead with a small radiative capture cross section over the whole range of neutron energies, the contribution of inelastic scattering gammas can be comparable with that of capture gammas.

The differential characteristics of capture gamma radiation are also significantly different for light and heavy media. The energy spectrum of capture gamma radiation in light materials is complex. It is continuously deformed as the thickness of the shielding layer is increased, and for thicknesses greater than 40 g/cm^2 it has the same shape as in an infinite medium. It is typical of heavy materials that the gamma spectrum varies slowly with increasing shield thickness. The shape of the gamma spectrum in such shields is similar to that resulting from the radiative capture of neutrons from a source having a soft spectrum, since multiply scattered gammas make a small contribution. The angular distribution of capture gamma rays at exit from a shielding layer of light material is strongly anisotropic and varies with the layer thickness. In heavy materials the angular distribution is significantly less anisotropic and varies slowly with the layer thickness.

LITERATURE CITED

1. Yu. A. Kazanskii et al., Physical Investigations of Reactor Shields [in Russian], Atomizdat, Moscow (1966).
2. D. I. Broder, K. K. Popkov, and S. M. Rubanov, A Compact Reactor Shield [in Russian], Atomizdat, Moscow (1967).
3. T. A. Germogenova, A. P. Suvorov and V. A. Utkin, in: Problems in the Physics of Reactor Shielding, No. 2 [in Russian], Atomizdat, Moscow (1966), p. 22.
4. V. I. Zhuravlev et al., The Solution of the Transport Equation in Slab Problems (ROZ-5 Program), Part 1 [in Russian], Preprint IPM SSSR (1972).
5. A. A. Abagyan et al., Fourth International Conference on Reactor Shielding, Paris, October 9-13, 1972, Paper No. 13-2, 18.
6. A. A. Abagyan et al., in: Abstracts of papers of the All-Union Scientific Conference on Shielding against Ionizing Radiations from Nuclear-Industrial Installations [in Russian], MIFI, Moscow (1974), p. 28.

ABSTRACTS

EFFECT OF PROTON IRRADIATION ON THE OPERATION OF A SCINTILLATION COUNTER

B. V. Gubinskii, É. M. Iovenko,
V. A. Kuz'min, V. G. Mikutskii,
and V. N. Nikolaev

UDC 539.1.074.3

The effects of proton irradiation (E_p = 18 MeV, flux $\Phi = 6 \cdot 10^{10}$ and $6 \cdot 10^9$ cm^{-2}, density $2 \cdot 10^4$ cm^{-2} ·sec^{-1} and E_p = 360 MeV, $\Phi = 10^6$, $8 \cdot 10^6$, and $1.46 \cdot 10^7$ cm^{-2}, density $1.05 \cdot 10^5$ cm^{-2} ·sec^{-1}) on an NaI(Tl) crystal were studied.

The changes taking place in the counting characteristics, the differential spectrum, and the position of the photopeak corresponding to the γ-radiation of ^{137}Cs (recorded before and after irradiation of the crystal) were estimated. The original counting characteristics were determined for an energy-discrimination threshold of U_g = 20, 40, and 60 keV.

Figures 1 and 2 show the counting characteristics measured before and a time Δt after irradiation of the crystals and the character of the changes taking place in these characteristics respectively.

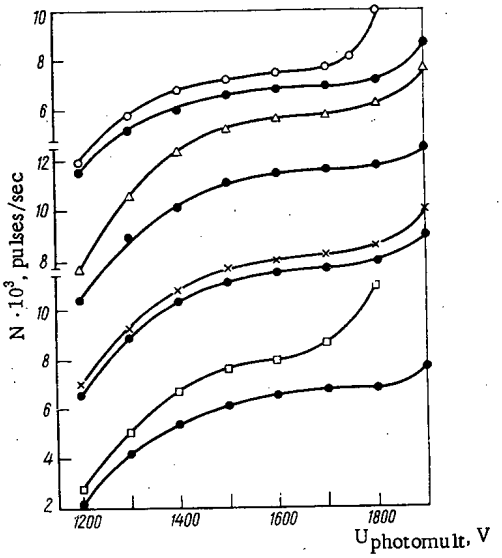

Fig. 1

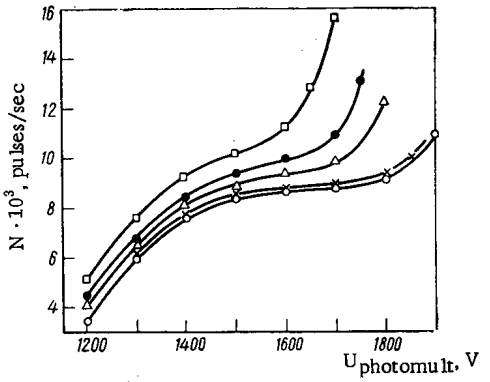

Fig. 2

Fig. 1. Counting characteristics of an FÉU-70 + NaI(Tl) scintillation counter before and after irradiation of the crystals: ●) characteristics before irradiation □) Δt = 6 min, E_p = 360 MeV, $\Phi = 8 \cdot 10^6$ cm^{-2}, U_g = 40 keV (No. 580); ×) Δt = 6 min, E_p = 360 MeV, $\Phi = 10^6$ cm^{-2}, U_g = 40 keV (No. 592); Δ) Δt = 4 min, E_p = 100 MeV, $\Phi = 4.1 \cdot 10^{-7}$ cm^{-2}, U_g = 20 keV (No. 624); ○) Δt = 8 min, E_p = 18 MeV, $\Phi = 6 \cdot 10^9$ cm^{-2}, U_g = 40 keV (No. 712).

Fig. 2. Counting characteristics of an FÉU-70 + NaI(Tl) scintillation counter obtained at various times Δt after the irradiation of crystal No. 605 with 300 MeV protons at a flux of $1.46 \cdot 10^7$ cm^{-2}: ○) original; □, ●, Δ, ×) Δt = 8; 35; 80; 270 min respectively.

Translated from Atomnaya Énergiya, Vol. 38, No. 6, pp. 411-417, June, 1975.

Analysis of the resultant data shows that after proton irradiation the most important change which occurs in the counting characteristic is an upward displacement of the latter. This may be associated with the development of induced activity (characterized by the emission of γ-quanta and β-particles with a mean energy of the order of 1 MeV and a mean half life of 30-40 min) in the crystal and the sheath around it. The radioactive nuclei arising in the crystal may be identified, for example, on the basis of the probability of star formation at the heavy and light nuclei under the influence of the protons. These nuclei include ^{122}I, ^{124}I, ^{126}Sb, ^{125}Sn, ^{123}Sn, ^{24}Na, ^{18}F, ^{29}Al, ^{120}S.

Thus for the irradiation fluxes studied the change in the slope of the plateau is very slight, and has no serious effect on the operation of the scintillation counter. The counting error associated with irradiation diminishes with time and is no greater than about 5% some 2-3 h after the end of irradiation, depending on the particular sample. The change fluctuates considerably for different crystal samples.

Original article submitted March 27, 1974

EXPERIMENTAL DETERMINATION OF THE TEMPERATURE DEPENDENCE OF THE THERMAL CONDUCTIVITY OF URANIUM DIOXIDE UNDER CONDITIONS OF REACTOR IRRADIATION

B. V. Samsonov, Yu. G. Spiridonov, N. A. Fomin, and V. A. Tsykanov

UDC 621.039.542.34(063)

Experimental data relating to a determination of the thermal conductivity of uranium dioxide at 0-2800°C based on the radial heat-flow method are presented. The measurements were carried out on fuel-element samples containing compact uranium dioxide with a density of 10.4-10.7 g/cm^3 and an oxygen coefficient of 2.01±0.01 V in a stainless steel can 32.5 × 1 mm in diameter. The temperature of the surface and center of the core were measured with VR5/VR20 thermocouples calibrated over the whole range of working temperatures. In order to find $\lambda(T)$ at temperatures above 2300°C, i.e., after the central thermocouple had failed, experiments were carried out using a molten central zone of the fuel, with corresponding analysis after removal from the reactor.

The power of the fuel element was determined calorimetrically, using a calibrated electric heater. The depression of the neutron flux in the fuel elements was found from the fission density measured with 90%-enriched metallic uranium indicators. The distribution of the neutron flux with respect to the height of the fuel element was determined from the activation of copper indicators.

We found that in the temperature range 0-2800°C the thermal conductivity of uranium dioxide was described to an error no greater than 5% by the equation

$$\lambda(T)=\frac{55}{560+T}+0.942\cdot10^{-12}T^3,\ \text{W/(cm}\cdot{}^\circ\text{C)}.$$

The resultant $\lambda(T)$ relationship is recommended for use in thermophysical calculations of fuel elements based on compact uranium dioxide fuel made by the technology employed for VVÉR-440 reactors.

Original article submitted April 21, 1974

MECHANICAL STRENGTH OF URANIUM FIELD-EMITTERS

A. L. Suvorov, G. M. Kukavadze,
D. M. Skorov, B. A. Kalin,
A. F. Bobkov, V. A. Fedorchenko,
B. V. Sharov, and G. N. Shishkin

UDC 535.82:546.791

The mechanical properties of thin acicular tungsten and α-uranium samples were studied with the aid of a field-emission ion microscope. The chief aim was to determine the limiting strength and the mode of deformation of the uranium samples; the experiments with tungsten were treated as standards. The samples were loaded directly in the field-emission microscope, using the strong electric field required to form images of the sample surfaces. The technique of preparing the uranium field-emission samples was described in [1]. Since one cause of sample deformation and rupture in the field-emission microscope was the asymmetry of the sample, the sample profiles were carefully monitored, first in the optical microscope, and after field-emission ion-microscope analysis in the electron microscope.

Rupture of the samples was indicated by a sharp change in the contrast of the field-emission ion image (or the complete disappearance of the latter). Calculation of the stresses σ_K corresponding to rupture was based on the equation $\sigma = F^2/8\pi$, where F is the electric field strength, proportional to the sample potential. The resultant σ_K values for tungsten and α-uranium were respectively $(1.31 \pm 0.15)\cdot 10^{10}$ and $(1.13 \pm 0.20)\cdot 10^{10}$ N/m^2 (sample orientiation along the [011] and [010] directions respectively). The mean diameters of the samples were ~1000 Å. The tungsten samples analyzed numbered 18 and the uranium 10 (altogether 50 uranium samples were examined in various imaging gases; only eight were ruptured by the field). The corresponding value of σ_K for tungsten obtained in [2] using an analogous technique was $(2.06 \pm 0.18)\cdot 10^{10}$ N/m^2, which agrees with the results of the present investigation within the limits of experimental error.

The values of the normal stresses σ_0 in the samples on imaging in various imaging gases are presented in Table 1, together with the corresponding deformations ε.

A comparison between the theoretical strengths σ_T of tungsten and α-uranium calculated from the equation $\sigma_T = \eta G$, where $\eta = 0.133$ from [3], G is the shear modulus (for tungsten $G = 14.85\cdot 10^9$, for α-uranium $G = 7.35\cdot 10^9$ N/m^2) shows that these are respectively $1.98\cdot 10^9$ and $0.97\cdot 10^9$ N/m^2. Thus the results here obtained lend weight to the assertion that the true theoretical strength is realized in such crystals (whiskers); this situation is promising from the point of view of verifying theory and also for the extensive practical use of the whiskers for example, as a base for modern composite materials.

TABLE 1. Calculated Values of Various Parameters

Imaging gas	F_0, b/Å	σ_0, N/m^2	ε, %	
			W	α-U
H_2, Ar	2,2	$2{,}1\cdot 10^8$	0,63	1,9
Ne	3,5	$5{,}3\cdot 10^8$	1,6	4,8
He	4,4	$8{,}4\cdot 10^8$	2,5	7,5
Evaporation mode	5,7 (W)	$1{,}41\cdot 10^9$ (W)	4,2	7,4
	4,35 (α-U)	$8{,}2\cdot 10^8$ (α-U)		

LITERATURE CITED

1. A. L. Suvorov et al., At. Énerg., 36, No. 1, 14 (1974).
2. R. I. Garber, Zh. I. Dranova, and I. M. Mikhailovskii, Dokl. Akad. Nauk SSSR, 174, 1044 (1967).
3. J. Hirth, Relative Structure and Mechanical Properties of Metals, Vol. 1, London (1963), p. 218.

Original article submitted July 1, 1974
revision submitted January 28, 1975

DOSE DISTRIBUTION IN A TISSUE-EQUIVALENT MEDIUM FROM A PLANE THIN ISOTROPIC ALPHA-PARTICLE SOURCE

D. P. Osanov, V. P. Panova,
Yu. N. Podsevalov, and É. B. Ershov

UDC 621.039.538.7

A general method is presented for calculating the dose distribution in a tissue-equivalent medium from a plane thin isotropic source of alpha particles of energy $E_0 \leq 9$ MeV having a surface source strength σ.

The dose rate at point A (Fig. 1) due to all alpha particles reaching it with residual energy between 0 and E(x) is

$$P(x) = k \int_0^{E(x)} \frac{dN(x)}{dE}(E) \frac{dE}{dr}(E)\, dE, \tag{1}$$

where N(x) is the flux density of alpha particles at depth x, and the conversion factor k depends on the choice of units. It is obvious that $dN(x) = (\sigma/2)(\rho d\rho / r^2) = (\sigma/2)(dr/r)$. Then

$$P(x) = k\frac{\sigma}{2} \int_0^{E(x)} \frac{dE}{r(E)} = k\frac{\sigma}{2} \int_0^{E(x)} \frac{dE}{R_0(E_0) - R(E)}, \tag{2}$$

where $R(E_0)$ and R(E) are respectively the total and residual alpha particle ranges.

Equation (2) can also be derived by starting from the definition of dose rate as the derivative of the energy flux density with respect to the depth of the absorber P(x) = dW/dx. The determination of the dose function P(x) is reduced to the correct determination of R(E) for a tissue-equivalent material.

We have found that our results on the energy dependence of alpha particle ranges in a tissue-equivalent material and the data cited in the literature are best approximated by the expressions

$$\begin{cases} R(E) = 6.3E, & 0 < E < 3.5 \text{ MeV}; \\ R(E) = 13.5E - 25.5, & 3.5 < E < 9 \text{ MeV}. \end{cases} \tag{3}$$

By substituting (3) into (2) and integrating we obtain

$$P(x) = c\sigma \ln \frac{R(E_0)}{x}, \quad x > [R(E_0) - 22], \ \mu;$$

$$P(x) = c\sigma \left[\ln \frac{R(E_0)}{x} + 0.47 \ln \frac{R(E_0 - 22)}{x} \right], \quad x < [R(E_0) - 22], \ \mu. \tag{4}$$

Here $c = 28(\text{rad/min}) \cdot (\text{cm}^2/\mu\text{Ci})$, σ is in $\mu\text{Ci/cm}^2$, and x and r are in μ.

The accuracy of Eq. (4) was tested experimentally for ^{239}Pu alpha particles. The dose distribution from a plane thin alpha particle source in direct contact with a tissue-equivalent absorber was determined

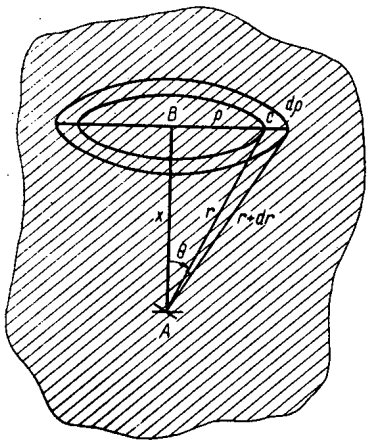

Fig. 1. Diagram for derivation of formula.

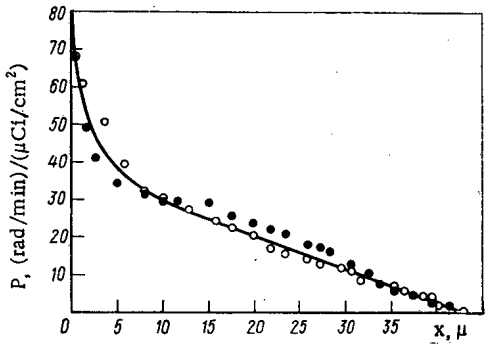

Fig. 2. Comparison of calculated (Eq. (4)) and measured dose distributions for ^{239}Pu alpha particles: ○) semiconductor detector; ●) scintillation detector.

by measuring the spectrum of alpha particles (dN(x)/(dE))(E) penetrating various depths (x) of the absorber. The measurements were made with a silicon semiconductor surface barrier detector and a CsI(Tl) scintillation crystal 70 μ thick on a light pipe. The energy resolution for 5.14 MeV alpha particles was 2.2% for the semiconductor and 6% for the scintillation spectrometer.

The total energy release rate W(x) behind an absorber of thickness x was determined by the measured functions (dN(x)/(dE))(E)

$$W(x) = \int_0^{E(x)} \frac{dN(x)}{dE}(E)\, E\, dE. \qquad (5)$$

It is clear that P(x) = $-$dW(x)/dx.

The calculated and experimental results are in good agreement (Fig. 2). Thus the absorbed dose rate in biological tissues from plane thin sources of alpha particles of energy $E_0 \leq 9$ MeV can be calculated from Eq. (4) using the alpha particle ranges given by (3). The error in determining the dose rate does not exceed 15%.

The dose rate in tissue-equivalent material from a thick tissue-equivalent alpha particle source can be calculated from Eq. (4) by using the method described earlier.

LITERATURE CITED

1. D. P. Osanov et al., Meditsinskaya Radiologiya, 5, 44 (1971).

Original article submitted August 19, 1974

RECOVERY OF THE INTEGRATED SPECTRUM OF NEUTRONS IN THE ENERGY RANGE 0.1-3 MeV BY THE EXTRAPOLATION METHOD

R. D. Vasil'ev, E. I. Grigor'ev,
G. B. Tarnovskii, and V. P. Yaryna

UDC 621.039.57

The proposed extrapolation method of recovering the integrated spectrum of neutrons in the range 0.1-3 MeV is based on the use of, first, experimental information on the spectrum of neutrons in the range 0.5-3 MeV obtained by means of a collection of threshold detectors and, second, a priori information on the used spectrum in the range 0.1-3 MeV, which makes it possible to extrapolate the spectrum into the region in which information is not available.

The integrated spectrum was recovered by an approximation by the method of least squares. An optimal approximating function was obtained: $g(E) = \varphi_{>E}(E)/\varphi_s$ (where $\varphi_{>E}(E)$ is the energy dependence of the integrated neutron flux density; φ_s is the integrated flux density of neutrons with energy greater than the effective reaction threshold $^{32}S(n,p)^{32}P$) in the form $g(E) = a_1 f(E) + a_2$, where a_1 and a_2 are parameters which must be determined; f(E) is a function specified with allowance for the reactor type as follows: for the fields of a water-moderated water-cooled reactor $f(E) = \exp(-0.8E)$, for the fields of graphite and heavy-water reactors and also for neutron fields with $g_{Np} > 11$ and $g_{Np} < 6$

$$f(E) = \exp[-(\lg E + 2.2)^2 \cdot 0.15],$$

and for the remaining cases

$$f(E) = \exp(-0.8E)\, E^{0.04(g_{Np}-7.5)^2-0.35};$$

here, the neutron energy is expressed in megaelectron volts; $g_{Np} = \varphi_{Np}/\varphi_s$ corresponds to the reaction $^{237}Np(n,f)$.

For measurements, one is recommended to use the neutron activation sets developed and supplied by the All-Union Scientific Research Institute of Physicotechnical and Radiotechnical Measurements. These

include five "detector—source" activation sets: $^{103}Rh—^{241}Am$ in a cadmium screen. $^{115}In—^{51}Cr$, $^{199}Hg—^{139}Ce$, $^{58}Ni—^{58}Co$, $^{32}S—^{32}P$ and one "detector—detector of fission fragments" fissile set: ^{237}Np—mica.

We investigated the problem of determining the error of the spectral coefficient g(0, 1) for the energy 0.1 MeV and formulas are given for its calculation.

The main advantage of the extrapolation method is that it ensures a correct result when a spectrum is recovered on the basis of little information. This is confirmed by comparison of the results of measurements obtained by this method and other methods for different types of static and pulse reactors. At the present time, the extrapolation method has been standardized and is used to solve applied problems of solid-state physics.

Original article submitted August 19, 1974

DETERMINATION OF TRACES OF NITROGEN IN PURE METALS BY GAMMA ACTIVATION

A. F. Gorenko, A. S. Zadvornyi, A. P. Klyucharev, and N. A. Skakun

UDC 539.172.3: 543.064: 621.039.32

The most sensitive method available at the present time for determining the mean content of nitrogen impurities in representative samples (5-10 g) of various pure metals is γ-activation analysis. After irradiation of the samples the radioactive isotope ^{13}N is separated, this being the product of the nuclear reaction $^{14}N(\gamma, n)^{13}N$ ($T_{1/2}$ = 10.1 min, β^+); selective deposition and a measurement of the isotope activity follows. In this operation the influence of activities induced in other impurities and the matrix by the γ-irradiation is eliminated.

Samples of Be, Y, V, and Nb were irradiated with γ-quanta obtained by the retardation of 25 MeV electrons (at a current of 18 μA) in a tungsten converter 2 mm thick. The metals were packed in aluminum cans and transported to and from the irradiation site by pneumatic post. A standard with a known N content was irradiated at the same time as the samples.

The ^{13}N isotope was separated from the irradiated samples and standards in a furnace at T = 1200°C. Using a helium flow, the ^{13}N and other gases were passed to a zeolite trap cooled with liquid nitrogen. In the path of the flow was a solid-particle filter followed by copper shavings heated to 500°C in which the nitrogen oxides were deoxidized. Absorption of halides took place over silver shavings heated to 350°C. The activity deposited in the zeolite was recorded by means of a fast—slow coincidence scintillation spectrometer with an efficiency of 1-2%. The absorption of $^{11}C^{15}O_2$ took place in ascarite. The efficiency of the absorption of ^{13}N from the gas flow passing through the zeolite was almost 100%.

The following traces of nitrogen were found (wt.%): Be (10^{-3}-10^{-5}), Nb ~ 10^{-3}, Y ~ 10^{-5} and V ~ 10^{-3}. These characteristics of the method influencing the accuracy and reproducibility of the results are discussed.

Original article submitted September 24, 1974

MICROSCOPIC DISTRIBUTION OF IONIZATION EVENTS IN AN IRRADIATED MEDIUM AS A CHARACTERISTIC OF THE QUALITY OF IONIZING RADIATION

I. B. Keirim-Markus, A. K. Savinskii, and I. V. Filyushkin

UDC 539.12.08

The traditional way of characterizing the quality of the radiation by the average linear energy loss of charged particles (L) is today recognized as inadequate [1]. In this connection, one seeks new parameters and functions which more adequately describe the spatial distribution of energy transferred to a medium. Of the functions of such kind one already knows the radial distribution of the energy transferred to the medium in the tracks of charged particles [2], which in contrast to the linear energy loss gives an idea of the two-dimensional spatial distribution of the transferred energy.

As a further characteristic one can take the spatial microdistribution of events of ionization (excitation) in the irradiated medium, which enables one to take into account the volume distribution of the transferred energy in small regions within the track.

One seeks the average distribution (or mathematical expectation) of the initial distances between the ionization (excitation) events when a charged particle passes through the medium. The required distribution $\Delta P(\rho, E)$ is the conditional probability of finding an ionization event in unit volume of a thin spherical layer of radius ρ with center coinciding with an arbitrary ionization event. It can be represented in the form

$$\Delta P(\rho, E)=\frac{2\pi}{L(E)}\int_0^\infty rD(r, E)\,\overline{D}(\rho, E, r)\,dr+\frac{1}{L(E)}\int_{E_\delta} E_\delta f(E, E_\delta)\,\frac{2\pi}{L(E_\delta)}\int_0^\infty rD(r, E_\delta)\times\overline{D}(\rho, E_\delta, r)\,dr\,dE_\delta, \quad (1)$$

where E and L(E) are the energy and linear energy loss of the charged particle; D(r, E) is the value of the radial distribution of the transferred energy of the particle at distance r from the track axis; $\overline{D}(\rho, E, r)$ is the mean value of the radial distribution of the transferred energy on a sphere of radius ρ with center at distance r from the track axis (the same notation with E replaced by E_δ applies to δ electrons); $f(E, E_\delta)$ is the spectrum of the δ electrons generated by the first particle in all generations.

Calculations of $\Delta P(\rho, E)$ for particles with effective charge Z* from 1 to 8 and energies up to 100 MeV showed in particular that the function $\psi(\rho) = 4\pi\rho^2\Delta P(\rho, E)$ depends solely on the ratio of the effective charge of the particle to its velocity, Z^*/β. In Fig. 1 these functions are shown for a set of values of the parameter.

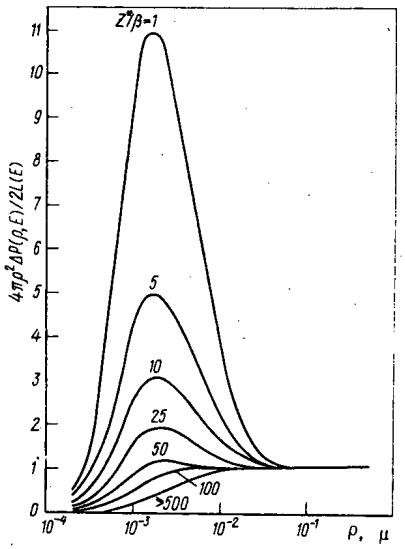

Fig. 1. Microdistribution of distances between events in the tracks of charged particles of arbitrary species and energy in a tissue-equivalent medium.

It follows from geometrical arguments that $\psi(\rho) \to 2L(E)$ as $\rho \to \infty$ (we ignore the variation of L along the track). In this connection, the function $\psi(\rho)/2L(E)$ for large ρ must become equal to unity. It can be seen from the figure that indeed $\psi(\rho) = 1$ for $\rho \geqslant 300$ Å, i.e., at such distances the proposed characteristic of the quality of the radiation no longer gives additional information compared with the linear energy loss.

At shorter distances, down to interatomic distances, the required distribution is different for different particles and is determined by the parameter Z^*/β.

The distribution $\psi(\rho)/2L(E)$ at distances ~16 Å has a maximum, whose value is the larger, the smaller is Z^*/β. This form of the function is due to the contribution of the concentration of ionization events in the cloud of δ electrons which surround the core of the charged particle's track.

This distribution together with the existing linear energy loss and radial distribution of the transferred energy can serve as an additional characteristic of the quality of the radiation when one considers radiation events characterized by interaction lengths $\leqslant 300$ Å.

LITERATURE CITED

1. ICRU, Rep. No. 16, Washington (1970).
2. I. K. Kalugina et al., At. Énerg., 34, No. 4, 298 (1973).

Original article submitted January 24, 1974

ALLOWANCE FOR FLUCTUATIONS IN THE IRRADIATION DOSE OF LUNGS BY HIGHLY ACTIVE PARTICLES

O. M. Zaraev and B. N. Rakhmanov

UDC 621.039.7

In real conditions one observes cases when several or just one highly active aerosol particle is retained in the breathing organs. The existing methods enable one to calculate the dose averaged over a large number of individuals. To choose a "risk criterion" of internal irradiation in such situations one requires the distribution of doses within individuals.

To estimate the potential danger of radioactive aerosols one must take into account two independent processes: 1) aerosol particles reaching the windpipe and being retained in different parts of the breathing organs; 2) the removal of aerosol particles from the breathing organs.

In the development of a method of probabilistic estimation of doses of internal irradiation it was assumed, first, that the "history" of each particle is independent of the "history" of the other particles and, second, the material is removed dynamically, i.e., the rate of removal is proportional to the amount of retained material. If n particles are retained in the breathing organs, the probability of their being removed in time t_n is

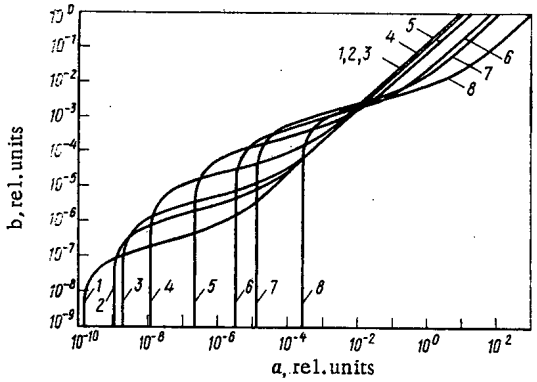

Fig. 1. Maximal irradiation dose of a lung for which the probability of being exceeded is 0.05% for different $d_{a,\mu}$: 1) 0.4; 2) 0.8; 3) 1.0; 4) 2.0; 5) 4.0; 6) 6.0; 7) 8.0; 8) 10.0.

$$\Gamma(t_n)=\frac{(\lambda n)^n}{(n-1)!}\,t_n^{n-1}e^{-\lambda n t_n},$$

where λ is the constant for the removal of the radioisotope from the breathing organs. With a probability of 99.95% one can assert that the removal time of one particle exceeds by not more than 7.6 times the average removal time of the same amount of radioactive material uniformly distributed among many particles. The mathematical model developed applies to any organ from which the removal is described by an exponential law.

As the risk criterion when a relatively small number of radioactive particles get into the breathing organs one must evidently take the so-called local absorbed dose, i.e., the radiation energy absorbed in 1 g of the irradiated tissue. The radiation danger cannot be estimated by the formal comparison of this dose with the maximally allowed dose since the latter is essentially the tissue average, i.e., it refers to unit mass of the complete organ.

In this connection, it is desirable to determine the tissue-averaged absorbed doses from radioactive particles calculated on the basis of the one-component variant of the exponential model of their removal with effective constant λ_{eff} and with allowance for the statistical nature of the processes of arrival and removal of the aerosol particles.

The processes of deposition and removal of the particles are independent. The probability that the mean-tissue dose absorbed in part j of the breathing system after the inhaling of an aerosol during time τ with mean number $\bar{N}$ of particles that arrive is the quantity D, equal to

$$V(D)=\Sigma\omega_j(n)\,W_n(D),$$

where $\omega_j(n)=\frac{(\bar{N}P_j)^n\exp(-\bar{N}P_j)}{n!}$ characterizes the process of inhaling of the particles and their deposition in part j of the breathing system; $W_n(D)=\left(\frac{\lambda_{eff}}{P_1^0 q_1}\right)\frac{D^{n-1}}{(n-1)!}\exp(-\lambda_{eff}D/P_1^0 q_1)$ characterizes the process of removal of the particles; D is the maximal irradiation dose of the lung; P_j is the probability of deposition of a particle in part j of the breathing system; P_l^0 is the power of the mean-tissue dose from a source with activity 1 μCi; q_1 is the activity of one particle.

The average dose adsorbed in part j of the breathing system is

$$\bar{D}=\int_0^\infty DV(D)\,dD=\frac{P_1^0\bar{N}P_j q_1}{\lambda_{eff}}.$$

Here, $\bar{D}$ does not depend on the number of retained particles but is entirely determined by the total amount of the radioisotope retained in part j.

Figure 1 shows universal curves which enable one to calculate the maximal irradiation dose of the breathing organs of an individual as a function of the number of radioisotopes that arrive averaged for the complete contingent of workers. For convenience, $\bar{Q}$ and D_{max} are given in relative units a and b, which are related to the corresponding absolute values through the parameters of the aerosol particles by

$$\bar{Q}=a\frac{q_1}{\sqrt{\rho}},\ \mu\text{Ci};$$

$$D_{max}=b\frac{q_1P_1^0}{\sqrt{\rho}\,\lambda_{eff}},\ \text{rem}.$$

The linear sections of these dependences correspond to the arrival amounts at which the fluctuation of the doses has no practical importance.

Original article submitted January 31, 1975

LETTERS TO THE EDITOR

CALCULATION OF HETEROGENEOUS NUCLEAR REACTORS BY THE METHOD OF INSERTED ELEMENTS

I. S. Slesarev and A. M. Sirotkin

UDC 539.125.52:621.039.51.12

With the appearance of computers, finite-difference schemes are widely used in reactor calculations. However, difficulties in their application to calculations of nuclear reactor models which are complex in composition, have led to the development of variational-difference methods which are suitable for the calculation of more realistic models [1]. A general approach is given below to the construction of a sufficiently versatile scheme of reactor calculation, which is suitable both from the point of view both of knowledge of the reactor composition and of the improvement of the local approximation and increase of the asymptotic convergence of the algorithm. By using the proposed method, the possibility emerges for the effective calculation of a reactor with an almost arbitrary disposition and geometry of its zones.

In the majority of cases, the nuclear reactor model can be represented in the form of a system consisting of arbitrarily disposed zones of quite simple geometrical shape. We designate as a reactor element the phase volume of space variables bounded by some external surface. In particular, the boundaries of the element can be the boundary of the zones. A zone is the simplest element. Thus, the reactor consists of elements inserted one in the other (see Fig. 1). We shall assume the outside element to be dominant in relation to the element completely inserted in it. The insertion of element n in m is equivalent to the subordination of the first element to the element m. Elements which do not have a common volume are assumed to be independent. Suppose that the neutron field Φ in the reactor is described by a diffusion equation with zero boundary conditions at the outer surface of the reactor. In order to construct a scheme for calculation, we shall use the variational formulation of the problem [1], which consists in the requirements of extremal properties of the functional, obtained by taking account of the starting equation. In diffusion problems, the solution belongs to a class of continuous functions with a continuous derivative $\mathbf{D}\mathbf{r}(d\Phi_r/dn)$ at the inside boundaries, where $D(\mathbf{r})$ is the step-continuous coefficient of diffusion.

It is obvious that the solution of the problem of quasicritical distribution of neutrons in a reactor can be represented in the form of a sum of sufficiently continuous functions, defined inside each of the elements and vanishing at their boundaries. We represent the approximate solution of the problem in the form of a set of polynomials. We shall assume that to the outside element $n = 0$, an arbitrary polynomial P_0 is assigned, which satisfies the zero boundary conditions at the boundary of this element and coincides with the boundary of the reactor. In each element $n = 1, 2, \ldots$ we define an additional polynomial P_n, not identically equal to zero only inside this element and vanishing at its boundary. The solution of the starting equation inside the element n will be found in the form $\Phi_n = P_0 + \ldots + P_n$ so that in the composition of Φ_n in addition to P_n are included polynomials of those elements which are subordinate to element n. This construction, first of all, leaves the solution continuous for any degree of approximation and takes account of the possible discontinuities of the derivatives; secondly, it permits local inhomogeneities in the solution to be described effectively, and which originate because of the change of properties in a heterogeneous reactor; thirdly, it preserves the generality of the structure of the scheme in all practically important cases.

In constructing the polynomials P_n with the properties mentioned (and, consequently, also of the coordinate functions [1]) the following approach is recommended. Functions of the type $W_n = \omega_n(x, y, \ldots)x^{\alpha} \cdot y^{\beta}$ are chosen as ordinate functions, where ω_n is a positive continuous function within the element n, having bounded and continuous partial derivatives and satisfying the conditions

Translated from Atomnaya Énergiya, Vol. 38, No. 6, pp. 419-420, June, 1975. Original article submitted April 22, 1974.

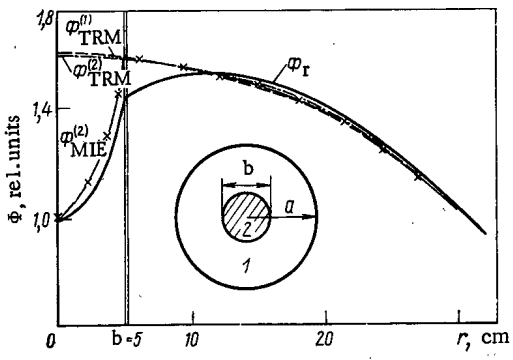

Fig. 1. Quasicritical neutron distribution in a reactor consisting of two elements. 1) Principal element (active zone, a = 50 cm); 2) subordinate element (rod, b = 5 cm); Φ_r is the precise solution of the problem.

$$\operatorname{grad}\omega_n \neq 0;\ \omega(x, y, \ldots) = 0 \text{ for } x, y, \ldots \in \Gamma_n,$$

where Γ_n is the boundary of the element n. There exist [2] simple general rules of construction of the function ω for elements of different geometrical shape, which permits a reactor of complex construction to be calculated. A proof of the completeness of the chosen type of coordinate functions can be found in [2].

The asymptotic convergence of variational methods of the type being discussed depends to a strong degree on the continuity of the solution. Traditional direct methods under these conditions have a slow convergence. The special method of constructing the coordinate functions in the method of inserted elements permits the class of functions to be expanded only by selecting the coefficients being varied. Hence, a higher asymptotic rate of convergence results, which is characteristic of this method.

Let us consider the structure of the matrix operators originating during the calculation of the reactor. A system of equations can be obtained for the unknown coefficients A with the coordinate functions W in the polynomials $P_n = \sum_{j=1}^{K_n} A_j W_j$ by using the extremal properties of the functional and the chosen coordinate functions (K_n is the number of unknown parameters A_j in the element n). It will have the form

$$\hat{R}A = \frac{1}{k_{eff}}\hat{B}.$$

The independence of a part of the elements leads to discharging of the matrix with zeros and, as a consequence, to its better conditionality. The singularities of the matrix structure permit the problem of its transformation for solving the problem to be simplified.

When approximating the solution with power series, the quantities representing integrals of the coordinate functions with the operators of the equation and forming the matrices $\hat{R}$ and $\hat{B}$, can be calculated a priori and included in the composition of some library, if the geometry of the elements and their neutron-physical properties are known. The possibility of creating a library gives appreciable advantages in solving the problem on a computer: it dispenses with the necessity of carrying out a large volume of calculations during integration of the coordinate functions.

The inherent form of the setting-up of the reactor composition is characteristic for the method of inserted elements. The setting-up procedure can be formalized by analogy with the block structure used in machine languages of the ALGOL type.

The proposed method, based on the special structure of the coordinate functions used, permit the accuracy of the calculation of the neutron distribution in any part of the reactor to be locally increased (in accordance with an accurate geometric form of the elements) without the necessity of increasing the accuracy (and, this means, also the difficulties of the calculation) in the entire reactor, which is characteristic with combined methods.

In order to illustrate the possibilities of the method, we shall consider the simplest problem of calculating a one-dimensional reactor with a cylindrical active zone, at the center of which is positioned an absorbing rod (see Fig. 1). The characteristics of the zones in one-group approximation are: diffusion coefficients $D_{a.z}$ = 2 cm; D_{rod} = 0.5 cm; absorption cross-section $\Sigma_{a.z} = 0.005\ cm^{-1}$; $\Sigma_{rod} = 0.03\ cm^{-1}$; secondary neutron generation cross-section $\nu\Sigma_{f,\,a.z} = 0.01\ cm^{-1}$. The accurate value for the neutron multiplication factor (with rod) is k_{eff} = 0.95, and the efficiency of the rod is Δk_{eff} = 8.65%. These same characteristics were calculated by means of the algorithms of the traditional Ritz method (TRM) and the method of inserted elements (MIE). In the TRM-method, the neutron distribution was found in the form $\Phi_{TRM} = (a^2 - z^2)(A_0 + A_1 r + \ldots)$. In this case, the problems are solved in the two simplest approximations with one (Φ^1_{TRM}) and two (Φ^2_{TRM}) unknown coefficients A_0 and A_1. The error in estimating Δk_{eff} varied from 33% for Φ^1_{TRM} to 30% for Φ^2_{TRM}. In the MIE method, the solution of the problem was found in the form

$$\Phi^{(1)}_{\text{MIE}} = (a^2 - r^2)\,\widetilde{A}_0 \quad \text{in the entire reactor;}$$

$$\Phi^{(2)}_{\text{MIE}} = \begin{cases} (a^2 - r^2)\,\widetilde{A}_0 & \text{in the active zone,} \\ (a^2 - r^2)\,(\widetilde{A}_0 + \widetilde{A}_1 r) & \text{in the rod.} \end{cases}$$

The solutions of $\Phi^{(1)}_{\text{MIE}}$ and $\Phi^{(1)}_{\text{TRM}}$ by definition coincided. The error in estimating Δk_{eff} in the MIE-method varied from 33% for $\Phi^{(1)}_{\text{MIE}}$ to 16% for $\Phi^{(2)}_{\text{MIE}}$. The solution of the problem was simpler in the case of $\Phi^{(2)}_{\text{MIE}}$ than in $\Phi^{(2)}_{\text{TRM}}$ because of the special properties of the matrix operator.

LITERATURE CITED

1. S. G. Mikhlin, Variational Methods in Mathematical Physics [in Russian], Nauka, Moscow (1970).
2. L. V. Kantorovich and V. I. Krylov, Approximation Methods of Higher Analysis [in Russian], Fizmatgiz, Moscow (1962).

TRANSIENT CHANGES OF THE THERMOELECTRIC CHARACTERISTICS OF THERMOCOUPLES BY THE ACTION OF REACTOR RADIATION

V. P. Kornilov and É. B. Pereslavtsev

UDC 621.039.531

Transient changes of thermo-electromotive force (e.m.f.) appear by the action of reactor radiation, depend on its intensity and vanish when the radiation is cut off. The well-known experiments give different results for the determination of these changes: less than 1% of the measured temperature [1-3] and 3 to 5% [4,5]. As a rule, the procedure for determining the transient effects of changes of the thermo-e.m.f. of a thermocouple by the action of reactor radiation is based on the calibration of the thermocouple relative to datum points — the melting (setting) points of pure metals in eutectic alloys directly in the active zone of the reactor. For example, in [3], the transient changes of the thermo-e.m.f. are measured by chromel—alumel and iron—constantan thermocouples under the following irradiation conditions: neutron radiation flux density $\varphi = 10^{16}$ n/(cm^2·sec) (fast neutrons); $\Delta\tau = 11\,\mu$sec; γ-radiation dose intensity $P = 10^{10}$ R/h. Changes of the thermo-e.m.f. amounted to 2 to 4°C at the melting (setting) point of tin [3]. The authors of [3] interpret these changes by local γ-heating of the working junctions of the thermocouples.

Experiments carried out on the SM-2 reactor in the Scientific Research Institute of Nuclear Reactors (NIIAR) with $\varphi_{th} = 3.3 \cdot 10^{14}$ n/(cm^2·sec), $\varphi_{fast} = 3.7 \cdot 10^{14}$ n/(cm^2·sec) for $E_n \geq 0.75$ MeV and $P = 9.9 \cdot 10^5$ R/sec, permitted transient changes to be detected, equal to +26°C for chromel—alumel and —16°C for tungsten—rhenium (VR-5/20) thermocouples. The measurements were carried out at the setting point of aluminum [5].

In all the experiments to determine the transient changes of thermo-e.m.f., a calibration of the thermocouple was carried out immediately at the instant of irradiation at the temperature of intensive annealing of the radiation defects formed and with low radiation ($\sim 10^{17}$-10^{18} n/cm^2). The amount of radiation defects in the crystal structure of the thermoelectrodes formed in this case, conditioned by the action of the neutron irradiation, is very insignificant (< 0.01% at.) and cannot be the source of the transient changes in the thermo-e.m.f.

One source of transient thermo-e.m.f. changes may be induced currents in the thermocouple loops. These currents are due to free charges originating at the electrodes and in the measurement lines, in consequence of electrons knocked out of the thermoelectrodes and the thermocouple sheath by γ-quanta. With an unfortunate choice of the measurement circuit, the induced current will distort the useful signal of the thermocouple. The induced current is independent of the time of irradiation but is proportional to the γ-radiation intensity.

TABLE 1. Thermoelectric Characteristics of Thermocouples [$\varphi_{th} = 1.44 \cdot 10^{14}$ n/(cm^2·sec); $\varphi_{fast} = 1.75 \cdot 10^{13}$ n/(cm^2·sec), for $E_n \geq 1.15$ MeV]

Integrated neutron flux density, n/cm^2		E_{av}, mV	T_{av}, °C	$\Delta T_{mean\ square}$, °C	Cycle
thermal	fast				
$5{,}2 \cdot 10^{17}$	$6{,}3 \cdot 10^{16}$	17,350	1086	0,35	Setting
$1{,}4 \cdot 10^{18}$	$1{,}26 \cdot 10^{17}$	17,385	1089	0,38	"
$1{,}56 \cdot 10^{18}$	$1{,}89 \cdot 10^{17}$	17,275	1082	2,25	Melting
$2{,}08 \cdot 10^{18}$	$2{,}52 \cdot 10^{17}$	17,348	1086	0,20	Setting

Translated from Atomnaya Énergiya, Vol. 38, No. 6, pp. 420-422, June, 1975. Original article submitted May 13, 1974; revision submitted December 13, 1974.

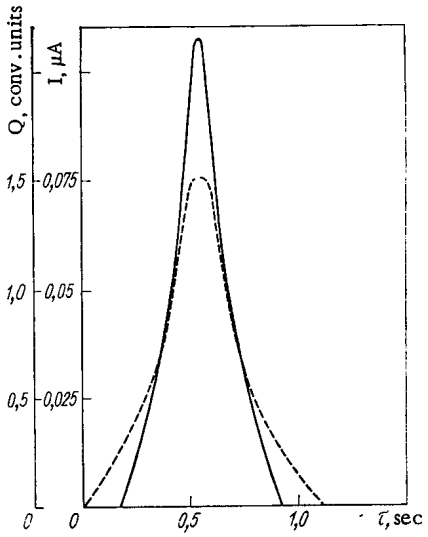

Fig. 1

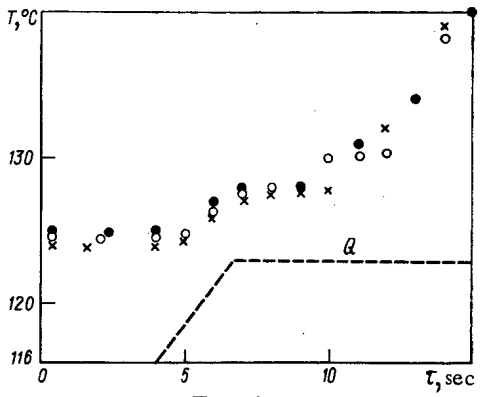

Fig. 2

Fig. 1. Induced current in KTMS-2 × 0.2 (chromel—alumel) cable. The dashed curve is the intensity profile (Q).

Fig. 2. Calibration of thermocouples at the setting point of the alloy 44.5% Pb + 55.5% Bi: •) VR-5/20; ×) Chromel—alumel; ○) chromel—Copel.

The induced current for a thermocouple cable of KTMS-2 × 0.2 (chromel—alumel) was measured in the IRG reactor [6] at a γ-radiation dose intensity of $P = 3 \cdot 10^6$ R/sec and $\varphi \leq 10^{15}$ n/(cm^2·sec) (fast and thermal neutrons). Its magnitude was ~0.1 μA (Fig. 1). Depending on the choice of the measurement circuit, the induced thermo-em.f. due to this current, will distort the useful thermocouple signal. For example, for a thermocouple made from KTMS-2 × 0.2 (chromel—alumel) cable, with an insulated working junction and using a measuring device with a grounded input, the induced thermo-e.m.f. of chromel—alumel, chromel—Copel and VR-5/20 thermocouples were also measured at a temperature of 125°C (the setting point of the eutectic alloy 44.5% Pb + 55.5% Bi), $\varphi \leq 2 \cdot 10^{14}$ n/(cm^2·sec) (fast and slow neutrons) and $P = 5 \cdot 10^5$ R/sec.

The results of the measurement of the thermo-e.m.f. of the thermocouples are shown in Fig. 2. It can be seen from the figure that a temperature, constant in time, corresponding to the alloy setting cycle, was observed for some time during operation of the reactor, but the thermo-e.m.f. of the thermocouple increased somewhat with the appearance of radiation (up to 30 μV for VR-5/20 and up to 400 μV for chromel—Copel thermocouples). The increase of the thermo-e.m.f. of the thermocouples investigated in the presence of radiation can be explained by local heating of the working junctions of the thermocouples, due to the absorption of γ-radiation. The calculation showed that this heating may amount to 3 to 5°C with a spatial energy release in Kh18N10T steel equal to ~10^8 W/m^3.

Calibration of the VR-5/20 thermocouples was carried out at the melting (setting) point of copper. The construction of the thermocouples investigated was: diameter of thermoelectrodes 0.2 mm; insulation — alundum; sheath — molybdenum and tantalum, with diameter 0.8 mm; the working junction was made concurrent with the sheath. The experimental results are shown in Table 1 [at the melting (setting) point of copper, 1083°C].

It can be seen from the table, that the readings of all thermocouples, within the limits of error of the temperature measurement (1%), corresponded to the handbook value of the melting (setting) point of copper.

Thus, in the experiments carried out by the authors, the contribution of transient changes in the thermoelectric characteristics of thermocouples did not exceed magnitudes which lie within the limits of the standard variance of calibration variations, established by GOST.

LITERATURE CITED

1. R. Carrol and P. Reagon, ORNL-p-1066 (1965).
2. W. Strum and R. Jonnes, Rev. Sci. Instrum., 25, 392.
3. G. Dau, R. Bourassa, and S. Kuton, Nucl. Appl., 5, No. 5 (1968).

4. G. Bianchi and S. Moretti, Energ. Nucl., 11, No. 8 (1964).
5. N. V. Markina, B. V. Samsonov, and V. A. Tsykanov, Fizika Metallov i Metallovedenie, 32, No. 4 (1971).
6. I. V. Kurchatov et al., Third Geneva Conference, Report No. 322a [in Russian] (1970).

OXIDATION OF SOLID SOLUTIONS OF URANIUM AND NIOBIUM MONOCARBIDES

V. G. Vlasov, V. A. Alabushev, and A. R. Beketov

UDC 546.261(791+882):546.21

Data hitherto published [1] provide a reasonable account of the behavior of uranium carbide containing refractory carbides in air, but offer no conclusions regarding the actual mechanism of the oxidation process.

In this paper we shall present the results of an investigation into the oxidation of UC—NbC solid solutions at 300-1100°C for oxygen pressures from 3.6 to 20.2 mm Hg. The characteristics of the original samples are given in Table 1.

TABLE 1. Physicochemical Properties of the Original Samples

Values of the coefficients in the formula $U_xNb_yC_z$			Pycnometric density, g/cm^3	Lattice parameters, Å
x	y	z		
0,69	0,31	0,97	11,42	4,805
0,56	0,44	1,00	10,41	—
0,33	0,67	0,99	9,40	4,592
0,08	0,92	1,00	8,19	4,505
0,01	0,99	1,00	7,81	4,477

The preparation of the samples, the determination of the proportions of their components, and the experimental methods involved were described in [2-8]. The impurity content of the present set lay within the limits of analytical accuracy. The single-phase character of the samples was monitored by x-ray diffraction and metallographic analysis.

It was initially established that, for niobium carbide contents of less than 30 mol. %, the alloys ignited spontaneously, so that it was impossible to study the oxidation kinetics of uranium carbide with low NbC contents.

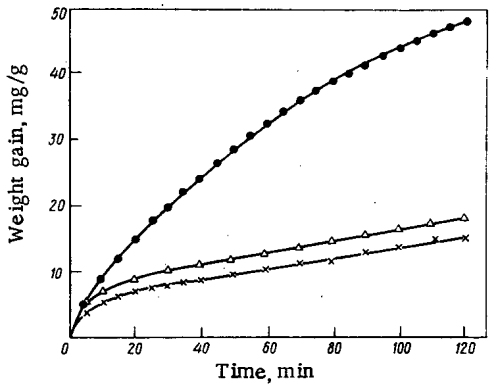

Fig. 1

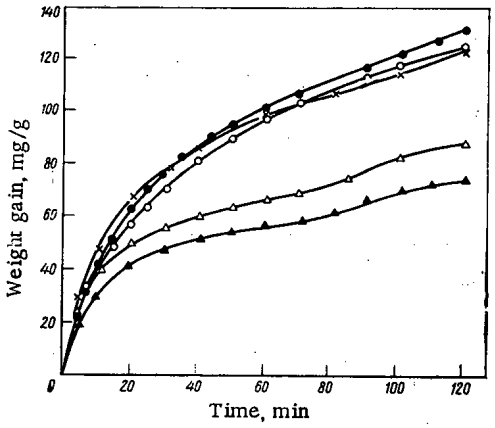

Fig. 2

Fig. 1. Oxidation isotherms (400°C) of carbide solid solutions of the following compositions: •) $U_{0.56}Nb_{0.44}C_{1.00}$; Δ) $U_{0.08}Nb_{0.92}C_{1.00}$; ×) $U_{0.01}Nb_{0.99}C_{1.00}$.

Fig. 2. Oxidation isotherms (900°C) of carbide solid solutions of the following compositions: •) $U_{0.69}Nb_{0.31}C_{0.97}$; ○) $U_{0.56}Nb_{0.44}C_{1.00}$; ×) $U_{0.33}Nb_{0.67}C_{0.99}$; Δ) $U_{0.08}Nb_{0.92}C_{1.00}$; ▲) $U_{0.01}Nb_{0.99}C_{1.00}$.

Translated from Atomnaya Énergiya, Vol. 38, No. 6, pp. 422-425, June, 1975. Original article submitted June 17, 1974.

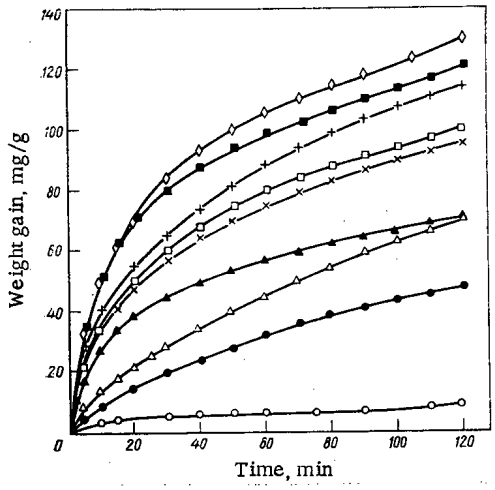

Fig. 3

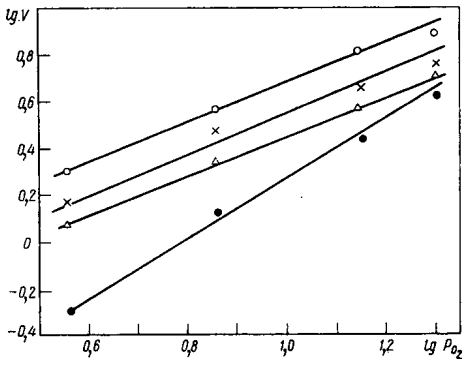

Fig. 4

Fig. 3. Oxidation isotherms of samples with the composition $U_{0.33}Nb_{0.67}C_{0.99}$ for P_{O_2} = 7.2 mm Hg: ○) 300; ●) 400; △) 500; ▲) 600; □) 700; ◇) 800; ■) 900; +) 1000; ×) 1100°C.

Fig. 4. Effect of a change in oxygen pressure on the oxidation of samples of composition $U_{0.33}Nb_{0.67}C_{0.99}$ at 600°C for various degrees of oxidation, mg/g: ○) 5; ×) 10; △) 20; ●) 30.

The principal results of our investigations into the oxidation kinetics of UC—NbC solid solution at 400-900°C are presented in Figs. 1 and 2. It follows from the results presented that the influence of the alloying additive depends not only on its concentration but also on the temperature. Whereas at 900°C a change in the NbC concentration from 31 to 67 mol.% has hardly any effect on the corrosion resistance of the alloy, at 400°C this only applies to NbC contents of no greater than 44 mol.%. The corrosion resistance of the samples increases considerably for high NbC concentrations and relatively intensive levels of oxidation (at 900°C, for example, in the case of more than 20 mg/g oxidation).

Figure 3 illustrates the influence of temperature on the oxidation of samples of composition $U_{0.33}Nb_{0.67}C_{0.97}$ at 300-1100°C for an oxygen pressure of 7.2 mm Hg. For samples of other compositions the kinetic relationships are analogous. We may distinguish two temperature ranges: 300-800°C, in which the temperature coefficient is positive, and 800-1100°C, in which it is either negative or zero. This latter is characteristic of the oxidation of solid solutions containing more than 50 wt.% NbC.

The values of the apparent activation energy determined for all compositions of the solid solutions studied and for various oxygen pressures fluctuate from 12 to 16 kcal/mole.

The influence of oxygen pressure on the oxidation rate was studied for samples of composition $U_{0.33}Nb_{0.67}C_{0.99}$ (Fig. 4). At 600°C an increase in the oxygen pressure accelerated the reaction in accordance with the equation

$$V = kP_{O_2}^n,$$

where V is the velocity of the reaction, k is a certain constant, P_{O_2} is the gas pressure, n is the power index. We see from Fig. 4 that the power index changes during the reaction. For degrees of oxidation equal to 5, 10, and 20 mg/g, n = 1; for 30 mg/g, n = 1.3. At 900°C for an oxygen pressure of under 7.2 mm Hg, n = 1; for higher pressures n = 0.22.

The oxide phases were identified by metallographic and x-ray analysis. Figures 5 and 6 illustrate diffraction recordings of the oxide layers formed on samples of compositions $U_{0.08}Nb_{0.92}C_{1.00}$; $U_{0.33}Nb_{0.67}C_{0.99}$. Solution of the diffraction patterns shows that the introduction of oxygen into the lattice of the mixed carbide leads to phase separation of the solid solution, with the formation of uranium and niobium oxycarbides. Poorly-crystallized niobium pentoxide appears after the formation of large quantities of UO_2 and U_3O_8. On the background of the diffuse Nb_2O_5 peaks we find peaks of an unknown phase; identification of this phase based on the data presented in [9] showed that it might belong to the niobium suboxides, in particular NbO_x. A crystalline Nb_2O_5 phase is formed in the initial stages of the process at temperatures of over 600°C. At 800°C and over the first oxide layer contains the phases NbO_2, UO_2, Nb_2O_5 but not U_3O_8.

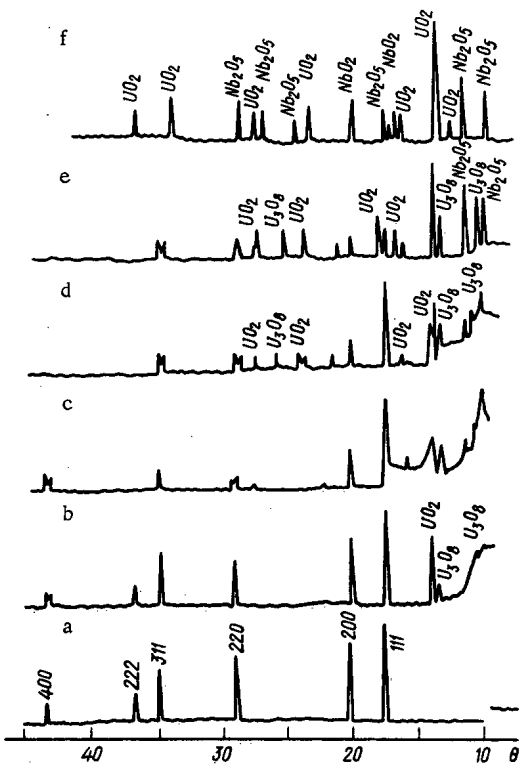

Fig. 5

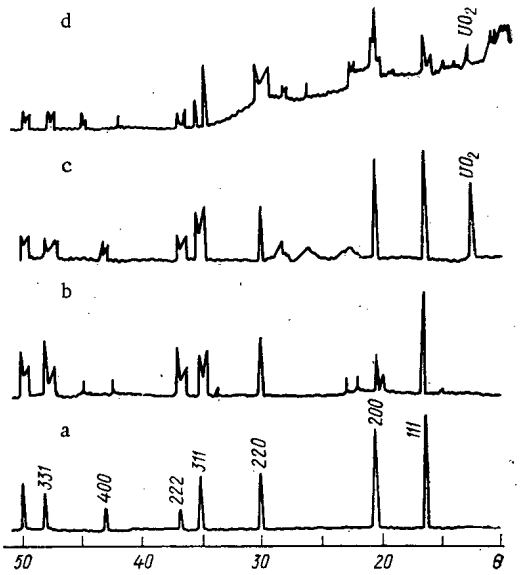

Fig. 6

Fig. 5. Diffraction recordings of the oxide layers formed on samples of composition $U_{0.33}N_{0.67}C_{0.99}$: a) original sample; b) powder flaking off at 300°C; c), d), e) substrate under the oxide layer at 400, 500, and 600°C; f) top sintered oxide layer at 800°C.

Fig. 6. Diffraction recordings of the oxide layers on samples of composition $U_{0.88}Nb_{0.92}C_{1.00}$: a) original sample; b), c) oxide film with a violet tint at 400 and 500°C; d) oxide film of green color at 500°C.

Increasing the amount of NbC in the alloy opposes the rupture of the samples. In the fracture surface of samples oxidized at temperatures above 800°C several layers may be distinguished. At the top there is usually a sintered oxide layer of violet color, adjacent to a black, compact film, under which lie layers exhibiting interference colors.

DISCUSSION OF RESULTS

Oxidation of UC—NbC solid solutions starts with the adsorption of oxygen and the formation of uranium and niobium oxycarbides on the surface. The introduction of oxygen atoms into the lattice of the solid solution is accompanied by the release of an equivalent amount of free carbon. Subsequent attachment of oxygen leads to the preferential oxidation of the uranium oxycarbide, with the formation of UO_2 and U_3O_8. The niobium oxycarbide is stabler with respect to oxygen, and oxidizes at later stages in the process. The great corrosion resistance of niobium oxycarbide is evidently associated with the formation of niobium suboxides of variable composition on its surface. On the basis of metallographic and x-ray analyses, it is reasonable to assume that the Nb_2O_5 phase is formed directly from the suboxides, by-passing other stable lower oxides. During the oxidation of the mixed uranium and niobium carbides in the temperature and oxygen-pressure ranges under consideration, a scale consisting of individual phases (uranium and niobium oxides) is formed; this appears especially for low NbC contents and relatively low temperatures. In this case self-ignition of the samples occurs as a result of the low protective properties of the scale, all the more so in view of the fact that, at the boundaries of the adjacent oxide phases, the sample is almost unprotected from the direct action of the oxygen. At high temperatures the niobium suboxides are unstable, and the difference between the rates of formation of Nb_2O_5 and the uranium oxides is negligible. As a result of this, a layer of oxide of uniform thickness is formed, and the conditions for the self-ignition of the samples are no longer operative.

At 600°C and over, the carbon in the scale interacts with the oxygen. The change in the index n of the equation as the oxidation process develops, and also the results of chemical analysis show that intensive combustion of the carbon takes place as the degree of oxidation increases, since a thick layer of scale develops, preventing the access of oxygen to the phase interface, so that the combustion of the carbon becomes the preferred reaction.

At 800°C and over, the scale sinters, the degree of sintering increasing with temperature. The sintered oxide film impedes the access of oxygen to the surface of the oxidized sample and the release of the gaseous reaction products CO and CO_2 from the latter. Carbon monoxide and amorphous carbon in the oxide layers promote reduction reactions at elevated temperatures. This may well explain the appearance of lower niobium oxides and the absence of the uranium mixed oxide from the scale, as well as the reduction in the total rate of oxidation with rising temperature. The phase U_3O_8 only appears at the final stages of the process.

Since the value of the apparent activation energy depends little on the composition of the solid solution, the degree of oxidation, and the oxygen pressure, it is reasonable to assume that the rate of oxidation is in all cases determined by the supply of the oxidizing gas through the porous scale, i.e., the formation of the oxide takes place at the boundary of the carbide as a result of the preferential diffusion of oxygen through the scale.

LITERATURE CITED

1. Physicochemistry of Alloys and Refractory Compounds Containing Thorium and Uranium [in Russian], Nauka, Moscow (1968).
2. V. A. Alabushev, Candidate's Dissertation [in Russian], Ural. Poli. Inst., Sverdlovsk (1974).
3. V. A. Vlasov et al., At. Énerg., 36, No. 3, 207 (1974).
4. B. V. Linchevskii, Technique of Metallurgical Experiments [in Russian], Metallurgiya, Moscow (1967).
5. H. Müller, High-Purity Gases [Russian translation], Mir, Moscow (1968).
6. V. S. Saltykova et al., Methods of Complete Chemical Analysis for Complex Rare-Metal Minerals [in Russian], Nauka, Moscow (1972).
7. P. Ya. Yakovlev, Determination of Carbon in Metals [in Russian], Metallurgiya, Moscow (1972).
8. V. K. Markov et al., Uranium, Methods of Its Determination [in Russian], Atomizdat, Moscow (1964).
9. I. I. Kornilov et al., Interaction of Refractory Metals of the Transition Groups with Oxygen [in Russian], Nauka, Moscow (1967).

SPECTRAL CHARACTERISTICS OF THE BACKGROUND NOISE IN THE PRIMARY LOOP OF AN ATOMIC GENERATING PLANT

K. A. Adamenkov, V. I. Gorbachev,
Yu. V. Zakharov, V. P. Kruglov,
S. A. Paraev, Yu. A. Reznikov,
and R. F. Khasyanov

UDC 621.039.564.2

An important prequisite to the application of the acoustic emission method [1-3] for the nondestructive testing of equipment is the determination of the frequency range in which the acoustic emission signals are reliably recorded when background noise is present in the testpiece and its auxiliary equipment. We have studied the background noise in the VVÉR-440 III section of the Novovoronezh atomic electric power

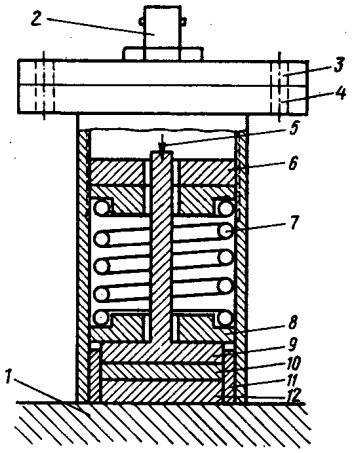

Fig. 1

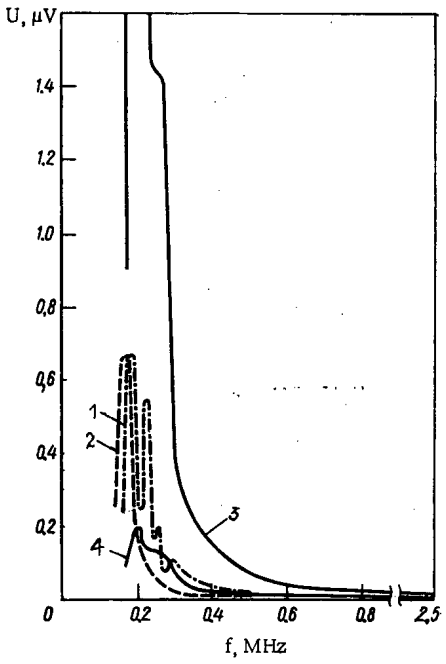

Fig. 2

Fig. 1. Schematic of piezoelectric transducer. 1) Testpiece; 2) connector; 3) cover; 4) casing; 5) conductor; 6) adjusting nut; 7) spring; 8) Teflon bushing; 9) current collector; 10) damper; 11) Teflon mandrel; 12) piezoelectric element.

Fig. 2. Spectrum of primary-loop background noise. 1) Wideband piezoelectric transducer on MCP cover plate; 2) wideband transducer on duct valve lock-band; 3) 0.2 MHz resonance transducer on MCP cover plate; 4) 2.0 MHz resonance transducer on MCP cover plate.

Translated from Atomnaya Énergiya, Vol. 38, No. 6, pp. 425-426, June, 1975. Original article submitted January 14, 1975.

generating plant. The investigations were carried out in the frequency range from 0.2 to 2.5 MHz with the reactor operating at full capacity.

We recorded the background noise with piezoelectric transducers mounted by means of permanent magnets on the cover plate of the main circulation pump (MCP) and on the lock-band of the primary-loop duct valve. The construction of the transducer is illustrated in Fig. 1. The transducers had two types of piezoelectric elements: commercial TsTS-19 lead zirconate—titanate ceramic with resonance frequencies of 0.2 and 2.0 MHz, and specially designed wideband elements of the same ceramic with a pass band from 0.6 to 2.5 MHz at the half-power points. The wideband elements enabled us to record the acoustic noise of the primary loop with a flat response over a wide frequency interval, and with the resonance elements we were able to estimate the noise levels at separate frequencies. The acoustic noise signals picked up by the piezoelectric transducers were sent to a wideband preamplifier situated in the immediate vicinity of the transducer. The amplifier signals were sent along an rf cable to the input of the main amplifier and then to the input of a V6-1 selective voltmeter and S4-8 spectral analyzer.

The spectral characteristics of the background noise are shown in Fig. 2, from which we see that the operation of the primary-loop equipment of the atomic generating plant is attended by strong noise in the frequency range below 500 or 600 kHz. From 500 kHz to 2.5 MHz the noise amplitude is low. It is evident from a comparison of curves 1 and 2 that the noise spectrum recorded on the duct valve does not contain the strong noise signals recorded on the MCP at frequencies above 200 kHz. Damping of the high-frequency components of the spectrum apparently causes the noise of the operating MCP to be filtered in transmission through the metal of the conduit, and mainly the low-frequency components of the MCP noise spectrum prevail outside the reactor casing.

A comparison of curves 3 and 4 shows that the use of high-frequency resonance piezoelectric transducers to record acoustic emission signals significantly lowers the level of the detected background noise signals, thereby permitting more reliable extraction of the useful signals.

It is evident, therefore, that frequencies above 500 kHz are relatively devoid of background noise signals created by the operating MCP and coolant conduits.

LITERATURE CITED

1. R. S. Sharpe (editor), Research Techniques in Nondestructive Testing, Academic Press, New York —London (1970).
2. R. Zipfai and D. Harris, Materials Research and Standards, 11, No. 3, 8 (1971).
3. Yu. I. Bolotin et al., Defektoskopiya, No. 6, 5 (1971).

PORES IN HELIUM-SATURATED NICKEL UNDER IRRADIATION BY NICKEL IONS

S. Ya. Lebedev, S. D. Panin, and S. I. Rudnev

UDC 621.039.51

It is of interest to clarify the effect of helium on the process of formation of pores in the crystal lattice of a metal irradiated by accelerated ions. In [1-3] the effect of helium on the magnitude of the flowing of structural steels under irradiation by carbon ions and protons was investigated, as well as its effect on nickel and copper under bombardment of nickel and copper ions.

The purpose of the experiments performed consisted in clarifying the effect of helium on the processed pore formation in nickel under irradiation by nickel ions over a wide range of concentrations. The procedure for irradiating and investigating samples are analogous to those expounded in [4, 5]. Strips of annealed nickel 0.2 mm thick were subjected to preliminary irradiation by helium ions having an energy of 70 keV on an ILU-100 accelerator. Saturation with helium was carried out without heating, and the target was mounted at an angle of 15° with respect to the ion beam. The helium concentration in the sample ranged from 10^{-4} to 10 at.%. Thermokinetic analysis performed according to the described procedure [6] demonstrated good agreement between the actual helium content in the sample and the calculated value. After irradiation by helium disks having a diameter of 3 mm were cut out from the nickel strips; these disks were then thinned electrolytically on the side opposite the irradiated side for study by the method of transmission electron microscopy. Irradiation with Ni^+ ions having an energy of 46 keV was carried out at a temperature of 520°C until an integral dose of 10^{17} ions/cm^2 was attained. The irradiation time was 1.5 h.

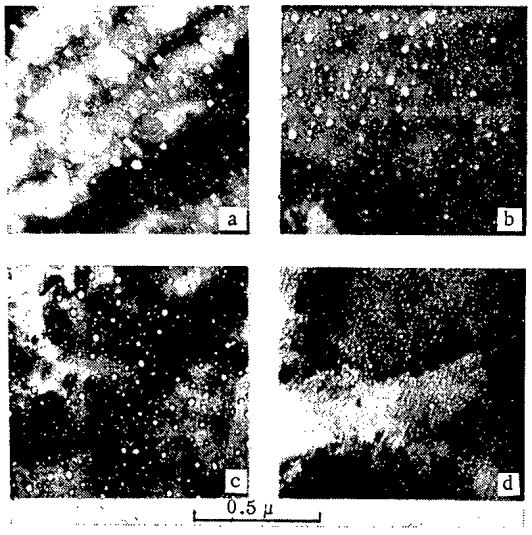

Fig. 1

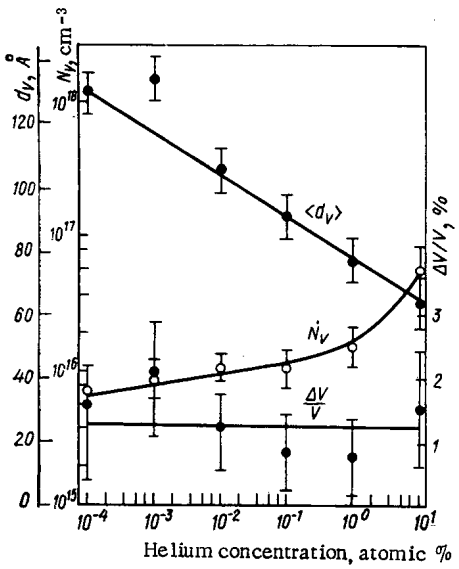

Fig. 2

Fig. 1. Microstructure of irradiated nickel for a helium concentration in the sample (atomic %): a) 10^{-3}; b) 0.1; c) 1; d) 10.

Fig. 2. Effect of helium concentration on the variation of the average pore size d_V, the pore density N_V and the volume of the sample $\Delta V/V$.

Translated from Atomnaya Énergiya, Vol. 38, No. 6, pp. 426-427, June, 1975. Original article submitted July 10, 1974.

Certain typical microstructures of the irradiated samples are illustrated in Fig. 1. The distribution of the pores on the inspected area of the samples was uniform. It is evident that, to the extent that the helium concentration increased, the pore density likewise increases, while the size of the pores decreases. The size of the pores having a facing ranged from 20 to 280 Å.

Figure 2 displays the dependences which characterize the effect of helium concentration on the average pore size, the pore density, and the variation of the volume of the investigated sample as a result of the development of porosity. Beginning with the helium concentration of 0.1 at.%, the density of the pores increased abruptly. At a low concentration (from 10^{-4} to 10^{-2} at.%) the role played by the helium atoms in the process of pore formation in nickel was negligible. Thus, the increase in helium concentration by a factor of 100 leads to an increase in pore density by only a factor of 1.5. The effect of helium at concentrations above 0.1 at.% is more perceptible. An increase in helium concentration by a factor of 100 changes the pore density by a factor of 5.3. The change in volume ($\Delta V/V$) is independent of the concentration of implanted helium within the limits of the measurement error.

Consequently the helium atoms merely stimulate the process of cavity nucleation. An increase in the number of helium atoms does not alter the magnitude of the swelling of the irradiated metal.

LITERATURE CITED

1. R. Nelson, D. Mazey, and J. Hudson, in: Proc. Reading Conf. on Voids Formed by Irradiation of Reactor Materials, BNES, Harwell (1971), p. 191.
2. D. Keefer and A. Pard, J. Nucl. Mater., 45, 55 (1972/1973).
3. J. Delaplace, J. Nucl. Mater., 47, 278 (1973); L. Glowinski, et al., ibid., p. 295.
4. V. N. Bykov et al., Fiz. Tverd. Tela, 15, No. 3, 910 (1973).
5. S. Ya. Lebedev and S. D. Panin, Pribory i Tekh. Éksperim., No. 3, 179 (1973).
6. V. S. Karasev et al., At. Énerg., 34, No. 4, 251 (1973).

SCINTILLATING PLASTICS WITH IMPROVED RADIATION RESISTANCE

V. M. Gorbachev, V. V. Kuzyanov,
Z. I. Peshkova, É. A. Rostovtseva,
and N. A. Uvarov

UDC 539.1.074.3:539.1.04

The commercial scintillating plastic based on polystyrene containing 2% PPP* and0.02-0.06% POPOP, which is widely used for low-intensity neutron and γ-radiation, decreases in light output significantly under the effects of constant-intensity radiation [1] and pulsed radiation [2]. This paper discusses the results of a search for polystyrene-based scintillating plastics possessing more stable light output when subject to the action of hard x-rays. The prescription for the luminescent additives introduced into the polystyrene was selected on the basis of optimal matching between the spectral regions of luminescence and the maximum spectral sensitivity of the photodetectors. All samples had high transparency and allowed mechanical working. Samples containing 5-15% N by weight turned out to be unstable when stored; evaporation of the naphthalene produced surface cracking after 1-2 months. This effect was not present for lower naphthalene content (0.5-2%). Sample composition and relative light yield $\varkappa_{rel}$ is shown in Table 1 (d is thickness in cm).

The scintillators were irradiated by bremsstrahlung from a 15-MeV linear electron accelerator [3] at a dose rate of $2.5 \cdot 10^3$ rad/sec. The samples were in the form of rectangular prisms with a base 25 × 25 mm in size and thicknesses ranging from 1 to 50 mm. Light output from irradiated samples was recorded by means of a photocell which was separated from the scintillator and which was shielded against scattered radiation. The photocell current was registered on a recorder.

Particular samples showing high stability of light output when irradiated by a flux of constant intensity were studied for the effects of pulsed x-radiation. For this purpose, a pulsed light source which simulated the luminescence of the scintillaor [4] was turned on [4-6] approximately 100 μsec before the pulse from a high-power x-ray generator [5]. The light passing through the scintillator was recorded by a photocell and displayed on an oscilloscope. Assuming that irradiation of plastic scintillators leads simultaneously to degredation (quenching) of luminescence and to loss of transparency by the material,

*PPP is paraterphenyl; POPOP, 2,2'-p-phenylene-bis-(5-phenyloxazole); PPO, 2,5-diphenyloxazole; N, naphthalene; St, stilbene; T, tolan; An, anthracene.

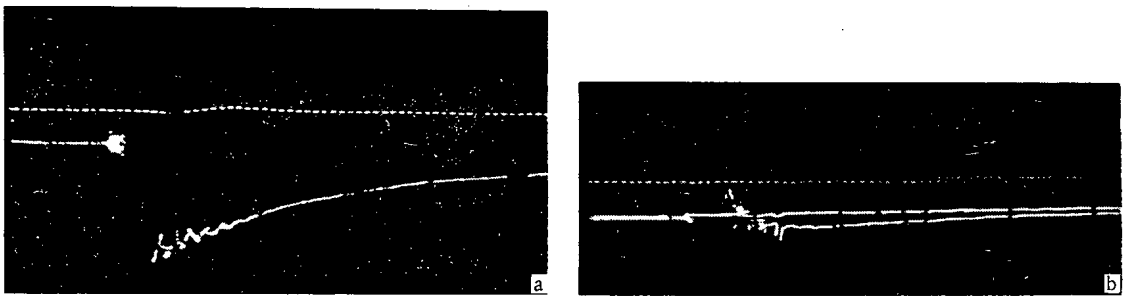

Fig. 1. Oscilloscope traces of the change in scintillator transparency for pulsed irradiation. Sweep time is 130 μsec; vertical sensitivity is 1 V/cm.

Translated from Atomnaya Énergiya, Vol. 38, No. 6, pp. 427-429, June, 1975. Original article submitted July 10, 1974.

TABLE 1. Characteristics of Radiation Effects on Certain Organic Scintillators with a Polystyrene Base

Additives, %	d	$\varkappa_{rel}$	μ_s, rad^{-1}	β_s, rad^{-1}	α_s, rad^{-1} · cm^{-1}
2 PPP	5	1	$8{,}1\cdot10^{-7}$	$1\cdot10^{-8}$	$3{,}2\cdot10^{-7}$
+0,06 POPOP	5	0,56	$2{,}6\cdot10^{-7}$	$6{,}8\cdot10^{-8}$	$7{,}2\cdot10^{-8}$
2 PPO					
2 PPO +0,06 POPOP	5	0,85	$2{,}4\cdot10^{-7}$	$1{,}14\cdot10^{-7}$	$7{,}4\cdot10^{-8}$
2 PPP +0,2 St	5	0,4	$7\cdot10^{-8}$	$1\cdot10^{-8}$	$3{,}7\cdot10^{-8}$
10 N +0,2 POPOP	5	0,7	$6\cdot10^{-8}$	$4{,}5\cdot10^{-8}$	$5{,}6\cdot10^{-9}$
0,5 N +0,2 POPOP	5	0,53	$2{,}4\cdot10^{-8}$	$1{,}57\cdot10^{-8}$	$3\cdot10^{-9}$
0,5 N +0,02 POPOP	5	0,36	$1{,}25\cdot10^{-8}$	$1{,}9\cdot10^{-8}$	$2\cdot10^{-9}$
St	2		$1{,}85\cdot10^{-7}$		
T	2		$1{,}74\cdot10^{-7}$		
N	2		$1{,}63\cdot10^{-7}$		
2 T +0,2 An	2	0,037	$1{,}87\cdot10^{-7}$		
2 N +2 St	2	0,11	$1\cdot10^{-7}$		
2 N +0,2 An	2	0,135	$9\cdot10^{-8}$		
2 PPP	2	0,78	$5\cdot10^{-7}$		
2 PPP +2 T +0,2 An	2	0,17	$9\cdot10^{-8}$		
15 N	2	0,15	$< 2\cdot10^{-8}$		$< 1\cdot10^{-8}$
2 PPP +2 St	2	0,1	$9\cdot10^{-8}$		
15 N +0,2 POPOP	2	0,75	$9\cdot10^{-8}$		$< 4\cdot10^{-8}$

the combined effect of these processes can be represented as the product of the two functions $f_1 = J/J_0 = 1/(1 + \beta D)$, which describes the reduction in intensity of luminescence [6] and $f_2 = S/S_0 = (1-e^{-\alpha Dh})/(\alpha Dh)$, which describes the loss of light output because of reduction in sample transparency [2], where D is the absorbed dose; h is the scintillator height in cm; J_0, S_0 and J, S are respectively the luminescence intensity and sample transparency before and after irradiation.

When $\beta D < 1$ and $\alpha Dh < 1$, functions f_1 and f_2 are satisfactorily described by exponentials and their product is

$$f_1 f_2 = \frac{\varkappa}{\varkappa_0} \approx e^{-\left(\beta+\frac{\alpha h}{2}\right)D} = e^{-\mu D}.$$

By measurement and comparison of the sensitivity $\varkappa$ of samples of different thickness (~1 and 50 mm) before and after irradiation with a constant-intensity flux, we determined the coefficient of radiation quenching of luminescence β_s,* the coefficient of radiation absorption α_s and the total coefficient of radiation damage μ_s (see Table 1). The commercial plastic was found to have the highest coefficient of radiation absorption (i.e., the poorest radiation resistance), $\alpha_s = 3.2\cdot10^{-7}$ rad^{-1} · cm^{-1}. The value of α_s was approximately ten times less in samples containing paraterphenyl and stilbene and approximately 100 times less in samples containing naphthalene. All the samples containing paraterphenyl had similar values for the coefficient of radiation quenching of luminescence, $\beta_s \approx (1\text{-}2)\cdot10^{-8}$ rad^{-1}. Scintillators containing PPO are characterized by the largest value for this coefficient, $\beta_s \approx 1\cdot10^{-7}$ rad^{-1}.

With pulsed irradiation, loss of transparancy by the scintillator in the first microseconds after irradiation is considerably greater than with radiation of constant intensity. The commercial scintillator showed the greatest loss of transparency ($\alpha_p = 4.6\cdot10^{-5}$ rad$^{-1}\cdot$cm^{-1} for 5 μsec after irradiation). For a scintillator with 15% N and 0.2% POPOP, α_p was 17 times less than for the commercial scintillator ($\alpha_p = 2.7\cdot10^{-6}$ rad$^{-1}\cdot$cm^{-1}). Pure polystyrene, polystyrene with 15% N, added, and polystyrene with 0.5% N and 0.02% POPOP added had considerably greater radiation resistance. For a dose of 5400 rad, a decrease in their transparency was not registered by the equipment used, which corresponds to $\alpha_p < 6\cdot10^{-7}$ rad$^{-1}\cdot$cm^{-1} and is at least 70 times less than the value of α_p for the commercial plastic with a polystyrene base.

Oscilloscope traces (Fig. 1) exemplify the respective change in transparency after pulsed irradiation for the commercial scintillator (2% PPP + 0.06% POPOP) 30 mm thick at a dose of 3850 rad (Fig. 1a) and for a scintillator of improved radiation resistance (15% N + 0.2% POPOP) of the same size at a dose of 5000 rad (Fig. 1b). In the second case, the decrease in photocurrent after the radiation pulse is considerably reduced.

It is necessary to note that in scintillators containing 2% PPP and 0.2% St, the luminescence time for the fast component (contribution ~75%) is < 2 nsec and is 11 nsec for the slow component while in scintillators with 0.5% N and 0.02% POPOP added, the times are respectively 5.5 and 57 nsec (contribution 85%).

Thus we have shown experimentally that one can create polystyrene-based scintillators for which the transparency varies under the effects of radiation by factors of 10 to 100 times less than does the transparency of a commercial scintillator containing 2% PPP and 0.06% POPOP.

*Coefficients obtained with a radiation flux of stable intensity have the subscript "s"; those obtained with pulsed radiation have the subscript "p."

LITERATURE CITED

1. I. M. Rozman and K. G. Zimmer, At. Énerg., 2, 54 (1957).
2. E. D. Beregovenko, V. M. Gorbachev, and N. A. Uvarov, At. Énerg., 34, 124 (1973).
3. T. N. Filimonova and A. M. Shmygov, Zh. Tekh. Fiz., 32, 1438 (1962).
4. K. V. Aleksandrovich et al., Pribory i Tekh. Éksperim., No. 3, 127 (1970).
5. K. F. Zelenskii et al., Pribory i Tekh. Éksperim., No. 4, 177 (1969).
6. J. Birks, Scintillation Counters [Russian translation], IL, Moscow (1955), p. 98.

SELECTING THE OPERATING POINT IN RESOURCE TESTS OF THERMIONIC CONVERTERS

V. I. Berzhatyi, A. S. Karnaukhov, and V. V. Sinyavskii

UDC 621.36.537.32

In tests of thermionic electrical generating elements and assemblies by the static method (by points) the volt—ampere characteristics of the constant thermal power q = const are usually determined. The temperature of the emitter field $T_e(z)$, including the maximum emitter temperature $T_{e.max}$, also varies along the q = const characteristics because of the variation of the current density j and the related electron cooling of the emitter [1]:

$$q_e = j\,(T_e,\ v)\,[v + \varphi_C\,(T_C) + 2kT_e]. \tag{1}$$

For increasing current the emitter temperature will decrease along the q = const characteristic as a consequence of the redistribution of the component of emitter heat takeoff: the increase of the electron component of the thermal flux in accordance with Eq. (1), and the decrease of the radiant flux density as a result of the reduction of emitter temperature:

$$q_r = \varepsilon\sigma\,(T_e^4 - T_C^4). \tag{2}$$

Here v is the potential distance between the electrodes; φ_C is the work potential of the collector; T_e is the electron temperature of the collector; k is Boltzmann's constant; ε is the reduced emittance of the electrodes; σ is the Stefan—Boltzmann constant; T_C is the collector temperature.

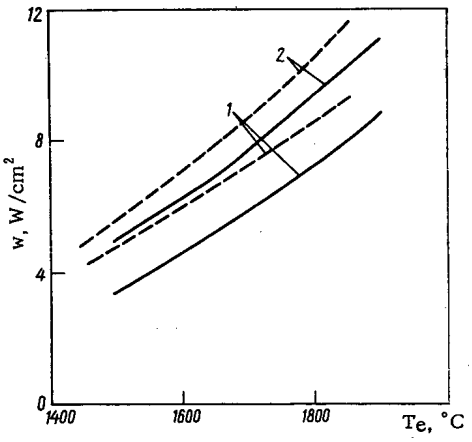

Fig. 1

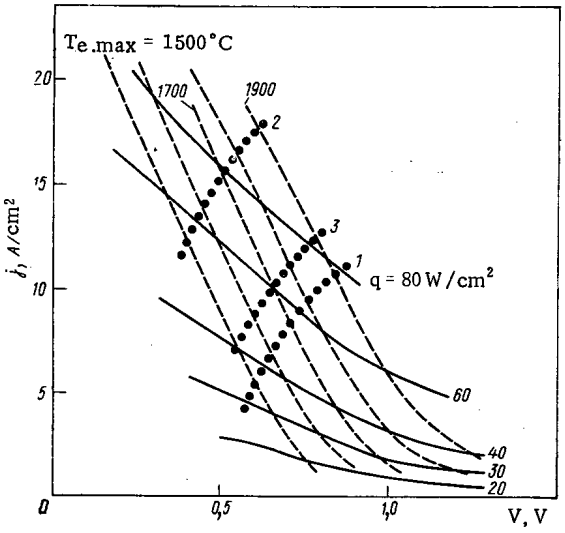

Fig. 2

Fig. 1. Dependence of the power of a thermionic electrical generating element on emitter temperature for the optimal points on the constant-thermal-power characteristics (1) and the constant-emitter-temperature characteristics (2).

Fig. 2. Set of constant-thermal-power and constant-maximum-emitter-temperature volt—ampere characteristics.

Translated from Atomnaya Énergiya, Vol. 38, No. 6, pp. 429-430, June, 1975. Original article submitted August 27, 1974.

Taking account of the fact that in resource tests of thermionic elements and assemblies a temperature "locking" of the results obtained is performed (for example, of the average electrical power density $\bar{w}(T_e)$ and the conversion efficiency $\eta(T_e)$), the point on the q = const characteristic at which this is done is not immaterial.

In [2-4], as a rule, there is no indication at what points on the characteristics the emitter temperature is determined. The results are usually referred to points on the q = const characteristics at which the maximum power is observed (for q = const characteristics the maximum efficiency is naturally also observed at these same points). However, in this case the experimental dependences $\bar{w}(T_e)$ obtained for the points on the q = const characteristics at which $\bar{w}$ is maximal do not correspond to the highest values of power which may be obtained at the same emitter temperatures. This is associated with the different spokes of the volt—ampere characteristics q = const and T_e = const and the resulting failure of the points on the q = const and T_e = const characteristics having the maximum electrical power to coincide. For an ideal thermionic converter the characteristics q = const and T_e = const cross at an angle determined by the conditions [5]

$$\left.\frac{\partial j}{\partial v}\right|_{q=\text{const}} \approx \left.\frac{\partial j}{\partial v}\right|_{T_e=\text{const}} \left(1-q_e \frac{\partial j/\partial T_e}{\partial q_e/\partial T_e+\partial q_r/\partial T_e}\right).$$

Whereas at low densities of the electric power w = jv (up to several W/cm^2) the slopes of the characteristics q = const and T_e = const are close and the points of interest to us practically coincide, with a growth of w the difference in the slope angles and the parameters of the considered points increases.

Figure 1 shows the dependences of the power on emitter temperature for an electrical generating element having a tungsten emitter and an interelectrode gap of 0.3 mm, both the average ($\bar{T}_e$; dashed lines) and maximum ($T_{e.max}$; solid lines) emitter temperatures being chosen as the independent variable. In Fig. 1 curves 1 correspond to the points on the q = const characteristics having the maximum power, while curves 2 correspond to the points on the T_e = const and $T_{e.max}$ = const characteristics having the maximum power. It can easily be seen that with increasing T_e the difference in the absolute values of w at the optimal points on the characteristics q = const and T_e = const increases. For the dependence w ($T_{e.max}$) the value of the difference is w times as great as a consequence of the different degree of nonisothermicity of the emitter at the optimal points on the q = const and $T_{e.max}$ = const characteristics, although its variation as a function of $T_{e.max}$ is less pronounced. As a result, for w = 5-10 W/cm^2 values of electrical power are realized at the optimal points on the $T_{e.max}$ = const characteristics which are 15 to 25% higher, or the same values of power may be obtained at values of $T_{e.max}$ which are 70 to 120°C lower than at the points on the $T_{e.max}$ = const characteristics corresponding to the optimal values of power. However, the transfer to the optimal point on the $T_{e.max}$ = const characteristic requires an increase in current density and heat evolution, as a result of which the efficiency for the considered points on the isothermal characteristics will be lower than it is for the q = const characteristics.

Thus, in tests of thermionic elements and assemblies having a high power density, in which the problem is to obtain the maximum values of power while restricting $T_{e.max}$, the optimal operating point will not correspond to the points on the q = const characteristics having the maximum power. The choice of the required operating point may be made from a set of q = const and $T_{e.max}$ = const volt—ampere characteristics which has been calculated for the tested elements or assemblies; this is very important in resource tests.

A typical set of characteristics for elements with a polycrystalline-aggregate tungsten emitter, an interelectrode gap of 0.3 mm, and an optimal cesium vapor pressure and collector temperature is illustrated in Fig. 2 (it was calculated from the algorithm of [5]). Curve 1 applies to operating points at which the maximum power density w is realized for a stipulated thermal flux density q on the emitter, while curve 2 corresponds to operating points at which the maximum w may be obtained for a stipulated $T_{e.max}$. Moreover, this same diagram shows curve 3 representing the geometric locus of the points at which the maximum efficiency of the $T_{e.max}$ = const characteristics is observed.

LITERATURE CITED

1. V. A. Maksimov and S. A. Titkov, Zh. Tekh. Fiz., 39, No. 1, 166 (1969).
2. R. Howard and J. Danly, in: Thermionic Energy Conversion [Russian translation], Atomizdat, Moscow (1971), p. 110.
3. J. Holland et al., ibid., p. 119.

4. A. Ester et al., ibid., p. 142.
5. Yu. A. Broval'skii et al., in: Reports of Soviet Scientists to the Second International Conference on Thermionic Energy Conversion [in Russian], Izd. VNIITI, Moscow (1969), p. 281.

NEUTRON RESONANCES IN ^{181}Ta AT 2-70 eV

T. S. Belanova, A. G. Kolesov,
V. A. Poruchikov, S. M. Kalebin,
and V. S. Artamonov

UDC 621.039.556

Measurements of σ_t for the isotope ^{181}Ta were made by the time-of-flight method at the SM-2 reactor. A neutron burst was created by a selector with three synchronously revolving rotors suspended in a magnetic field [1]. The neutron detector was a band of helium counters. The spectrometer resolution was 70 nsec/m.

Metallic tantalum of high purity containing 99.9% ^{181}Ta was studied. Measurements were made with samples of three thicknesses: $132.5 \cdot 10^{20}$, $44.2 \cdot 10^{20}$, $5.5 \cdot 10^{20}$ nuclei/cm^2.

Resonance parameters of neutron levels in the energy range 2-70 eV were determined from the measured transmission. The statistical error of the measurements was $\leq 1.5\%$. The neutron background level was 1-2%.

Up to 40 eV, the neutron resonance parameters were calculated by the shape method from the one-level Breit—Wigner formula, and by the area method above 40 eV. In using the area method, the value of the radiation width was assumed to be 65.5 MeV. It was obtained by averaging the radiation widths Γ_γ over the 10 resonances in the neutron energy region 10-40 eV. Table 1 presents the values we obtained for the neutron resonance parameters.

A value for the potential scattering cross section $\sigma_p = 9.8 \pm 1.0$ b, which is in agreement with earlier values [2,3], was calculated together with the calculation of the resonance parameters in the energy region 2-70 eV.

The data obtained for the level parameters in ^{181}Ta are in basic agreement with earlier data [4-6]. One should note the first determination of a weak level at 34.28 eV. Apparently it was not observed previously in the background from the strong level at 35.16 eV. A rather strong level at 18.6 eV with $g\Gamma_n = 0.4$

TABLE 1. Resonance Parameters for ^{181}Ta

$E_0 \pm \Delta E$, eV	$\Gamma_\gamma \pm \Delta\Gamma_\gamma$, MeV	$g\Gamma_n \pm \Delta g\Gamma_n$, MeV	$g\Gamma_n^0$, MeV	σ_0, b
4,28±0,01 *	(65,5)	1,81±0,06	0,87	19 000±1000
10,37±0,03	76,5±3,5	1,68±0,07	0,52	5 520±60
13,89±0,06	57,4±3,3	0,50±0,02	0,13	1 625±30
20,35±0,07	51,8±4,5	0,48±0,02	0,11	1 174±30
22,78±0,09	65,7±10,0	0,10±0,01	0,02	171±10
24,00±0,09	76,4±7,3	2,53±0,19	0,52	3 590±70
30,08±0,12	57,1±16,6	0,15±0,05	0,027	223±20
33,51±0,13 †	—	—	—	—
34,28±0,15	60±10	0,10±0,02	0,02	130±20
35,16±0,20	70±11	5,2±0,6	0,88	4 800±100
35,95±0,20	67±8	6,63±0,60	1,11	6 000±900
39,2±0,20	64±10	23,0±6,0	3,7	14 000±1000
49,23±0,20 *	(65,5)	0,53±0,07	0,075	420±40
57,65±0,30 *	(65,5)	0,18±0,04	0,024	125±30
58,99±0,30 *	(65,5)	0,08±0,02	0,01	57±10
63,22±0,30 *	(65,5)	2,30±0,15	0,29	1 400±600

*Area method

†Very weak resonance.

Translated from Atomnaya Énergiya, Vol. 38, No. 6, pp. 430-431, June, 1975. Original article submitted December 9, 1974.

MeV has been cited [6, 7]. We did not observe a level at 18.6 eV. If this level does exist, then judging from the value for its neutron width it should be comparable with the neighboring levels at 13.89 and 20.35 eV which we observed and for which $g\Gamma_n$ is respectively 0.50 and 0.48 MeV.

We did not observe the level at 55.8 eV with $g\Gamma_n = 0.1$ MeV [6] possibly because the measurements were made with thin samples.

In the present work, the energy region 2-70 eV was considered sufficiently resolved to permit calculation of the average spacing $\bar{D}$ in the spin state for ^{181}Ta and of the neutron strength functions S_0: $\bar{D} = 4.21 \pm 0.98$ eV and $S_0 = 1.96 \cdot 10^{-4}$.

LITERATURE CITED

1. S. M. Kalebin et al., in: Proceedings of Conference on Neutron Physics [in Russian], Pt. II, Naukova Dumka, Kiev (1972), p. 267.
2. H. Lion and L. Rainwater, Phys. Rev., C6, 435 (1972).
3. R. Fluharty et al., Phys. Rev., 103, 1778 (1956).
4. R. Ya. Dol'nitsyn, in: Proceedings of Working Conference on Slow Neutrons [in Russian], Dubna (1961), p. 57.
5. J. Garg, L. Rainwater, and W. Havens, Conf. on Study of Nuclear Structure with Neutrons, Antwerp (1965), p. 95.
6. Neutron Cross Sections, BNL-325, Second Edition (1966).
7. I. A. Radkevich and V. V. Vladimirskii, At. Énerg., No. 5, 55 (1956).

COLLABORATION DAYBOOK

The fifth meeting of KNTS on atomic power plant water systems was held in Ostrava, Czechoslovakia, from February 25 to 27, 1975. USSR proposals for the purification of coolant and radioactive discharge waters of 1000 MW(e) water-cooled, water-moderated power reactors were discussed. It was stressed that the technical solutions presented provide for operation of the atomic power plant with maximum use of a recirculating water supply and a minimum discharge of radioactive wastes into the environment.

Reports of specialists from Bulgaria, Hungary, East Germany, and the USSR on the regeneration of boric acid from discharge and drain waters of the primary loop were discussed, as were reports of specialists from Bulgaria, the USSR, and Czechoslovakia on the development and use of magnetic filters to purify the primary coolant and the secondary loop water of atomic power plant reactors.

A delegation of USSR specialists proposed a plan for a set of unified methods for estimating the properties and qualities of ion-exchange resins for nuclear power. KNTS for the most part approved this plan and recommended using it as a basis for the preparation of the final version.

Discussion led to an agreement on a working plan for a program of cooperation of the COMECON member countries on "water systems, water preparation, and problems of monitoring the tightness of atomic power plant fuel element cladding" during 1976-1980.

The seventh meeting of KNTS on the reprocessing of irradiated fuel was held in Brno, Czechoslovakia from March 17 to 21, 1975. Problems of the further cooperation of COMECON member countries in the field of reprocessing of spent fuel elements from atomic power plants during 1976-1980 were discussed in detail, and a working plan of cooperation was agreed upon. Reports of work performed in COMECON member countries in 1974 in accord with the program of cooperation, and papers on the work of KNTS were discussed. A plan of general instructions on the transport of spent fuel of the COMECON member countries was also discussed. A plan was made for presentation to the standing committee.

Simultaneously with the KNTS meeting a conference of specialists was held on the technical tasks in the working plan on "The development of methods and devices for monitoring and controlling the technological processes in the regeneration of spent fuel elements."

The seventh KNTS meeting on fast reactors was held in Minsk from March 31 to April 3, 1975. There were reports of Czechoslovakian specialists on progress in completing research on fast reactors, and communications of specialists from Hungary, Poland, the USSR, and Czechoslovakia on the development of methods and devices for monitoring fast reactor cores, and studies of methods for increasing heat transfer. Plans for future work on all these matters were firmed up.

There was a discussion of paper PK IAÉ on KNTS projects completed during 1972-1974 on cooperation in "Research on fast power reactors."

Recommendations of the conference of specialists from the COMECON member countries on nuclear data (Obninsk, November, 1974), and preparations for a conference on various aspects of the safety of sodium—water steam generators were discussed.

Plans were discussed for experimental and construction work on high-power fast reactors during 1977-1980, and reports on other KNTS commissions were discussed. Agreement was reached on all problems.

The conference of COMECON member country specialists on the standardization of radiation-shielding and radiation technology products was held in Moscow from April 15 to 18, 1975. There was agreement

Translated from Atomnaya Énergiya, Vol. 38, No. 6, pp. 432-433, June, 1975.

on standards for lead shielding blocks (general technical requirements). There was agreement on standards and technical conditions for solid lead shielding blocks, and ports with ball and socket joints. A plan was discussed for the development of COMECON standards by 1976 and the order of development of programs of the complex standardization of radiation and radiation-shielding technology products during 1976-1980.

A COMECON standard for equipment used in working with radioactive materials (general technical requirements) was discussed, and the subsequent order of its development was agreed upon. The order of formulating working plans on "Scientific and technical cooperation during 1976-1980," and a preliminary notice for the next conference of specialists in Poland during September, 1975 were settled.

The conference participants exchanged opinions on standardization of "Laboratories for working with sources of ionizing radiations. Classification and general technical requirements," and "Aerosol filters for nuclear technology." Plans were made for further development and coordination.

The twentieth meeting of the working group on reactor science and technology and atomic power was held in Eisenach, East Germany, from April 15 to 18, 1975. Scientific and technical cooperation during 1976-1980 was agreed upon for the following topics: "Research, development, and improvement of water-cooled, water-moderated (WCWM) reactors, in particular the production of 1000 MW(e) reactor installations of the WCWM type," "Research on critical heat loads in fuel rod bundles in stationary and nonstationary heat-transfer regimes," and "Determination of optimum strategies in the development of nuclear power within the COMECON framework." A communication from a delegation of USSR specialists on the work performed during 1971-1975 on "Monitoring and control of nuclear reactors and atomic power plant equipment" was discussed. A proposal was made for a program and forms of cooperation on "The development and introduction of monitoring and control systems using computers for 400 MW(e) and 1000 MW(e) WCWM reactor installations."

Proposals were discussed for cooperation in the development of large power reactors, the use of nuclear power reactors for the combined production of electrical power and low-temperature heat, and the nuclear power fuel cycle. A communication from specialists on "Research on the physics of shielding atomic power plant reactors" was discussed.

There was agreement on the program for a seminar on "Experience in the construction and operation of WCWM reactor installations."

BOOK REVIEWS

E. M. Filippov

NUCLEAR GEOPHYSICS*

Reviewed by J. A. Czubek

In 1962 E. M. Filippov published "Applied Nuclear Geophysics" (Izd-vo AN SSSR, Moscow, 1962). This was the first review in the world of applications of nuclear methods in geophysics and geology. In the next 11 years it remained the only complete handbook, and references to it can be found in many articles from the USSR and elsewhere.

In 1973, Filippov published a new book, "Nuclear Geophysics," in two volumes. In this, in contrast to the first book, he pays less attention to theoretical problems. He considers mainly practical results obtained by using nuclear geophysics in the USSR and elsewhere.

The book consists of 36 chapters in seven sections. Twelve appendices give information on the methods and devices of nuclear geophysics. There are over 2000 citations of Soviet and foreign authors.

The first volume is devoted to methods based on measurements of natural radioactivity and methods based on applications of sources of alpha, beta, and gamma radiation. The author considers the interactions and transference of nuclear radiation in rocks, various nuclear methods, methods of measurement, ways of registering nuclear radiation, and the basic principles of design of radiometric apparatus and the possibilities of nuclear methods in various geological and geophysical investigations. In these sections the author does not consider machine processing of the data, though this question is becoming increasingly important as nuclear geophysics develops.

In the seventh chapter, which discusses errors of measurement, more attention should have been paid to the "dead time" of the apparatus, because this is also important at the present stage of development of nuclear methods.

The second volume mainly deals with neutron methods in nuclear geophysics. The author discusses their applications in determining the wetness of soils, the porosity of rocks, and their contents of various minerals. Comparatively little attention is paid to problems of lithological differentiation of the cross sections of boreholes with the aid of these methods (in combination with other geophysical methods).

Chapter 26 deals with the photoneutron method. Here foreign specialists will be most interested in the results of Soviet investigators on the study of cross sections of boreholes.

The sixth section deals with methods based mainly on the use of various accelerators (linear accelerators, betatrons, electron cyclotrons (microtrons), cyclotrons, neutron generators, neutron multipliers, and nuclear reactors). The use of these instruments to analyze rock samples is discussed in the broad-ranging Chapter 28. Here the author gives methods which form a basis for application of various nuclear reactions caused by ions, alpha particles, protons, deuterons, neutrons, gamma quanta, etc.

Methods of investigation of cross sections of boreholes with the aid of neutron generators are discussed in Chapter 29. This contains the physical principles of these methods, and gives the main theoretical results of Soviet geophysicists.

The last section deals with the combined applications of nuclear—geophysical methods to solve such problems as the study of lithology, the determination of porosity and density in rocks, and the concentrations

*(Proceedings of Institute of Geology and Geophysics, Siberian Branch, Academy of Sciences of the USSR, Nos. 40-41, "Nauka," Novosibirsk, 1973.)

Institute of Nuclear Physics, Cracow, Poland. Translated from Atomnaya Énergiya, Vol. 38, No. 6, p. 433, June, 1975.

of various minerals (oil, coal, boron, beryllium, aluminum, titanium, chromium, manganese, iron, nickel, copper, tin, antimony, barium, tungsten, molybdenum, mercury, the rare earths, potassium, uranium, thorium, etc.).

In conclusion I should like to express my delight at the way in which the author has managed to elucidate such a huge amount of material in a form accessible to a wide circle of geophysicists. This book, like the previous one, will be of use to students, graduates, scientists, and engineers working in the field of nuclear geophysics.

I am astonished that such a small number of copies (1200) has been printed: this is less than half the circulation of the first book!

SYMPOSIUM OF THE INTERNATIONAL AGENCY OF ATOMIC ENERGY REGARDING THE CHOICE OF AREAS FOR NUCLEAR INSTALLATIONS

N. P. Dergachev

The Symposium on the choice of areas for nuclear installations was held on December 9-14, 1974 and was attended by 230 representatives from 40 countries and a number of international organizations (International Commission on Radiological Protection, World Energy Conference, etc.). Some 43 papers were read and discussed. It was pointed out that present-day practice in the exploitation of a large number of nuclear installations, nuclear power stations, and fuel-cycle undertakings was consistent with the safety of the population and the environment when these installations operated under normal conditions. The dose levels in the surrounding territory associated with gaseous and liquid fall-out are very low — 5-30% of the natural background.

Only the slight chance of accidents makes nuclear installations a potential menace to the population. Hence the criteria governing the choice of sites for nuclear installations discussed in the contributions from a number of countries (United Kingdom, Soviet Union, United States, France, West Germany, etc.) made three principal demands: general engineering suitability; safety for the population and environment; social-economic propriety (taking account of the general feeling of the populace). Taking the most detailed and comprehensive paper as an example (No. 188/42, United States), it is interesting to examine the whole set of requirements imposed upon the siting of nuclear power stations.

I. General requirements.
   1. Energy requirements in the region in question.
   2. Closeness and accessibility of the power-supply system.*
   3. Size and number of the units (nuclear power stations) established in the area.
   4. Suitability of the area in question for other forms of production (industrial competitiveness).

II. Engineering requirements (characteristics of the site).
   1. Safety (geology, freedom from earthquakes; hydrology, prevention of flooding, degree of dilution of liquid radioactive waste; demography, low population density; meteorology, dilution and dissipation of gaseous fall-out.
   2. Functional requirements (presence and accessibility of cooling water; geology, permissible ground loading; accessibility of the site to adoption; presence of manpower and the necessary building materials).

III. Characteristics of the environment [ecological sensitivity of the flora and fauna on the earth and in the water to the action of effluents (radioactive, thermal, etc.) from the installation in the surrounding territory].

IV. Use of the earth in the region of the site.

*In the United States and a number of capitalist countries principal attention is paid to the closeness of the nuclear power station to the customer, so as to eliminate undue occupation of the ground by power lines.

Translated from Atomnaya Énergiya, Vol. 38, No. 6, pp. 434-435, June, 1975.

1. Compatibility of the nuclear installation with existing industries.
2. Existence of reserved sites (natural parks) of historical, archeological, or esthetic value.

V. Social—economic factors.

1. Cost of the ground.
2. Disposition of the owners of the ground.
3. Competition in the use of resources (earth, water).
4. Public opinion.

This paper deals with the method practised in the United States by which the fundamental governing and auxiliary criteria are chosen for various parts of the country on the basis of the foregoing requirements. Depending on local conditions the criteria are assessed on a ten-point basis, then the area (site) is assessed and chosen on a point basis. This method (known as the "sifting" technique) was illustrated in connection with the choice of sites for nuclear power stations in the state of Arizona. This state is characterized by the existence of large protected areas (national parks, reservations, etc.), seismic activity, poor water resources, and a relative low population density. Hence the accessibility of the ground for exploitation, the exclusion of earthquake-prone areas, and the existence of water resources (subsurface water) were adopted as main guiding criteria for determining nuclear power station sites. As auxiliary criteria, demography, meteorology (dilution of radioactive effluents), and the accessibility of the area for adoption were chosen.

Thus the main criteria were the engineering requirements; questions of ensuring the safety of the population were solved quite easily. This approach to the choice of sites is characteristic of countries possessing wide territories with a comparatively low mean population density.

A different solution is required in European countries, with their limited territory and high population density (West Germany, France, Denmark, Italy, etc.). Thus in paper No. 188/49 (West Germany) it was noted that, according to predictions for 1955, West Germany would build about 40 nuclear power stations with a total power of 100 million kW placed in the main industrial regions with a high population density and an average distance of 70-100 km between sites. Thus most of the country's population would live quite close to atomic power stations. If one also considers sites for radiochemical installations reprocessing the fuel and the transportation of irradiated fuel elements, it is easy to understand that the main question when siting nuclear power stations and other undertakings of the fuel cycle is that of ensuring the safety of the population under normal operating conditions and in the case of possible accidents. The situation in which a considerable proportion of the population of a country is subjected to the radioactive action of effluents from nuclear installations has led to a reconsideration of the limits of permissible levels of irradiation and to the introduction of a limit based on the genetically significant dose of 30 mrem/year over the whole body (France, West Germany, Denmark, Finland, Common Market countries, etc.). In determining the danger of a nuclear installation for the population, consideration is given to possible accidents involving the melting of the active zone of the reactor and the outflow of activity into the protective building. The leakage of radioactive fission products from the building to the extent of 0.1% per day is taken as acceptable. The limiting dose for individual members of the population during such an emergency is in the majority of countries taken as 25 rems over the whole body, 300 rem on the thyroid gland. The limiting permissible collective dose for the population in a radius of up to 100 km is set at 10^6 man-rems. In the event of a possible excess over the doses indicated in the case of individual members of the population, the latter should be evacuated to safe regions. In papers Nos. 188/6 (Denmark) and 188/7 (Finland) the dose loadings on the population were considered for the case of a serious accident in a nuclear power station, with the destruction of the protective building. It was shown that the limiting dose might be greatly exceeded for individual members of the population in the adjacent territory at distances of up to 10 km.

Methods of calculating the collective dose during a discharge from a nuclear power station were considered in papers Nos. 188/15 and 188/18 (France) in which a new method was developed for determining the dilution coefficient of radioactivity over large distances (up to 100 km). On the basis of experimental investigations coefficients, were proposed defining the vertical and transverse (to the wind direction) turbulent diffusions (σ_z and σ_y) in the form of equations $\sigma_i(t) = (A_i t)^{Ki}$, where A_i and K_i assume certain values (experimentally determinable) in successive time intervals after the discharge. By determining the concentration of radioactivity at various distances from the installations in a 20° sector and multiplying

this quantity by the population density at this distance, the collective dose in the sector may be determined. In this way it is possible to estimate the danger of placing a nuclear power station in a particular site in the case of a serious accident, in respect of the most unfavorable sector.

It is essential to organize a meteorological service in the region of the area selected. The great risk to the population of a serious nuclear accident requires careful consideration of all possible external causes of such accidents. Such causes include severe earthquakes, flooding, hurricances, the bursting of dams, crashing aircraft, explosions in neighboring undertakings, gas pipes, etc. In choosing the site it is essential to undertake investigations aimed at eliminating such dangers. This question was considered in detail in paper No. 188/58 (USA). It was noted that, in accordance with the rules laid down in the United States, in placing a nuclear power station or other nuclear installation on a site subject to any of these factors the risk of an accident should not exceed 10^{-7} per yr. Corresponding calculations should be made by the organizations granting the licences.

The characteristics of the siting of factories processing fuel elements were considered in papers Nos. 188/20, 188/21 (West Germany), 188/26 (India), and 188/59 (USSR). It was shown in these papers that in choosing a site for radiochemical factories it was important to curtail operations relating to the transportation of irradiated fuel and radioactive waste for long-term burial. In papers Nos. 188/21 and 188/20 (West Germany) the authors discussed the siting of radiochemical factories providing for the fuel cycle of atomic power stations with a steady power of ~50 million kW. Two versions were considered; siting the factory as close as possible to the majority of the planned nuclear power stations, and siting them in a region allowing the organization of long-term storage for the radioactive waste from the factories and nuclear power stations. It was shown that on ejecting the radioactive gases formed in the dissolution of fuel elements (^{85}Kr, ^{3}T) into a ventilation pipe 200 m high the concentration of radioactivity at ground level exceeded the permissible doses on the skin (over 100 mrem/year). It was noted that accidents in radiochemical factories were less dangerous as regards the scale of action on the population and surroundings than accidents in nuclear power stations, owing to the absence of high-pressure circuits and the lower yield of activity.

A number of communications discussed in the Symposium were devoted to the formation of public opinion in the country. Owing to incorrect information, possible dangers were sometimes overestimated, and a resistance was engendered to programs on the development of nuclear power and the siting of nuclear installations. In papers Nos. 188/39 (United Kingdom) and 188/56 (West Germany) the importance of careful explanatory work in connection with the population (exhibitions, models, lectures) so as to provide reliable and qualitative information as to the safety of nuclear installations was emphasized. Analogous comments were made in other papers.

An interesting paper regarding the underground siting of nuclear power stations came from the United States (No. 188/45). A layer of earth 10-30 m thick over the building housing the installation should eliminate risks to the environment and population in the event of a serious nuclear accident; in the opinion of the author this fully justified the additional erection costs, which would be no greater than 10%.

In conclusion, we may note certain new principles in the approach to the choice of sites for nuclear installations. It is considered in the United States and the United Kingdom that, in introducing powerful nuclear stations it is desirable (in view of the difficulty of obtaining a licence), to site several nuclear power-station units with a total power of up to 8-10 million kW on a single site. This approach greatly reduces the risk to the population, since the sites may be placed in regions with a low population density, while the probability of a serious accident for such a site will clearly remain at the same level as that of a single nuclear power station.

Choosing a site by the sea simplifies the organization of powerful cooling systems for nuclear power stations with seawater intake. However, this directly contradicts the necessity of bringing the nuclear power station close to the user.

ALL-UNION SCIENTIFIC CONFERENCE ON SHIELDING AGAINST IONIZING RADIATIONS FROM NUCLEAR-INDUSTRIAL INSTALLATIONS

V. P. Mashkovich

The conference was held in Moscow from December 17 to 19, 1974; 267 conference participants representing 77 organizations of various ministries, departments, and the Academy of Sciences of the USSR discussed 200 papers in two plenary* sessions and 16 sectional meetings.

A large fraction of the papers presented at the session on Theoretical Methods and Computer Programs for Calculating Distributions of Ionizing Radiations was devoted to further improvement of the Monte Carlo method and numerical methods for solving the transport equation, and to new programs for solving the neutron and γ-ray transport problem.

Three new modifications of the Monte Carlo method for computing local fluxes were presented: 1) the MDA method (1.26)† decreases the error in predicting the radiation field at the boundary between two media in deep penetration problems; 2) by combining the method of local flux calculation with the concept of a differential albedo (1.29) the radiation field in multisectional bent channels can be solved on medium scale computers; 3) the application of local flux calculations to a finite sized detector (1.42) improves the statistics and decreases the computing time by at least a factor of three in comparison with ordinary local flux calculations.

Recently there have been further developments in finite difference methods for solving the kinetic equation. The RADUGA multigroup complex of programs for two-dimensional shielding calculations, first developed in our country (1.4), was presented at the conference.

The family of widely used ROZ programs developed in the Soviet Union since 1959 was enlarged by the addition of three new programs for multilayer shields (1.9; 1.15; 1.16).

A complex of programs for medium scale computers was developed to obtain approximate solutions of two-dimensional shielding problems. These problems use removal theory for fast neutrons, the P_1 approximation for thermal and intermediate neutrons, and a point kernel and buildup factors for primary and secondary γ-rays (1.21).

The programs which have been written for reactor shield calculations include, for example, a complex program which takes account of primary and secondary radiations, and a multigroup program for calculating multilayer shields by the "diffusion removal" method.

A very large number of papers was presented at the session on New Results of Experimental and Computational Shielding Research. Among the measuring devices which have been constructed should be mentioned the set of five intermediate neutron converters in the B-2 beam of the BR-5 reactor (2.21) for simulating neutron spectra at the inside of a real shield, and the OR-M test stand (2.19) at the VVR-300 reactor (2.7) for basic measurements using a broad weakly diverging monodirectional beam of reactor radiations.

*The review papers presented at the first plenary session appear on p. 502 of this issue of the Journal.
† The numbers in parentheses refer to the numbers of the papers in the collection of abstracts.

Translated from Atomnaya Énergiya, Vol. 38, No. 6, pp. 436-437, June, 1975.

Papers were presented on studies of γ-ray distributions; the spatial, angular, and energy distributions of scattered and reflected reactor γ-rays for shields of tungsten (2.73), lead (2.74), graphite and depleted uranium (2.75), were investigated; studies were made of the γ-distributions beyond lead shadow shields in a water medium (2.22), of collimated γ-sources with energies up to 20 MeV in water and aluminum (2.32), of the time dependence of the angular distribution for pulsed γ-sources (2.93), and a method was presented for taking account of scattered γ-radiation emerging from a volume source (2.77). A number of other investigations was reported (2.25; 2.87).

Interesting research has been performed on the propagation of neutrons in media: a comparison of fast neutron distributions in certain shielding materials calculated with the ROZ-5 program with measured values has led to refinements of a number of group constants (2.5); the relation of the fast neutron scattering function to the scattering cross section for neutrons transmitted through a shield and reflected has been determined (2.20); the neutron distribution in D_2O has been investigated (2.92); the fast neutron buildup factor for heterogeneous shields with an arbitrary arrangement of layers has been investigated (2.6); fast neutron distributions behind finite cylindrical media have been studied (2.41); new experimental information on intermediate neutron spectra in various shielding media has been obtained (2.42).

New experimental and computational information has been obtained on the quasialbedo of the neutron —γ type (2.1) and on the shaping of the capture γ-distribution inside and outside shields of various materials (2.1; 2.2; 2.40).

By using various modifications of the Monte Carlo method the time and spatial-energy distributions of neutrons and γ-rays have been calculated at the surface of separation between air—earth (2.12; 2.38; 2.59; 2.60; 2.65), air—water (2.26), and air—vacuum (2.39; 2.69; 2.70). The systematic results presented are distinguished by the detailed treatment of the time characteristics.

A special session was devoted to the study of charged-particle radiation fields. New experimental information on the characteristics of the fast electron distribution behind shields was compared with the extrapolated problem (2.16). Results were reported on a study of the transport of secondary γ-radiation formed in a heterogeneous shield on which a beam of high-energy protons is incident (2.80).

New results were reported in four papers on the calculation of albedos. It was established that 1) bremstrahlung from secondary charged particles makes a significant contribution to the characteristics of the albedo of high-energy γ-rays for heavy scatters, as much as doubling the values of the differential albedo (2.10); 2) monoenergetic sources of fast neutrons and hydrogenous media are characterized by a linear dependence of the integral neutron albedo on the ratio of the hydrogen cross section to the total cross section of a given reflector material (2.64); 3) the form of the angular dependence of the reflected neutrons is practically independent of the composition of the concretes considered with a hydrogen content of $6 \cdot 10^{21}$-$21.6 \cdot 10^{21}$ atoms/cm^3 (2.31).

Quantitative calculational information was reported on the penetration of radiation through shield inhomogeneities. The RZD program (2.3) and the Monte Carlo method (2.37) were used for neutrons, and the Monte Carlo method for γ-rays (2.24) and electrons (2.68). New experimental research on the propagation of slow and intermediate neutrons through a sodium neutron duct with borated walls in water (2.81) showed that borating the walls of the neutron duct can reduce the neutron flux at the exit of such an inhomogeneity by a factor of 10-100. Experiments at a high-energy proton accelerator (2.28) showed that a composite shield made of large blocks with through slits up to 10 mm wide and bond cracks up to 20 mm wide was practically as effective as a solid shield for a ratio of slit width to length less than 0.005.

New research on the physical, mechanical, deformational, and special properties of new boron containing barium—serpentine and lead—boron cements was reported (2.76). The radiation resistance of concretes was studied (2.15; 2.48). Preliminary data (2.15) indicate the possibility of replacing stainless steel by polymer concretes for lining various vessels used in nuclear power plants if the integrated radiation does not exceed $5 \cdot 10^8$ rads. An interesting paper (2.85) was presented on the search for the place in a layer of good heat-conducting material in a medium of low thermal conductivity where the peak temperature of the layer is least likely.

Several papers were devoted to techniques and instruments for measuring radiation fields, and to problems of radiation therapy.

Fourteen papers were discussed in the session on Nuclear Constants.

The creation of the ARAMAKO complex of programs for generating group constants for reactor-shield problems (3.3) must be counted as an important forward step. The program computes blocked constants by using a 26-group library of cross sections for the interaction of neutrons with matter in the subgroup representation of information on resonance parameters, and the OBRAZ complex of shielding programs (3.14) for calculating multigroup constants using the catalogue of neutron cross sections in the subgroup representation and elastic scattering anisotropy parameters. Other interesting programs form blocks of constants for calculating the penetration of γ-rays through matter by the Monte Carlo method (3.7), and calculate group removal cross sections (3.13).

It is important in performing any calculations to determine the effect of errors in the cross sections on the calculated results. Papers (3.4; 3.9; 3.10) were devoted to these problems.

In the session on Shielding of Nuclear Industrial Installations papers (20% of all papers) were presented on the biological shielding of various kinds of reactors (mainly atomic power plants), charged particle accelerators, space vehicles, and isotopic power generators.

Various aspects of the problem were touched upon: 1) data on radiation fields outside shields around various types of installations were analyzed and used to test the computational methods proposed; 2) a great deal of attention was paid to the design and construction of optimum and economically proven shields; 3) radiation protection during refueling, and ways of decreasing the radiation level from primary loops of atomic power plant reactors were discussed; 4) an approach to the solution of the problem of protecting the environment against atomic power plants using water-cooled, water-moderated power reactors, and the general principles of safety considerations were discussed (4.41); 5) it was shown that the information obtained at charged particle accelerators on conversion factors from particle flux density to equivalent dose rate for various types of corpuscular radiation can serve as the basis for the development of a health-hygiene irradiation norm.

Analysis of the paper presented shows that the creation of complexes of programs for calculating shields around nuclear industrial installations of various kinds significantly decreases shield design expenditures and gives more accurate information on radiation fields outside the shields.

The conference will undoubtedly contribute to the further development and coordination of research in our country on shielding against penetrating radiations.

It is proposed to publish the conference papers in 1975-1976.

FOURTH ALL-UNION CONFERENCE ON THE PHYSICS AND TECHNOLOGY OF HIGH VACUUM

G. L. Saksaganskii

The conference was held in Leningrad between October 29 and 31, 1974; six hundred delegates took part. Some two hundred papers and communications were presented on the following subjects; the physics and physical chemistry of surface and exchange processes in very high vacuum; the technology of very high vacuum in instrument making, high-energy physics, and nuclear physics; the calculation and design of very high vacuum systems; the condensation and cryosorption of highly-rarefied gases; vacuum technology in electrical-vacuum and thin-film instrument making; the automation of vacuum equipment and processes; instruments, apparatus, and scientific—methodical problems of vacuum measurements; vacuum metrology.

Opening the conference with a review paper "Creation of very high vacuum in the chambers of accelerators and storage rings used for counterflow collisions," Academician A. L. Mints emphasized the important role of the further development of very high vacuum technology in creating a new generation of accelerators, and especially accelerator—storage ring complexes. The average pressure in storage-ring chambers should be $\sim 10^{-10}$ mm Hg, while in the region corresponding to the interaction of counterflowing beams it should be under 10^{-11} mm Hg. The life-time of the stored beams and the level of background interactions with the residual gas then become acceptable for the initiation of physical experiments. In order to create such conditions it is essential to make a whole complex of technological constructional decisions, including the choice of the best pumps and pumping arrangements, the operating conditions of the vacuum system, construction materials, and methods of heat-treating the chambers and improving their surface finish.

One example considered was the vacuum system to the NAP-M storage ring (V. V. Anashin et al.). The storage-ring chamber, some 50 m long, is evacuated to $5 \cdot 10^{-10}$ mm Hg by means of combined titanium pumps with a delivery of 250 liters/sec each. Only under such vacuum conditions was it possible to observe the electron "cooling" of a proton beam experimentally. At higher pressures the electron cooling was masked by background interactions.

The replacement of oil-diffusion pumps by magnetic-discharge pumps in the vacuum system of the Institute of Theoretical and Experimental Physics synchrotron, even without the overhauling and cleaning of the vacuum chambers of the linear and annular accelerators, greatly increased the service reliability of the installation. In the I-2 linear accelerator breakdown ceased completely (K. K. Onosovskii et al.).

The important role of high-vacuum technology in solving problems of controlled thermonuclear fusion was noted by V. A. Glukhikh, and also in the review papers "Vacuum aspects of the design of experimental thermonuclear installations" by D. V. Serebrennikov et al. and "Light impurities in tokamaks" by E. A. Maslennikov et al. The first paper, in particular, considered the structural arrangement and design parameters of the vacuum system of a hypothetical reactor of the tokamak type. For evacuating the chamber a combined system of the module type is provided; it is based on cryosorption and compression pumps with a total delivery of $\sim 10^7$ liters/sec.

The conference papers reflected considerable improvements in computing methods of vacuum-system design. Some contributors analyzed the spatial distribution of the molecular flows in complex elements of vacuum systems (V. F. Golovinkin, L. S. Gurevich, A. M. Makarov, et al.). The use of the mathematical apparatus of the theory of radiant heat transfer enabled the molecular-flux-density surface-distribution functions to be constructed for various arrangements of the sorption-wall structures. A general criterion

Translated from Atomnaya Énergiya, Vol. 38, No. 6, pp. 437-439, June, 1975.

for the optimization of such structures was formulated; the criterion was based on the principle of making the fullest use of the sorbing properties of the wall at any point of the latter. The majority of existing pump systems of both the evaporating and absorption types were shown to have a low efficiency in this respect; arrangements more closely approximating the optimum were proposed.

An unconventional approach to the analysis of vacuum systems was set out by V. K. Grishin. Instead of such characteristics as the effective conductance and pumping speed, the author uses a group of integrated characteristics determining the mass transfer in the chamber under analysis (for example, the capture coefficient of structures with sorbing walls, the coefficient of restriction of the molecules to the object, and so forth). The mathematical apparatus of the theory of radiant heat transfer enables us to construct a closed system of equations on this basis; their solution gives a good idea of the spatial distribution of molecular concentration.

B. D. Ershov and G. L. Saksaganskii developed a method of analyzing vacuum systems with a complex geometrical structure (method of equivalent surfaces). The method lies in the successive simplification of the systems under analysis by replacing individual three-dimensional components with equivalent surfaces, to which certain characteristic functions are ascribed.

Among the many contributions relating to very-high-vacuum pumping devices, we may particularly note some papers on the creation of new electrophysical and cryogenic equipment. A series of magnetic-discharge pumps of the NMD diode type has been developed; these contain optimized electrode units and possess parameters substantially in advance of the commercially-produced NÉM and NORD pumps (O. K. Kurbatov et al.). The series includes pumps with deliveries of 6, 25, 63, 100, 250, 630 and 1000 liters/sec (referred to air) and a limiting residual gas pressure of $5 \cdot 10^{-10}$ mm Hg. The speed of the NMD systems is practically constant in the pressure range 10^{-8}-10^{-4} mm Hg; the pumps operate stably up to 10^{-9} mm Hg; the starting pressure is 10^{-2} mm Hg. The mass and size of these systems are smaller than those of commercial pumps by a factor of 1.5-2. The pumps are supplied by means of unified generation of three types with a no-load voltage of 7 kV. The pumps may be used in automatic-control systems.

For the high-speed evacuation of hydrogen in ion sources, heavy-current injectors, and experimental thermonuclear devices, extensive use will no doubt be made of sorption systems based on electric-arc titanium evaporators (L. P. Sablev et al.). Modified versions of these devices, in which the titanium is condensed on a water-cooled wall, are characterized by a high value of the getter use coefficient (up to 0.85); they are reliable in operation and have a delivery of up to 10^5 liters/sec (referred to hydrogen); the working pressure range is $5 \cdot 10^{-2}$ to 10^{-7} mm Hg.

For the prolonged evacuation of hydrogen at a very high vacuum (as indicated by Yu. A. Balovnev) the use of magnetic-discharge and palladium pumps operating together is extremely efficient. The palladium pump has a very high working pressure range (up to atmospheric pressure), a long operating life, and high specific characteristics: one such pump with a delivery of 600 liters/sec at 10^{-8} mm Hg weighs under 1 kg.

In recent years interest has arisen in a variety of new methods of cryopumping (condensation, cryosorption in layers of solidified gases, cryoadsorption on surface-active substances, and cryocapture). A paper by S. F. Grishin et al. described a very-high-vacuum cryogenic device comprising a backing pump and two condensation pumps. The pressure range of the system was 10^{-12}-760 mm Hg, the delivery (referred to hydrogen) 900 liters/sec for a liquid-helium consumption of $\sim$0.2 liter/day.

A paper by M. P. Larin et al. described several original pumps and traps based on cryosorption by layers of supercooled carbon dioxide and nitrogen condensates. Supercooling of the condensates was achieved by the evacuation of their vapor, so creating a porous block. The characteristics of one of the pumps were as follows: speed $\sim 10^4$ liters/sec, limiting residual pressure under 10^{-12} mm Hg, consumption of liquid helium 0.3 liter/h, mass less than 80 kg.

A number (around forty) of the conference papers discussed problems relating to the technology of high-vacuum systems and the construction of their component parts. An analysis of the service reliability of pumping equipment, fittings, vacuum gages, and other apparatus was presented by S. G. Appel' et al. A mathematical model of the breakdown of parts in a vacuum system and an attempt at predicting the reliability of projected vacuum installations were presented by E. A. Deulin et al.

On the whole the conference indicated a deeper interest and a more detailed understanding of the mechanisms underlying the interaction of rarefied gases with solid surfaces. The technique of cryogenic

evacuation is continuing to develop, and the foundations are being laid for the optimization of technological-construction decisions in relation to various parts of vacuum equipment, and also for a transition to automatic control. There is an undoubted tendency toward the detailed mathematical analysis of planned high-vacuum systems.

Some of the papers presented to the conference will be published in the collection "Problems of atomic science — physics and technology of high vacuum" (Khar'kov, 1974). Papers on the technology and equipment of electrical-vacuum products will be published in 1975 in the collection "Electronic technology." Most of the remaining papers will be deposited in the Central Scientific-Research Institute of Electronics.

BOOK REVIEWS

B. A. Ushakov, V. D. Nikitin,

and I. Ya. Emel'yanov

FOUNDATIONS OF THERMIONIC ENERGY CONVERSION*

Reviewed by Yu. I. Skorik

The purpose of the book under review is to acquaint the readership with the state of the art as a whole and to present its individual aspects.

In the first two chapters the authors acquaint the readership with the principal concepts of thermionic emission, devoting special attention to the work function of the electrodes.

Physical processes in a low-temperature plasma are considered theoretically in the third chapter. Equations for the transport of matter and energy in the interelectrode gap of the converter, which are in good agreement with the experimental data, are derived on the basis of simple reasoning. An analysis of the distribution of the plasma parameters over the gap and of the output characteristics of the converter for various operating modes gives evidence that the arc operating mode of the converter is the most efficient and promising.

Experimental material on the electrical and energy parameters of the converter — on the volt —ampere characteristics when electrodes made of the most promising materials are used — is displayed in the fourth chapter. The effect of the temperature of the electrodes and the interelectrode gap on the electrical characteristics is estimated. Recommendations are made on choosing the optimal working voltage. The material given may be used as the initial conditions in designing practical converters. The process of producing power in the converter is considered, and a procedure is expounded for the thermoelectric computation of an actual converter construction with presentation of certain results of numerical optimization computations indicating the strong effect of emitter nonisothermicity.

In the fifth and sixth chapters a general survey of thermionic power installations having a relatively low power rating and using various heat sources is given. Attention is focused on the possibility of using thermal pipes, and the physical processes that occur in them are analyzed.

The seventh chapter tells about the use of a thermionic converter in combination with a nuclear reactor as a source of heat energy. The peculiarities of the operation of converters in various aggregations are analyzed, including the effect of profiling the energy production in a reactor and the nonuniformity of heat production along the emitter length on the converter characteristics, the effect of gaseous fission products on the stability of the geometry of the converter sections, and the electrical characteristics. A review is presented of the principal trends in construction implementation of reactor—converters using examples of projects designed abroad and the creation in the USSR of the first reactor—converter in the world.

The latter chapter indicates the operating conditions and formulates the requirements governing the material of the sections of a converter which is built into a reactor; information of a specification character is presented concerning the properties of the possible structural materials, and recommendations are made for their selection.

The bibliography (240 titles) covers practically all Soviet and the majority of foreign publications on the given topic.

Note should be taken of the methodological consistency, the logical nature of the design, and the clarity of the description of the theory of thermionic conversion.

*Atomizdat, Moscow (1974).

Translated from Atomnaya Énergiya, Vol. 38, No. 6, p. 439, June, 1975.

A deeper elucidation of individual, very important problems is desirable (the effect of irradiation on the properties and stability of the structural materials, resource tests of converters, and analysis of the role of the fine crystallographic structure of the surface of the electrodes).

The Plenum/China Program

Research in the medical, life, environmental, chemical, physical, and geological sciences from the People's Republic of China

The 15 major scientific journals published in China since the Cultural Revolution are being made available by Plenum in authoritative, cover-to-cover English translations under the Plenum/China Program imprint.

These important journals contain papers prepared by China's leading scholars and present original research from prestigious Chinese institutes and universities. Their editorial boards are affiliated with such organizations as the Chinese Chemical Society, the Academia Sinica in Peking and its Institutes, and the Chinese Microbiological Society.

The English editions are prepared by scientists and researchers, and all translations are reviewed by experts in each field.

Journal Title	No. of Issues	Subscription Price
Acta Astronomica Sinica	2	$65
Acta Botanica Sinica	4	$95
Acta Entomologica Sinica	4	$95
Acta Genetica Sinica	2	$65
Acta Geologica Sinica	2	$75
Acta Geophysica Sinica	4	$95
Acta Mathematica Sinica	4	$75
Acta Microbiologica Sinica	2	$55
Acta Phytotaxonomica Sinica	4	$125
Acta Zoologica Sinica	4	$125
Geochimica	4	$110
Huaxue Tongbao — Chemical Bulletin	6	$95
Kexue Tongbao — Science Bulletin	12	$175
Scientia Geologica Sinica	4	$125
Vertebrata PalAsiatica	4	$95

For further information, please contact the Publishers.

SEND FOR YOUR FREE EXAMINATION COPIES

plenum

PLENUM PUBLISHING CORPORATION
227 West 17 Street, New York, N.Y. 10011
In United Kingdom 8 Scrubs Lane, Harlesden, London, NW10 6SE, England

Declassified and Approved For Release 2013/09/25 : CIA-RDP10-02196R000400050004-2